Polychromatic Determination of Spectral Response of PV Devices

by

Ira Devi Sara

Doctoral Thesis

Submitted in partial fulfilment of the requirements for the

award of

Doctor of Philosophy of Loughborough University

2 December 2013

Abstract

This thesis introduces a novel spectral response (SR) measurement technique using polychromatic filters (filters with very broad spectral transmittances) to determine SR of large area PV devices. Conventionally, SR of a photovoltaic (PV) device is determined by illuminating the device under test (DUT) with a series of monochromatic beams at different wavelengths as described in the international standard IEC 60904-8, or beams of limited spectral content using narrow band pass filters or monochromator. One significant problem associated with the application of the narrow band pass filters for a large-area SR measurement is that low light intensity produced on the measurement plane particularly in certain wavelength ranges: the ultraviolet and infrared. This can produce weak signal responses from a tested PV device. In addition, the imperfection of the filter's mounting position can shift the peak wavelength of the filter's transmittance at angle of incidence greater than 10°. This can cause stray light on the measurement plane. The proposed SR measurement method is called as '**the polychromatic SR fitting method**' or, in short, it is known as '**the polychromatic method**'. The advantage of this method is that higher beam intensity can be produced on the measurement plane as a result of large spectral transmittance of the polychromatic filters. This can improve the signal strength of a tested PV device. This new SR measurement method works by comparing the variations in the currents which are measured at different spectra to the currents which are calculated at the same spectral conditions using the SR model. Validations of this method for a large- and small-area SR determinations show that it is potentially feasible as a new technique for determining SR of a PV device with deviations within ±2% across the wavelength bands.

Keywords: *Photovoltaic, spectral response, monochromatic filters, polychromatic filters, fittings, spectral response measurement, spectral response model*

Nomenclature

I_o	Diode saturation current in Amperes	n	Ideality factor to represent the quality of a p-n junction
I_{01}	Diffusion diode saturation current due to the diffusion driven of charge carriers in Amperes	n_1	Ideality factor to represent the diffuse driven current
I_{02}	Recombination diode saturation current due to the drift driven of minority carriers in Amperes	n_2	Ideality factors to represent the drift driven current
K	Boltzmann's constant, 1.38066×10^{-23} J/K	T	Absolute cell temperature in Kelvin
Q	Electrical charge, 1.60219×10^{-19}C	V	Output voltage in volts
R_s	Series resistance	R_p	Parallel resistance
I_{sc}	Short-circuit current in Amperes measured at zero voltage bias	$\mu\tau$	Product of carrier lifetime and carrier mobility
$I_{sc,ref}(\lambda)$	Measured short-circuit current of the reference detector	d_i	Thickness of intrinsic layer of a-Si device
$I_{sc,DUT}(\lambda)$	Measured short-circuit current of the tested PV device	P_{in}	Incidence irradiance in Watts
V_{bi}	Built-in voltage	V_j	Voltage across the p-n junction
$A(\lambda)$	Absorbance	A	Cell' area in units of m^2
A_{ref}	Area of the reference detector	A_{DUT}	Area of the tested PV device
H	Planck's constant, 6.6262×10^{-34}Js	$\alpha(\lambda)$	Absorption coefficients

D	Film thicknesses	a	Rate of change (dimensionless)
χ	Sum of the squared errors (SSE)	c	Speed of light, 2.997925×10^8 m/s
λ	Specific narrow-band wavelength in nm	λ_o	Centre wavelength of absorption in nm
hc/q	Approximately 0.80655 for wavelength in units of μm	$E(\lambda)$	Spectral irradiance at the plane of array (W/m^2/nm)
$E_{ref}(\lambda)$	Standard spectrum as given in the standard IEC 60904-3 [1]	$E_{sim}(\lambda)$	Spectrum of solar simulator at the time of measurement
$QE_{top}(\lambda)$	External quantum efficiency of the top cell	$QE_{bottom}(\lambda)$	External quantum efficiency of the bottom cell
I_{ph}	Photocurrent in Ampere	SR	Spectral response in A.W^{-1}
$SR_{ref}(\lambda)$	Spectral response of the reference device	$SR_{DUT}(\lambda)$	Spectral response of the device under test
V_{oc}	Open-circuit voltage in volts	FF	Fill factor (dimensionless)
I_{mpp}	Current at the maximum power point in Amperes	V_{mpp}	voltage at the maximum power point in volts
P_{mpp}	Power at the maximum power point in Watts	λ_1 and λ_2	Wavelength ranges of device spectral interest
α	Material constant, for silicon $\alpha=0.473$meV.K-1	$E_{g0}(0)$	Bandgap energy at 0 K. For silicon PV device, $E_g(0)=1.17$eV
β	Material constant which combines all of the dimensional, doping and minority carrier transport parameters of a solar cell, For silicon, $\beta=636$K	E_{gT}	Bandgap energy at temperature T
P_1 to P_3	Absorption and reflection losses at the front glass and encapsulation layer	P_4 to P_7	Absorption curve in the active layer

I	Data point	y_i	Measured data point
$y(x_i/a)$	Calculated data point	σ_i	Standard deviation in each data point
N	Total points in the measurement	M	Number of fitted coefficients

Acknowledgments

All praise and thanks due to the Almighty Allah SWT, the Lord of the universe, may blessings and peace of Allah be upon the last Messenger and Prophet, Muhammad SAW, his family, companions and all those who follow his footsteps until the end of this universe. Without His help and guidance, this thesis will not be completed successfully.

I would like to express my deepest appreciation and gratitude to my supervisors, Prof. Ralph Gottschalg and Dr. Thomas R. Betts for their guidance, support, and inspiration particularly from the initial stage of my work. They always keep motivating me to be strong and to believe in myself that I can complete my research project successfully.

A special thanks to my funder, the Indonesian National Education Scholarship, for giving me opportunity and financial support to pursue the PhD study. I would like to give special thanks to my parents for always keeping me in their prayer, always supporting me particularly when I feel weak; to my sisters, Isna Keumala and Nadia Ulfah, for inspiring me to keep working hard to finish this work.

Many people have contributed in different ways toward the successful completion of this thesis. I cannot name them all individually, but I want to express my special thanks to all my colleagues at the Centre for Renewable Energy Technology (CREST) in the School of Electronic, Electrical and Systems Engineering: Dr. Martin Bliss who constantly assists me with the experiment; Blago and Michael for their insight about the spectral measurement; Alex Smith and Charles Greenwood for always be there to help me with their advice for the experiment and keep motivating me to complete this PhD work; My best friends: Noor Kasri, Farhana, Sa'adiah and Shalawati who always motivate me to be confident and pray for my success.

Contents

Lists of Figures

17

19

Lists of Tables

Chapter 1

Introduction

A standard test condition (STC) has been established to assess and compare performance of different types of PV devices under specific environmental conditions. At this condition, a PV device is measured at an irradiance of 1000 Watt/m^2 at angle of incidence of zero degree, temperature of 25°C and the spectral irradiance distribution at air mass (AM) 1.5 global [1].. However, information provided from the STC measurement is inadequate to predict energy delivered by a PV device accurately under real operating conditions. This is due to the power output of a PV device varies with temperature, intensity of incoming sunlight, angle of incidence and spectral irradiance conditions.

An accurate PV performance measurement at any environmental conditions requires information of spectral response (SR) of a tested PV device which is the ratios of the current generated from a PV device to the power at specific wavelengths of solar spectrum, temperature coefficients, and light transmission coefficients as shown in Figure 1.1. Due to the mismatch in the measured spectrum that is produced from a solar simulator to the reference spectrum and the mismatch in the spectral response between the reference solar cell and the tested PV device, the current measurement indoor becomes incorrect. To avoid this condition, the measured current needs to be corrected using the spectral mismatch correction factor which requires device spectral response in its calculation.

Environmental conditions:
- Temperature
- Irradiance
- Solar spectrum
- Angle of Incidence
- Wind speed
- Humidity
- Pressure

MEASUREMENTS

PERFORMANCE: Power; Efficiency

Energy Yield

Characteristics of a PV device:
- Temperature coefficients
- Irradiance response
- Spectral response
- Light transmission coefficient
- Characteristics at STC
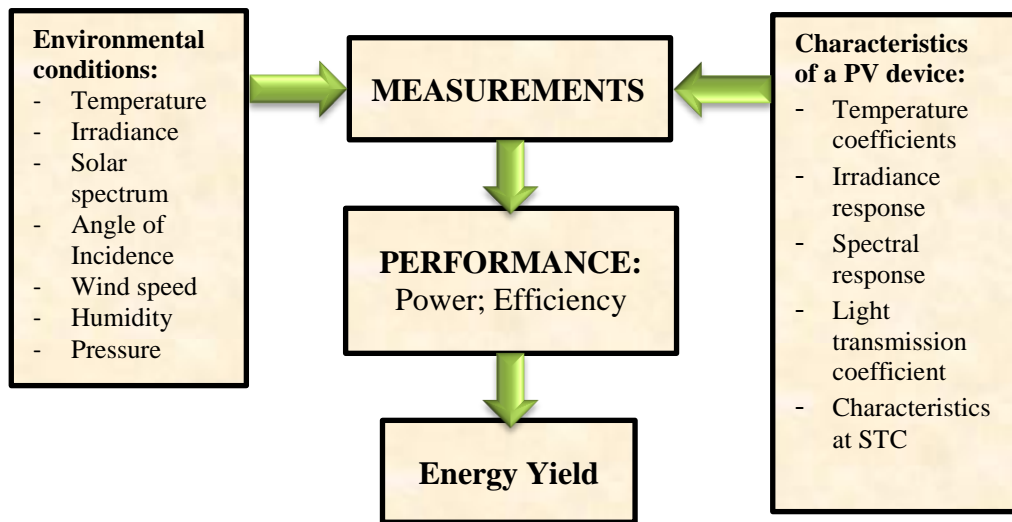
Figure 1.1: Requirements for an accurate energy yield prediction according to the draft standard IEC 61853

Conventionally, SR of a PV is measured using a series of different monochromatic beams as described in the standard IEC 60904-8 [4]. These monochromatic beams are produced by filtering the spectrum of a light source using different narrow bandwidth interference filters (filter-based method), a tuneable laser (differential spectral responsivity method) or using a monochromator (grating-based method).

Since most of commercial PV devices that are currently available on the PV market have a size up to 2 metres such as a polycrystalline module with a dimension of 1.6 m by 0.9 m, the requirement for a large-area SR measurement is very demanding. Due to the natural shape of the spectral light source used in the SR measurement, the light intensity of a xenon lamp after being filtered by some narrow band pass filters at specific wavelengths (the ultraviolet (UV) and near infrared (NIR)) are extremely low, i.e. 0.12 Watt/m^2 and 3.02 Watt/m^2. These extremely low intensity beams produce very weak response signals from the tested PV device, i.e. 9.27×10^{-5} A and 5.2×10^{-4} A. If these monochromatic beams are enlarged to illuminate the entire surface of a large-area PV device, its intensity will be reduced as well as the spatial uniformity of its irradiance on the measurement plane. As a consequence, the uncertainty in the SR determination becomes high. This bandwidth limitation has made the conventional SR measurement method more suitable for a small-area SR determination rather than for a large-area SR measurement. Another problem is that

the blocking region of an interference filter can shift to the higher transmittance region at higher angle of incidence such as 10° due to an imperfection in the mounting position. This can produce stray light on the measurement plane and leads to the systematic error in the spectral response measurement.

Aiming to solve the problem encountered in a large-area SR measurement, this thesis introduces **a new method for measuring SR of a PV device**. The proposed SR method is based on the application of polychromatic filters to provide higher beam intensity and larger beam size on the measurement plane. Polychromatic filters are the filters with a broadband spectral transmittance. Using filters with a wide spectral-band for SR measurement brings an advantage in terms of the beam intensity on the measurement plane. The beam intensity produced from the selected filters becomes higher than that is produced from the narrow band pass filters, as have been used in the monochromatic filter method. Introducing polychromatic filters for spectral response determinations can solve the problem of low beam intensity that is encountered in the application of a monochromatic filter. This simple approach can enhance the signal strength that is produced from a tested PV device. Hence, the proposed SR fitting method does not require the lock-in technique to detect weak response signals that are produced from the tested PV device and the bias lighting system. The types of filters used for this new SR measurement method are also considered to be cost-effective, compared to that are used in the conventional SR measurement method. It is expected that this new SR measurement approach can improve the accuracy in the SR measurement within an acceptable uncertainty and can be used to measure SR of any PV technologies.

1.1. Thesis Structure

The motivation and objective of the research is presented in Chapter 1. A fundamental knowledge on measurements and characterisations of photovoltaic devices is important to understand device performance and problems exist in the PV measurements. A brief review on characterisations and measurements of PV devices is presented in Chapter 2. This chapter also explains the effects of different environmental factors on the current-voltage characteristic curves of a PV device.

Chapter 3 introduces a new proposed approach for determining spectral response of different PV technologies. It also describes in more detail how the new SR method works to obtain SR of a PV device. A new spectral response model is introduced with a fitting algorithm to fit the currents. Lastly, a conclusion on the feasibility of the proposed concept for SR determination is drawn. Chapter 4 provides experimental evidences of the proposed SR method on a small-area measurement system. It also discusses several factors influencing the accuracy of the proposed SR method. Chapter 5 demonstrates the implementation of a polychromatic filter method for a large-area SR measurement. It explains the experimental setup of SR characterisation tools into the PASAN measurement system in use at the Centre for Renewable Energy System Technology (CREST). Finally, the feasibility and reliability of the polychromatic filter method for SR determinations of different size PV technologies is concluded in Chapter 6. In this chapter, the recommendation for future works related to the research area is presented.

Chapter 2

Characteristics and Measurements of Photovoltaic Devices

2.1. Introduction

This chapter provides the fundamentals required for understanding photovoltaic (PV) performance and reviews the methods currently in use for characterizing the performance of PV devices as a means to convert sunlight directly into electricity. Understanding of the performance characteristics of a PV device is essential knowledge for predicting energy yield under a specific operating condition. These performance characteristics are discussed in section 2.2. Since the performance of a PV device depends on the operating condition, therefore it is essential to comprehend factors affecting their performance. These factors are the irradiance, temperature, angle of incidence and solar spectrum (section 2.3). Section 2.4 explains the types of measurements required to obtain the performance characteristics. It also includes the measurement methods. Finally, a conclusion is presented.

2.2. Performance Characteristics of Photovoltaic Devices

Characteristics of PV devices include spectral response, temperature coefficients for current, voltage and power at the maximum point; series and shunt resistances; current at the short-circuit condition; voltage at the open-circuit condition; power at the maximum point; fill factor; and efficiency. These device characteristic parameters are used to indicate the performance of a PV device as power generation under certain environmental conditions and employed as input parameters in the energy yield calculation. Of these parameters, the open-circuit voltage (Voc), the short-circuit current (Isc) and the maximum power point (Pmpp) constitute

significant points in the current and voltage (I-V) characteristic curve of a PV device as shown in Figure 2.1 [5].
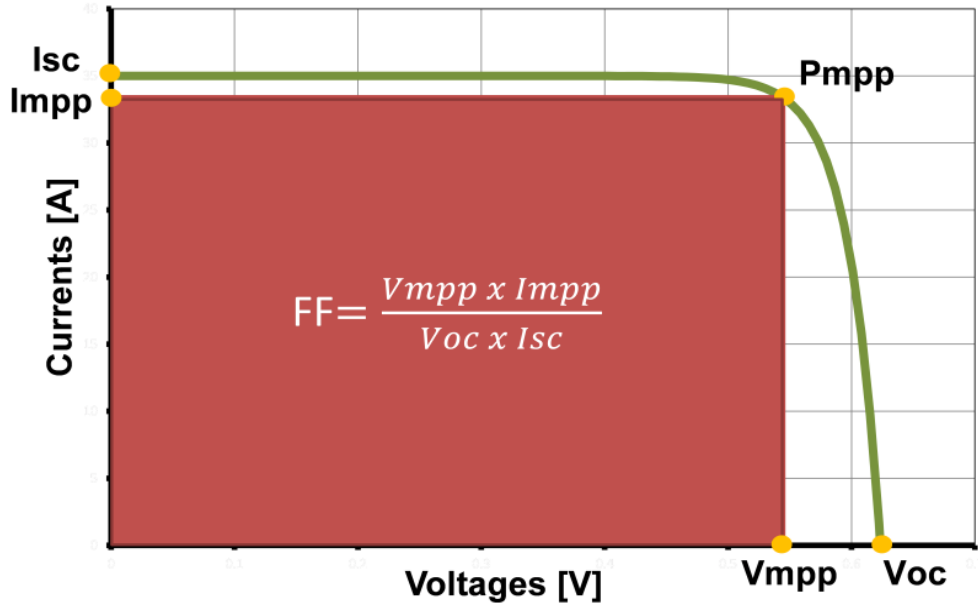
Figure 2.1: A typical current and voltage curve of a PV device

The short-circuit current is the maximum current generated from a solar cell at zero voltage. At this condition, the short-circuit current becomes equal to the photocurrent [6]. Its magnitude is around 5% to 15% higher than the current at the maximum power point (Impp) [5]. The open-circuit voltage is a potential difference between the positive and negative contacts of a solar cell. It is the maximum voltage produced from a solar cell at zero current condition [6]. The magnitude of this voltage varies between different PV materials. For example, crystalline silicon solar cells have an open-circuit voltage of approximately 0.5 V to 0.6 V and that for amorphous silicon cells is 0.6 V to 0.9 V. The maximum power point is the maximum power produced from a PV device. This corresponds to the fill factor (FF), which is a square area under the I-V curve as shown in Figure 2.1. The fill factor represents a ratio of the maximum power to the product of the open-circuit voltage and the short-circuit current as expressed in equation (2.3).

$$I_{ph} = A \int_{\lambda_1}^{\lambda_2} SR(\lambda) \cdot E(\lambda) d\lambda \qquad (2.1)$$

27

$$V_{oc} = \frac{nkT}{q} ln \left(\frac{I_{ph}}{I_o} + 1 \right) \qquad (2.2)$$

$$FF = \frac{I_{mpp} \times V_{mpp}}{I_{sc} \times V_{oc}} \qquad (2.3)$$

A simple circuit model is used to explain the relation of those electrical characteristics in a solar cell. It starts with an ideal model which describes a solar cell as a current source as shown in Figure 2.2. When there is no light radiating a solar cell, the current produced is called the dark current (I_D) as written in equation (2.4). In the presence of light, a solar cell generate the photocurrent which opposes the dark current and its value is proportional to the amount of the incident light and cell's spectral response as shown in equation (2.1).
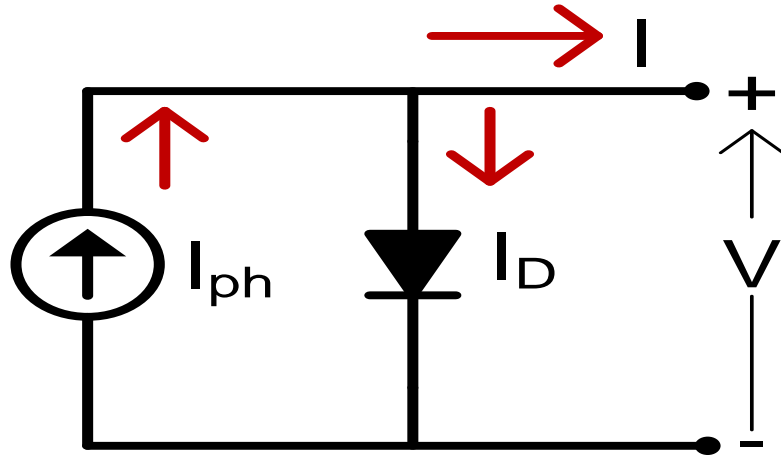
Figure 2.2: An ideal model of a solar cell

In this light condition, the total current (I) generated by an ideal PV device is calculated by subtracting the photocurrent generated to the dark current as shown in equation (2.5):

$$I_D = I_0 \left[e^{\frac{q(V)}{nkT}} - 1 \right] \qquad (2.4)$$

$$I(V) = I_{ph} - I_D \qquad (2.5)$$

Unfortunately, this ideal solar cell never exists in real operating conditions. Due to manufacturing defects such as a poor p-n junction quality (impurities near a p-n junction), a shunted path is formed and causes part of the generated photocurrent

flowing through it [6]. This reduces the total current output at the PV device terminal. The shunted path is represented by the shunt or parallel resistance (Rp). Another factor causing losses in a PV device is the series resistance (Rs) that exists between the interconnected layers such as the electrical contact and the front surface [7]. As a result, an equivalent circuit model of a commercial solar cell becomes as shown in Figure 2.3. This model is known as the one-diode model.
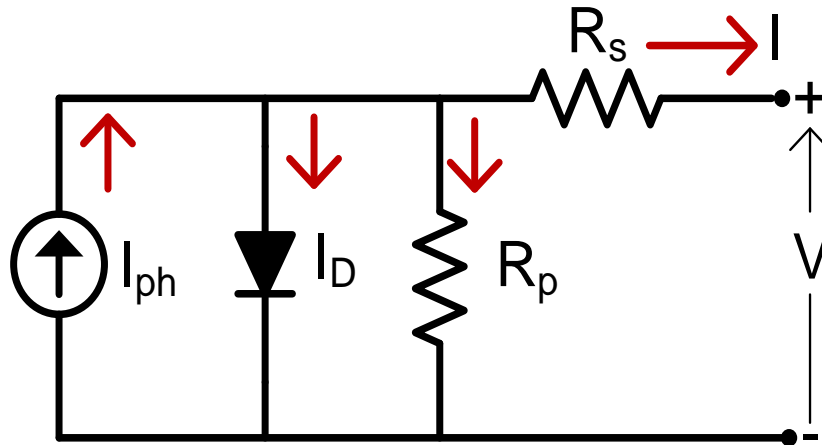
Figure 2.3: An equivalent circuit diagram of one-diode model

The current and voltage relationship of a one-diode model is shown in equation (2.6).

$$I(V) = I_{ph} - I_0 \left[e^{\frac{q(V+IR_s)}{nkT}} - 1 \right] - \frac{(V+IR_s)}{R_p} \qquad (2.6)$$

The shape of the I-V curve and the area under the curve are influenced by the shunt and series resistances which represent losses in a solar cell [7]. Ideally, the series resistance should be zero and the shunt resistance should be extremely high to prevent current flowing through the p-n junction of a solar cell [6]. These ideal conditions can never be found in commercial solar devices. Effects of varying the shunt and series resistances on the shape of the I-V curve are shown in Figure 2.4 and Figure 2.5.

As can be seen in the two figures, variations in the series and shunt resistances affect the fill factor and power at the maximum power point. Higher series resistances are resulted from low doping densities and poor conductivity of materials used for the

29

contacts [8]. For example, crystalline solar cells have contacts made from aluminium paste which has higher conductivity compared to that are used for thin film solar cells. Lower shunt or parallel resistances indicate leakage current through the p-n junction of the PV device.
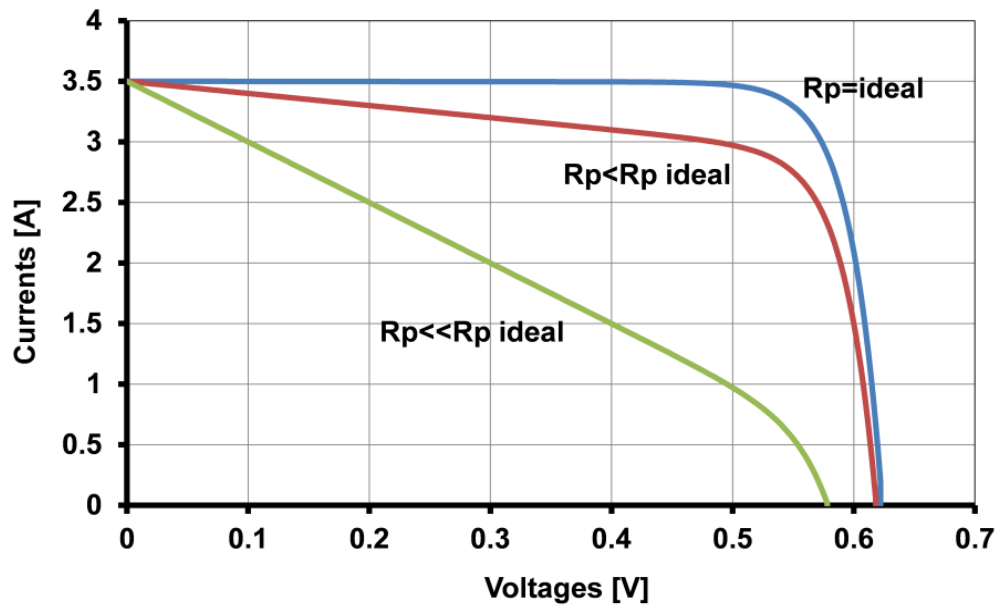
Figure 2.4: Effects of varying shunt resistances to the shape of an I-V curve of a solar cell
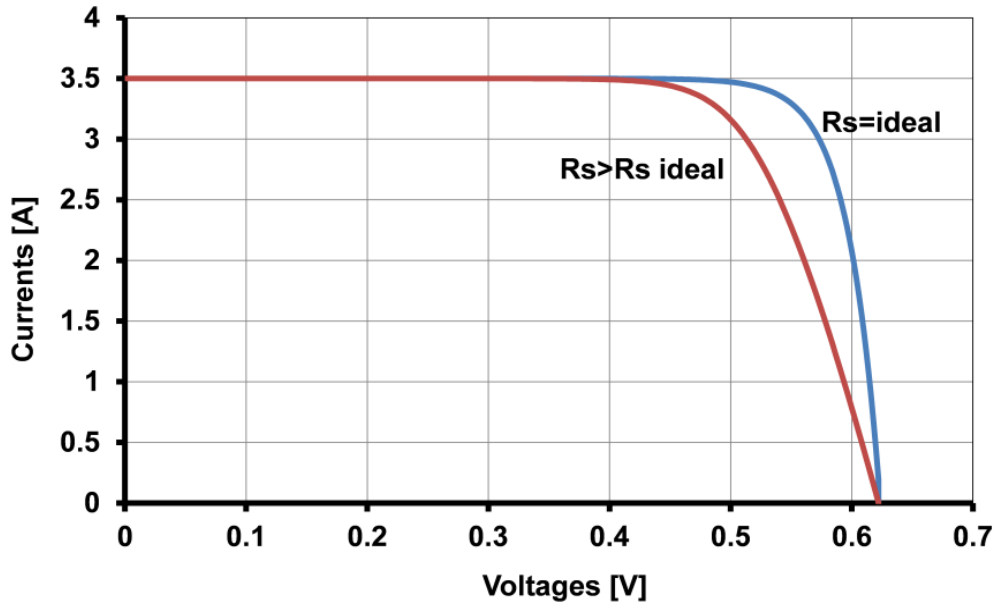
Figure 2.5: Effects of varying series resistances to the shape of an I-V curve of a solar cell

However, any solar cells have certain characteristics. To accurately model a PV device, a one-diode model needs to be modified in order to consider the recombination losses due to drift currents at the depletion area [6]. The modification is made by adding a second diode into the one-diode model to represent a drift current as shown in Figure 2.6. A mathematical model used to express the relation of the current to voltage of two-diode models is written in (2.7) [9].

$$I(V) = I_{ph} - I_{01}\left[e^{\frac{q(V+IR_S)}{n_1 kT}} - 1\right] - I_{02}\left[e^{\frac{q(V+IR_S)}{n_2 kT}} - 1\right] - \frac{(V+IR_S)}{R_p} \qquad (2.7)$$
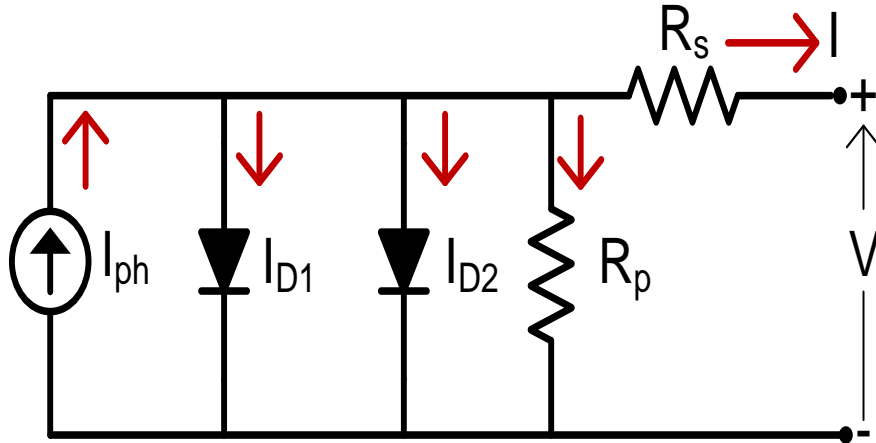
Figure 2.6: An equivalent circuit diagram of two-diode model

Due to short diffusion lengths in doped amorphous silicon (a-Si) solar cell, an intrinsic layer (*i*-layer) is added in between its p-n junction for optimum photon absorptions. This layer extends the distance (thickness) of the p-n junction which results in an increase in the electric field across the junction and the probability of successful charge separation across the junction [8]. The presence of dangling bonds in amorphous silicon cells causes recombination losses in the *i*-layer. These losses reduce the photocurrent generated by an amorphous silicon cell [10]. Therefore, its performance can be more suitably represented using a Crandall-Merten model as shown in equation (2.8):

$$I(V) = I_{ph} - I_{rec} - \left[e^{\frac{q(V+IR_S)}{nkT}} - 1 \right] - \frac{(V+IR_S)}{R_p} \qquad (2.8)$$

$$I_{rec} = I_{ph} \left[\frac{1}{\frac{\mu\tau}{d_i^2}(V_{bi}-V+IR_S)} \right] \qquad (2.9)$$

An extra term added to the one-diode model is called the recombination current which accounts for the loss in current due to recombination in the *i*-layer as shown Figure 2.7.
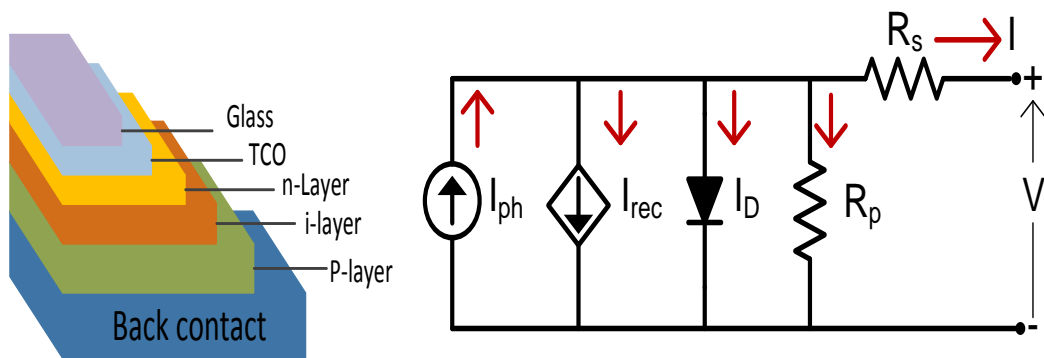
Figure 2.7: Structure of an amorphous silicon device and its equivalent circuit diagram

To characterise the performance of a solar cell under varying irradiances and temperatures, a solar cell needs to be represented using a dynamic model. This model consists of a current source (I_{ph}), a diode, a series and parallel resistance, and a parallel capacitance which composes of a transition and diffusion capacitance. These capacitances exist inside the space charge region and the bulk region of a solar cell [11]. A dynamic model of a solar cell is in Figure 2.8 [12].
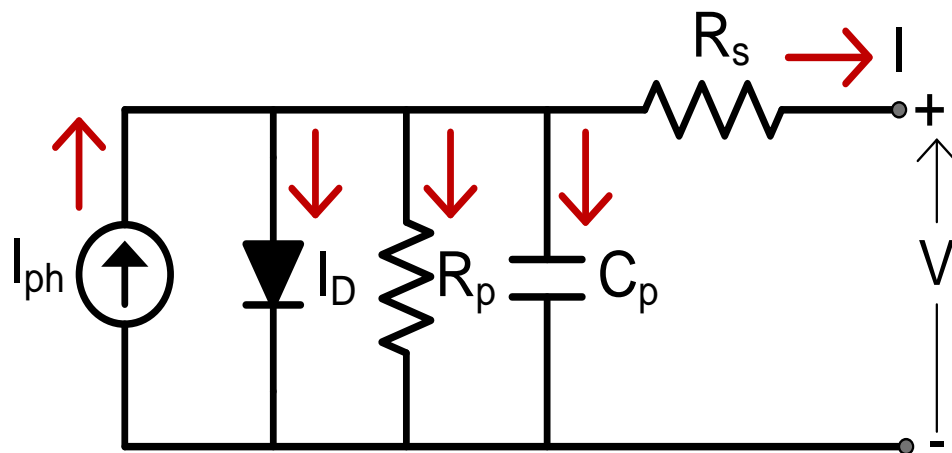
Figure 2.8: An equivalent circuit of a dynamic model for a solar cell

The current and voltage relationship of the dynamic model is mathematically expressed in the following equations [12][13]:

$$I = I_{ph} - I_D - I_p - I_c \qquad (2.10)$$

33

$$I_c = C \frac{\partial(V + IR_s)}{\partial t} + (V + IR_s) \frac{\partial C}{\partial t} \qquad (2.11)$$

Other currents are written in the same mathematical expression as shown in equation (2.6).

Certain types of solar cells consist of more than one p-n junction, which are known as multi-junction (MJ) solar cells. These PV technologies are derived from thin film devices. They are made to increase the conversion efficiency of a single-junction thin film PV device by increasing the light absorption into a wider range of solar spectrum. There are two types of these MJ PV devices commercially available on the PV markets: double-junction (2J) and triple junction (3J) PV devices. A double-junction solar cell is made by integrating two single-junction PV devices monolithically in series [14-17] as represented in Figure 2.9.
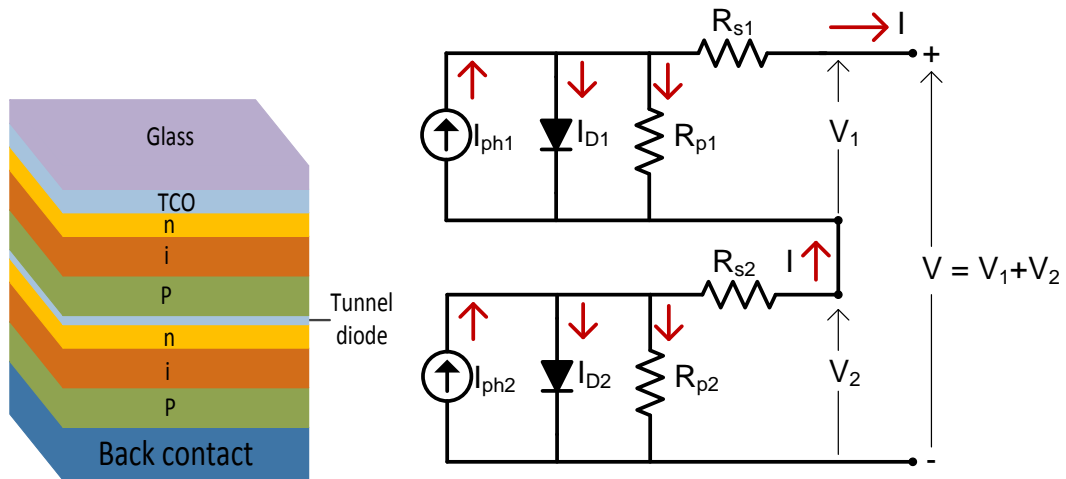
Figure 2.9: An equivalent circuit model for a double junction solar cell

In order to absorb different ranges of solar spectrum, sub-cells in a double-junction PV device are designed with different band gap energy [18, 19]. Generally, the band gap of the top cell is made higher than that of the bottom cell [20][21]. As a result, each cell has different spectral response [22][23]. Since both cells respond differently toward solar spectrum, matching current between the cells is rarely found under real operating conditions. The cell which produces less current becomes the current limiting for another cell and determines the total current flowing through the double-junction device [19, 24] as shown in Figure 2.10.

34

However, the rule to determine the total current of a MJ device is not always correct as has been mentioned above, where the least current in the MJ device becomes the total current of the MJ device. There is a device parameter in the MJ device that influences its total photocurrent generation. This parameter is the shunt resistance of the individual sub-cells of the MJ cell [25]. If one cell has low shunt resistance, the total current flowing through the device becomes greater than the lowest current and less than the highest current produced by the individual sub-cells as shown in Figure 2.11.
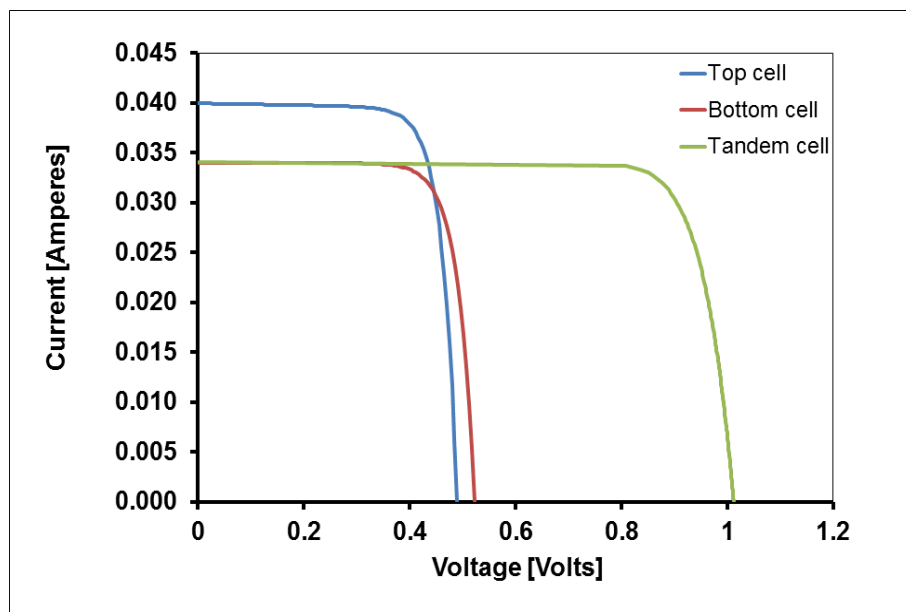
Figure 2.10: Current and voltage characteristic of a double-junction solar cell
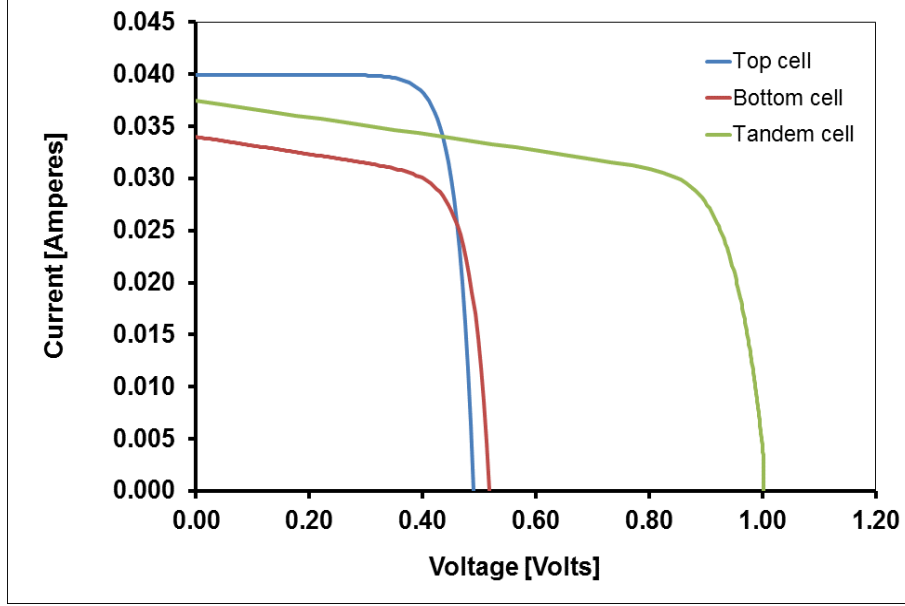
Figure 2.11: Changes in the current and voltage characteristic of a double-junction solar cell due to variations in sub-cells' shunt resistances

The photocurrent generated by the top cell can be determined by knowing the spectrum falling onto it and its spectral response (SR), as written in equation (2.13). The top cell becomes a spectral filter for the bottom cell and determines the amount of spectrum received by the bottom cell. To calculate the photocurrent generated by the bottom cell, it is important to know the unabsorbed spectra of the top cell. These unabsorbed spectra are modelled by using the quantum efficiency (QE) of the top cell [26]. By substituting the unabsorbed spectral component into equation (2.13) and replacing the QE_{top} with the QE_{bottom}, the photocurrent of the bottom cell is calculated as:

$$I_{ph,top}(\lambda) = A.(q/hc) \int_{\lambda_1}^{\lambda_2} \lambda E(\lambda) QE_{top}(\lambda) d\lambda \qquad (2.12)$$

$$I_{ph,bottom} = A.(q/hc) \int_{\lambda_1}^{\lambda_2} \lambda E(\lambda) \big[1 - QE_{top}(\lambda)\big] QE_{bottom}(\lambda) d\lambda \qquad (2.13)$$

Having understood the structure of different PV technologies, the following section presents the impacts of different environmental conditions on the performance of a PV device.

2.3. Effects of Environmental Conditions on the Performance of PV Devices

Electrical characteristics of a PV device are significantly affected by the operating conditions where the PV device is operating outdoor [27-30]. The effects can be clearly seen on how the shape of the current and voltage curve varies with changes in the environmental conditions [31]. There are four vital environmental conditions influencing the performance characteristics of a PV device. These environmental factors are the irradiance, temperature, solar spectral irradiance, and the angle of incidence (AOI) [32, 33, 34, 35, 36]. For energy yield prediction purpose, changes in the performance characteristics of a solar cell with environmental conditions should be quantified. The I-V characteristic at an STC is used as a reference to assess changes in the performance parameters of a PV device. Understanding the impacts of changes in these environmental factors on performance characteristics of a PV device is important for accurate PV measurements which will be relevant for Chapter 4 and 5 where an accurate current determination is very significant for an accurate spectral response determination. These environmental impacts on the performance of a PV device are discussed further in the following section.

2.3.1 Irradiance Effects

The sun's position in the sky varies at any time of the day and seasons of the year due to the earth's rotation around its axis and its evolution around the sun. This rotation has an impact on the amount of irradiance received at a typical site on the earth's surface. The annually average irradiance received at the outer atmosphere is 1367 W/m^2 at AM0 [5]. On a clear day, when the sun is positioned perpendicularly on a surface at sea level, the average irradiance reaching on the earth's surface is about 1000 W/m^2. This intensity is reduced depending on the atmospheric conditions particularly the cloud cover amount (clearness of the atmosphere), the sun's position in the sky and the distance that the sunlight passes through it [37, 38] and site's geographical condition [39].

The impacts of variations in the irradiance on electrical characteristics of a solar cell are shown in Figure 2.12.
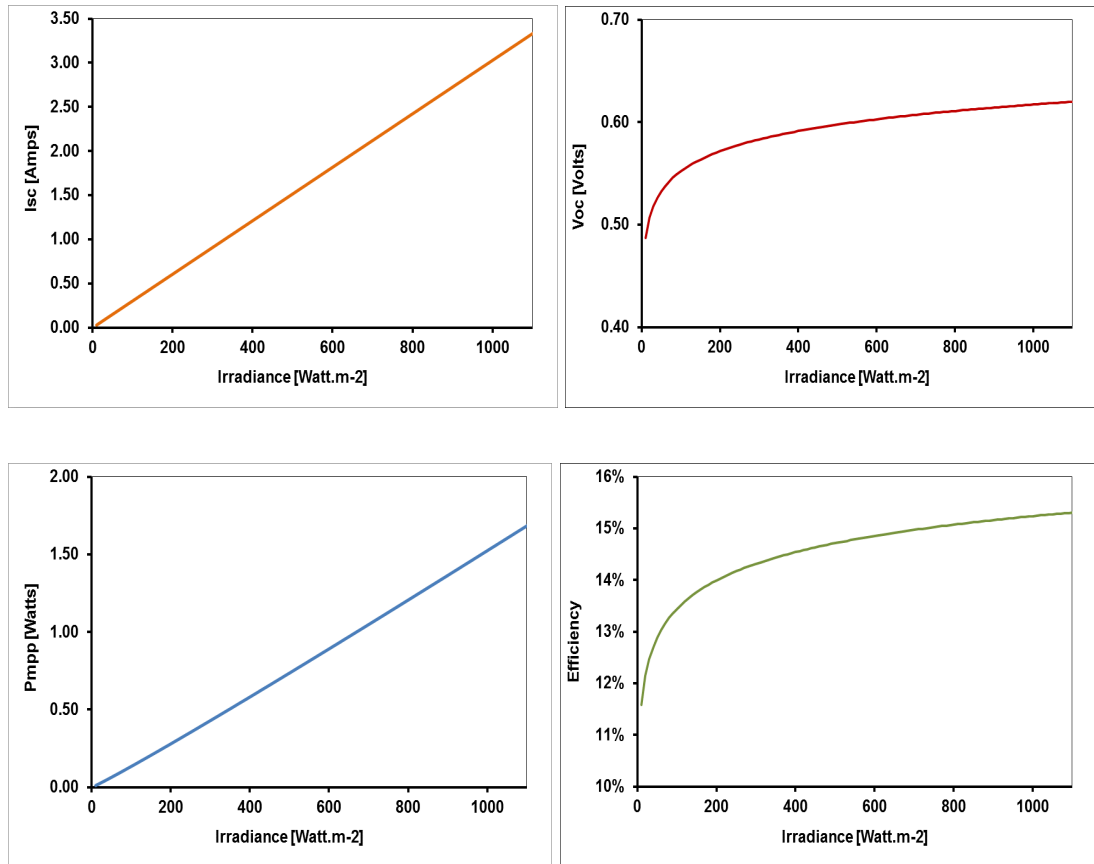
Figure 2.12: Effects of variations in Irradiance on electrical performance of a solar cell

As shown in Figure 2.12, the short-circuit current and the power at the maximum point vary linearly with the change in the irradiance level. This relationship only applies for linear solar cells (spectral response versus wavelength is constant). The open-circuit voltage and efficiency increase logarithmically with increasing irradiance intensity. Based on these relationships, it is important to monitor the irradiance level of a light source and to keep it at a desirable level during the current and voltage measurements in order to obtain accurate electrical characteristics of a tested PV device.

2.3.2 Temperature Effects

Temperatures have significant influences on the performance parameters of a PV device, particularly the open-circuit voltage and the power at the maximum point, which degrades rapidly with increasing temperatures. Changes in the open-circuit voltage with temperature occur because the band gap energy of a solar cell varies with temperature as expressed in equation (2.14) [40-42].

$$E_g(T) = E_{g0}(0) - \frac{\alpha T^2}{T+\beta} \qquad (2.14)$$

Changes in the band gap energy due to variations in the cell temperature affect the reverse saturation current of a solar cell as expressed in equation (2.15) [43]:

$$I_o = \beta T^3 exp\left[-\frac{E_{gT}}{kT}\right] \qquad (2.15)$$

Several factors such as the increase in the ambient temperature, the wind speed and the irradiance contribute to the increase in cell temperature. Effects of increasing cell temperature to the shape of I-V curve of a solar cell can be seen in Figure 2.13.
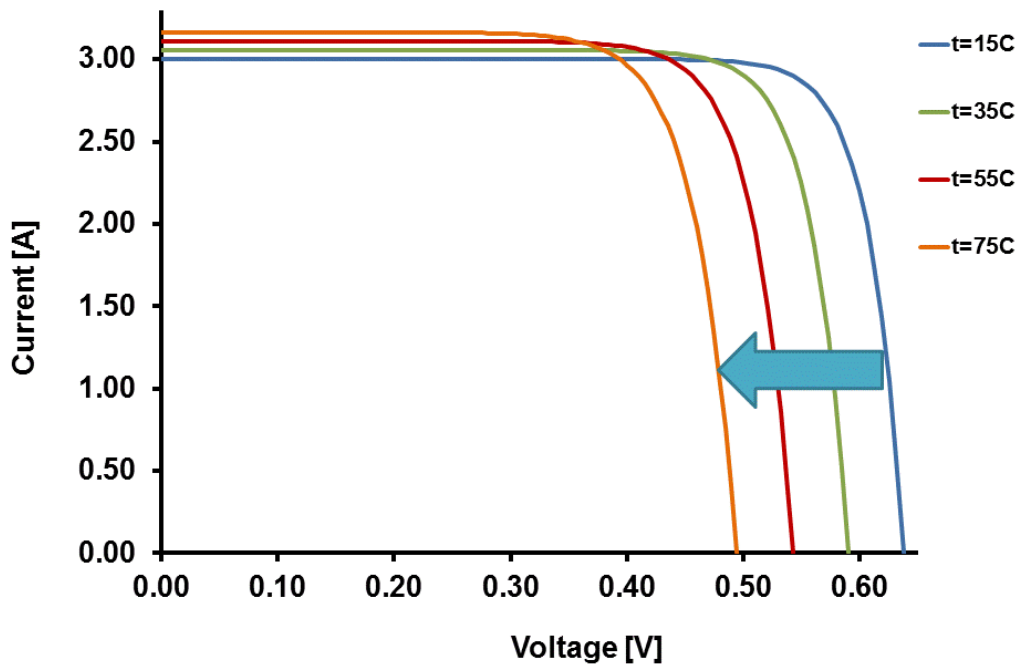
Figure 2.13: Changes in the I-V characteristic curves of a PV device with temperature

As shown in Figure 2.13, the increase in temperature has major impacts on the open-circuit voltage and the power at the maximum point. Changes in each of the electrical characteristic are given in Figure 2.14.
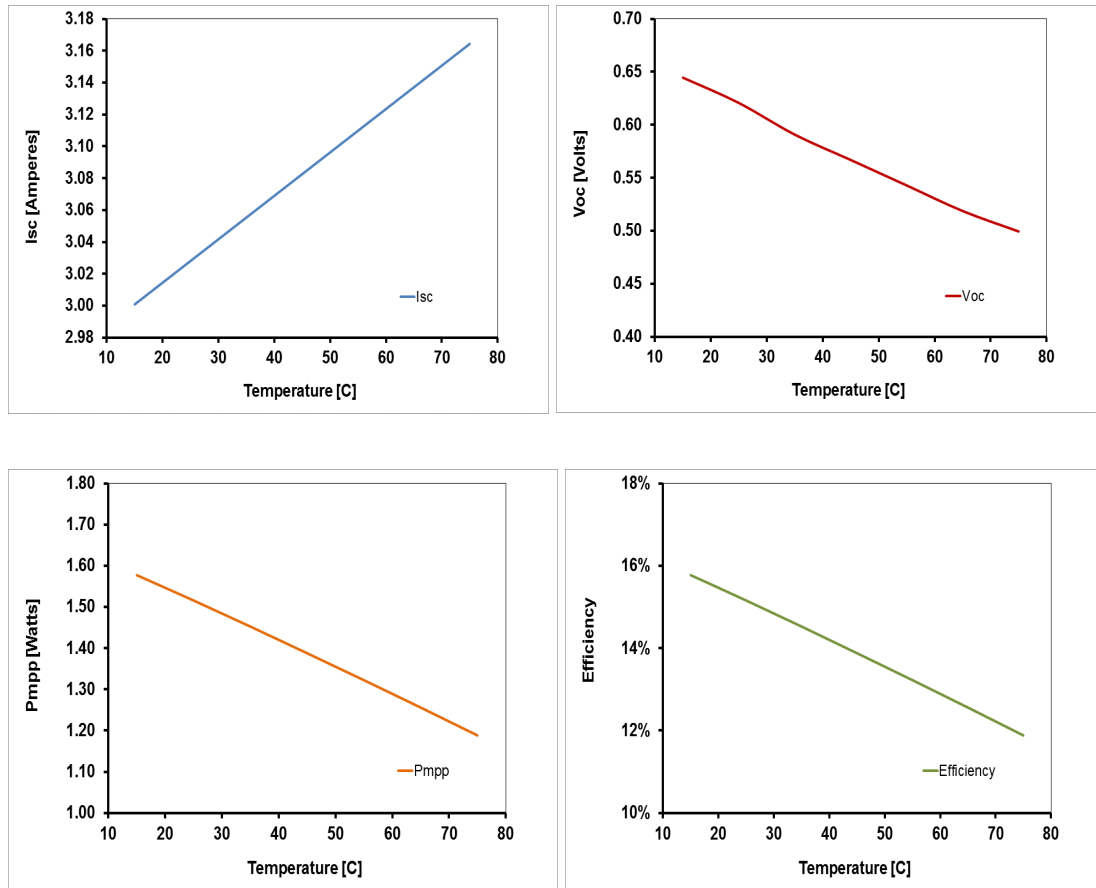
Figure 2.14: Effects of variations in temperatures on electrical performances of a solar cell

As shown in Figure 2.14, the open-circuit voltage decreases by 0.25% for every 1°C rise in temperature. The reduction in the power at the maximum point with an increase of 1°C in temperature is approximately by 0.65%. To avoid temperature effects on the open-circuit voltage and the short-circuit current of a tested PV device, the room temperature must be set at a fixed condition and the device temperature must be regulated using a temperature controller during the I-V measurement. In this way, the accurate I-V curve can be obtained as the device's temperature stays constant during the measurement.

2.3.3 Spectral Effects

Spectral irradiance is defined as the power density at a certain wavelength range of solar spectrum. It is given in units of $Watt.m^{-2}.nm^{-1}$ [5]. It is composed of X-rays, ultraviolet, visible light, infrared and radio waves. The distribution of the solar spectrum spans from 100 nm to about 1 mm. Based on the increasing order of wavelengths, the solar spectrum is classified into several regions as follows:

Regions	Wavelength range
Ultraviolet C (UVC)	100 to 280 nm
Ultraviolet B (UVB)	280 to 315 nm
Ultraviolet A (UVA)	315 to 400 nm
Visible light	380 to 780 nm
Infrared	700 nm to 10^3 nm

Table 2.1: Classification of spectral ranges [5]

Atmospheric elements such as air molecules, water vapour, dust, pollutants, ozone, oxygen and carbon dioxide affect the thickness of atmosphere and attenuate the amount of solar radiation reaching on the earth surface [38, 44, 45]. Air mass (AM) is used to quantify the thickness of the atmosphere. It is also defined as the distance the sunlight passes through. It is given in equation (2.16) [6]:

$$AM = \frac{1}{cos\,\theta} \qquad\qquad (2.16)$$

The angle between the point where the sun is exactly overhead (zenith) to the sun's position in the sky is denoted by θ and illustrated in Figure 2.15.
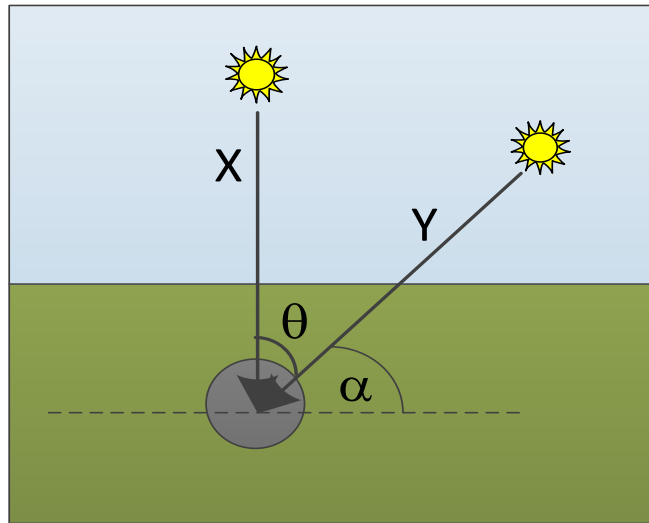
Figure 2.15: Illustration of the sun position in the sky and air mass calculation. X is the thickness of atmosphere; Y is the sun's position from horizontal and α is the altitude angle

Effects of the variations in air mass to the solar spectrum are shown in Figure 2.16. The solar spectrum at AM1.5g is a standard spectrum for measuring performance characteristics of a PV device [1, 46]. It is simulated when the sun is positioned at 48.2° from the zenith. The total irradiance over the entire wavelength range of spectrum AM1.5g is approximately 970 W.m^{-2}. The power density in the solar spectrum decreases as the air mass increases. The spectrum shifts toward the red range with increasing air mass as shown in Figure 2.16. The shift in the spectrum toward the long wavelength with increasing air mass reduces the generated photocurrent of a solar cell. How variations in the solar spectrum significantly affect the performance parameters of a PV device is shown Figure 2.17.
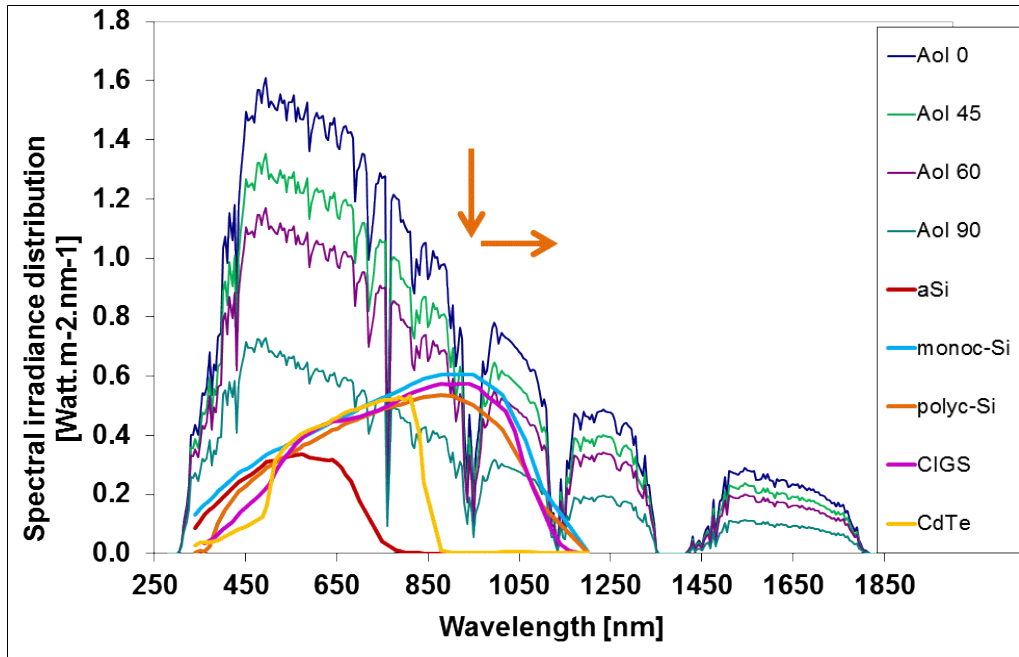
Figure 2.16: Variations in solar spectrum with air mass and their effects on the spectral response of different PV technologies
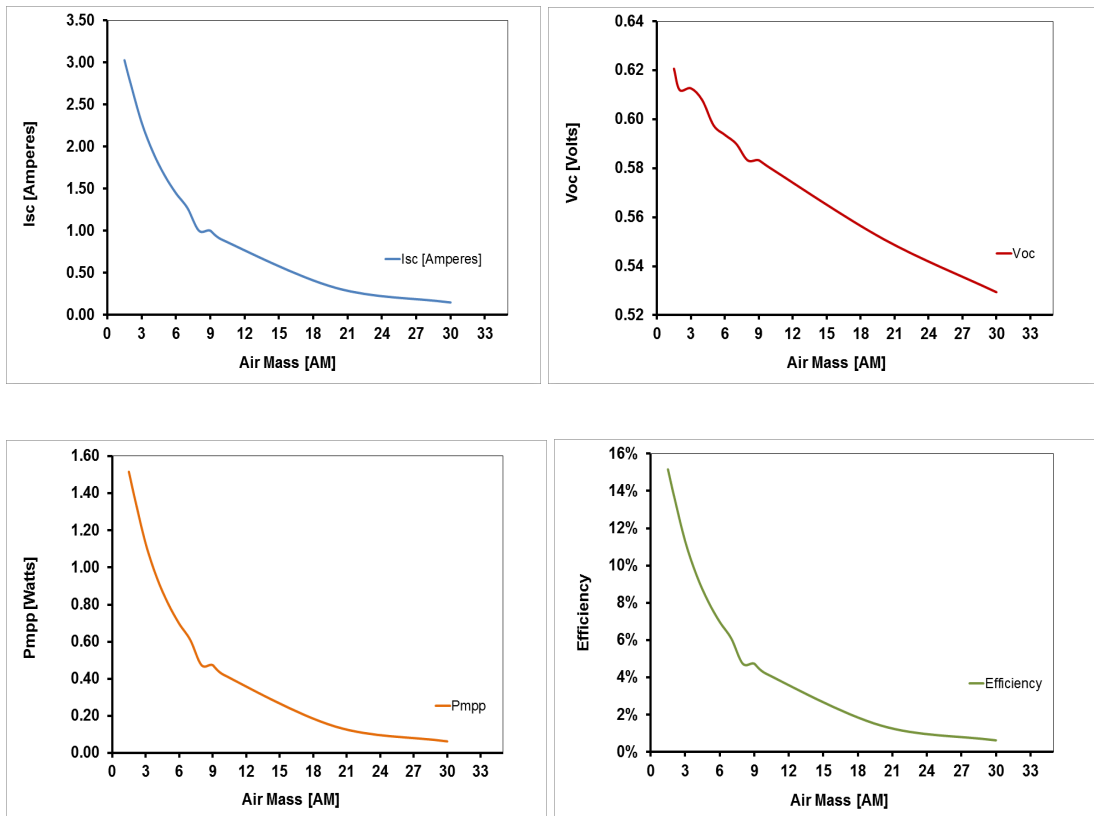
Figure 2.17: Changes in the current and voltage characteristic curves with air mass

43

As shown in Figure 2.17, all the electrical performance parameters reduce logarithmically with increasing air mass. Therefore, a correction factor is required for accurate current and voltage measurements if a tested PV device is measured indoor using a solar simulator which has different spectrum from a reference spectrum.

2.4. Performance Measurements of a PV Device

In this following section, two types of measurement methods are discussed for determining device characteristic parameters at certain operating conditions. These are the current and voltage characteristic and spectral response measurements.

2.4.1 I-V Characteristic Measurement

The current-voltage measurement is used to determine the performance parameters of a PV device at any specific environmental condition. A measurement at STC is currently used to retain a role in full performance characterisation as a normalising, or reference point.

The current-voltage (I-V) measurement system consists of a light source, power supply and a set of filters to reduce levels of irradiance; a monitor cell to measure irradiance incident on the measurement plane; a temperature sensor such as Pt100 to measure module temperature; a temperature controller to regulate the device temperature during the measurement; an electronic load to trace a full I-V curve; a current to voltage converter to record the current measurement and an adjustable measurement rig for mounting a tested PV device at certain angle of incidence. A schematic of the I-V measurement system is shown in Figure 2.18.
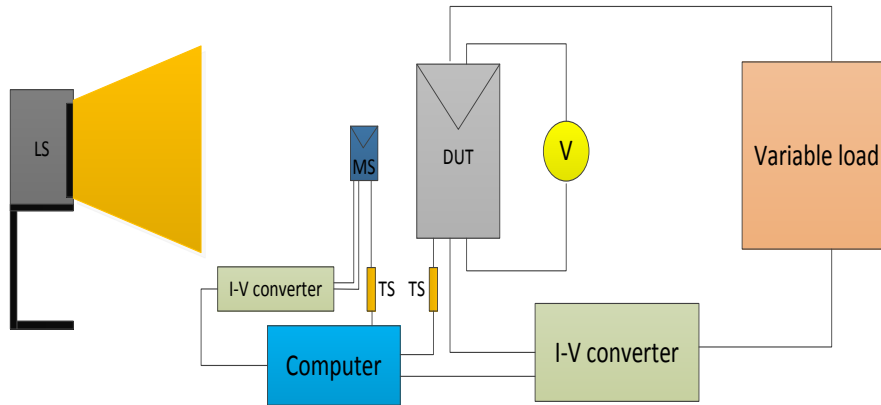
Figure 2.18: Layout of I-V measurement system, where MS is the monitor cell, TS is the temperature sensor and LS is the light source.

The procedures to perform the measurement of the I-V characteristic curve and requirement for test condition can be found in the standard IEC 60904-1 [47]. Before starting the I-V measurement, a tested PV device is mounted on a measurement plane and positioned perpendicularly toward the direct beam of a light source. A four-wire connection is used to connect the tested PV device to the measurement units as shown in Figure 2.18. The purpose of using the four wire connection is to eliminate losses along the cable in the current measurement and to obtain accurate voltage measurements [48]. The room temperature and irradiance are set and maintained at a fixed point during the I-V measurement. The device temperature is always monitored using temperature sensors that are attached at the rear surface of the tested PV device. To produce the full I-V curve when a tested PV device is illuminated, the current and voltage points of the tested PV device are varied using a variable load, which is connected in series with the tested PV device. There are several types of variable loads used in the I-V measurement, for example a variable resistor, a capacitor and a DC power supply. To measure a wide range of PV device's size and outputs, the variable load must have certain voltage and current ranges.

To obtain accurate performance parameters at STC, the light source that is used to simulate the sunlight in the I-V measurement needs to produce irradiance at 1000 W/m^2 and spectral irradiance at AM1.5 global as prescribed in the IEC standard 60904-1 [47] with a spectral range from 400 nm to 1100 nm. Other criteria that are required for accurate PV performance measurements are that the light source should

have stable and uniform irradiance intensity during the I-V measurement test with variations less than ± 2% over the measurement plane [49, 50].

These criteria are not ideal for a solar simulator. Most commercial solar simulators cannot fulfil these requirements to perform an accurate indoor testing for the I-V characteristic measurement of a PV device. Each lamp used in the solar simulator has a specific spectral shape, intensity and characteristics as shown in Figure 2.19.
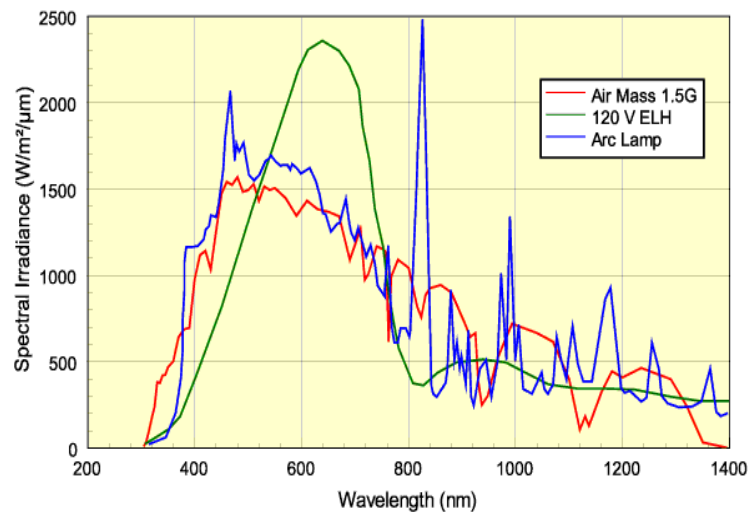
Figure 2.19: Light spectrum of typical solar simulators compared to a standard spectrum AM1.5g [51]

As it is apparent from Figure 2.19, the spectral irradiance that is produced from different light sources is far from matching the reference spectrum at AM1.5 global. According to the IEC standard 60904-9 for the spectral match, deviations in different spectral ranges of the light source's spectrum from the reference spectrum AM1.5 global should be within the following criteria [49]:

No.	Wavelength range in nm	Per cent of total irradiance
1	400 – 500	18,4
2	500 – 600	19,9
3	600 – 700	18,4
4	700 – 800	14,9
5	800 – 900	12,5
6	900 – 1100	15,95

Table 2.2: Specification required for matching spectrum AM1.5 defined for six wavelength intervals from 400 nm to 1100 nm

46

The tolerance for the percentages of the total defined irradiance are given in Table 3.3 If the I-V measurement is performed at STC, any deviations from the STC are considered as errors in the measurement and these contribute to measurement uncertainty. The most common error in the I-V measurement is the spectral mismatch error. As the light source's spectrum changes with pulse duration, lamp power and operation time, the mismatch between the light source's spectrum and the reference spectrum increases [50]. This spectral mismatch error affects the accuracy of the measured power at the maximum power point indoor. By applying the spectral mismatch correction factor [52] to the measured short-circuit current, the power measurement indoor is corrected. The calculation of the spectral mismatch factor is written as explained in the standard IEC 60904-7 [53, 54]:

$$MM = \frac{\int_{\lambda1}^{\lambda2} E_{ref}(\lambda)SR_{ref}(\lambda)d\lambda \int_{\lambda1}^{\lambda2} E_{sim}(\lambda)SR_{DUT}(\lambda)d\lambda}{\int_{\lambda1}^{\lambda2} E_{sim}(\lambda)SR_{ref}d\lambda \int_{\lambda1}^{\lambda2} E_{ref}SR_{DUT}(\lambda)d\lambda} \qquad (2.17)$$

As shown in equation (2.17), the calculation of spectral mismatch factor requires information of spectral response (SR) of a PV device under test (DUT) and the spectral irradiance of a light source. Providing the device's spectral response data is quite challenging [55] as it is not available from the device specification sheet because of measuring spectral response of a large-area PV module is still quite difficult and expensive. Therefore the spectral mismatch factor (MM) is still assumed unity because of the difficulty in obtaining the information of the device's spectral response data [48]. Using this assumption for the spectral mismatch factor can introduce a major deviation in the device's power at the maximum power point between the indoor and outdoor measurement as reported by Virtuani [11].

Other factors influencing the accuracy of the I-V characteristic parameters are variations in the spatial uniformity of irradiance with time, particularly for a continuous arc lamp solar simulator; temperature errors due to the temperature difference between the back surface of a PV device and the PV device itself, which is normally higher than the temperature at the back surface [48]; and variations in the cells' temperature in a PV module. For typical crystalline silicon devices, the temperature error is up to 2.5°C during the I-V measurement. Unstable cell

temperature affects the open-circuit voltage of a PV device under test, as have been mentioned in section 2.3.2.

The non-uniformity of irradiance on a measurement plane can be known by dividing area of the measurement plane into small areas and measuring the irradiance falling onto each area using irradiance sensors. Taking the ratio of the difference between the maximum and minimum irradiances to their total values, the spatial non-uniformity irradiance on the measurement plane is determined as shown in equation 2.18. [49]:

$$Non - uniformity(\%) = \left[\frac{maximum\ irradiance - minimum\ irradiance}{maximum\ irradiance + minimum\ irradiance}\right] x100\% \qquad (2.18)$$

The temporal instability of the irradiance at a measurement plane is obtained by measuring the irradiance falling onto the measurement plane over certain period of time. The calculation of the irradiance temporal instability is shown in equation 2.19.

$$Temporal\ instability(\%) = \left[\frac{maximum\ irradiance - minimum\ irradiance}{maximum\ irradiance + minimum\ irradiance}\right] x100 \qquad (2.19)$$

Here, the maximum and minimum irradiance are the measured irradiance over the measurement plane.

Apart from the temperature error and the spatial non-uniformity, the accuracy of the I-V measurement depends on the temporal instability and an illumination time of a light source. Therefore, the solar simulator that is used for simulating the natural sunlight in the I-V measurement test should meet the criteria as elaborated in the standard IEC 60904-9 [49]. Based on the criteria mentioned in the standard IEC 60904-9, commercial solar simulators are rated into different classes as shown in Table 2.3.

Characteristics	Tolerance		
	Class A	Class B	Class C
Spectral match	0.75 – 1.25	0.6 – 1.4	0.4 – 2.0
Non-uniformity of irradiance	± 2 %	± 5 %	± 10 %
Temporal instability			
- Short term	± 0.5 %	± 2 %	± 10 %
- Long term	± 2 %	± 5 %	± 10 %

Table 2 3: Classification of commercial solar simulators based on the spectral match, uniformity and temporal instability [49]

The least criteria that a solar simulator should have for the performance measurements of a terrestrial PV device is CBA, which means that a solar simulator must meet class C for spectral match, class B for irradiance uniformity and class A for temporal instability. To characterize PV performance parameters at STC, the solar simulator should produce an effective irradiance of 1000 $W.m^{-2}$ at the measurement plane and meet criteria required for matching spectrum AM1.5g as shown in Table 2.2 [1].

The following section will discuss the measurement of spectral response of a PV device.

2.4.2 Spectral Response Measurement

As has been mentioned in the previous section, SR of a PV device is one of important parameters in the spectral mismatch correction calculation. It is also used as a tool to estimate diffusion length of minority carriers, the optical losses due to encapsulation [56], to determine surface recombination velocity and layer thickness of a solar cell [57, 58] and to understand the current generation, recombination and diffusion mechanism in a PV device [59]. SR of a PV device is usually represented as function of wavelength (λ) in units of $A.W^{-1}$ [6] as shown in Figure 2.20.
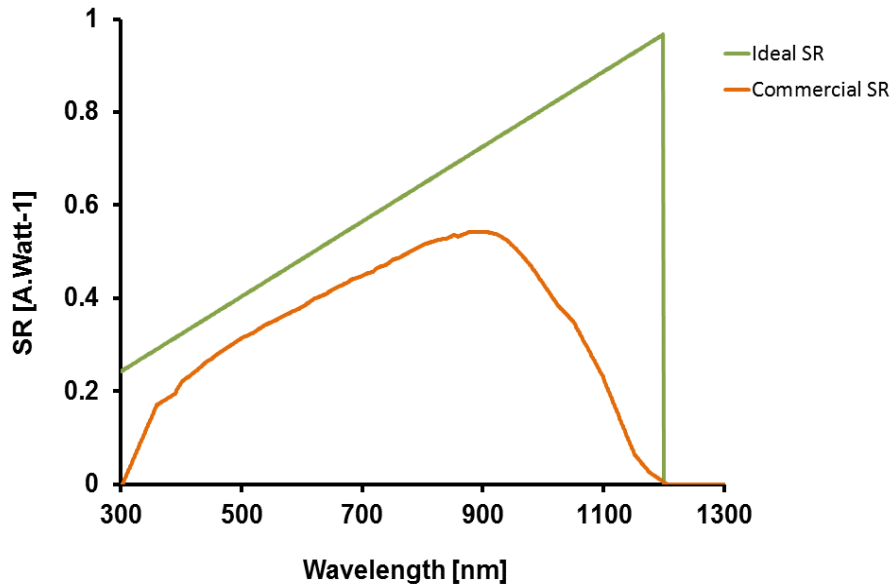
Figure 2.20: Spectral response of a typical PV device

Ideally, each incoming photon should produce one electron-hole pair. However, only higher energy photons or photons with energy levels equal to the band gap energy of a typical PV device can generate electron-hole pairs [6]. When the light enters a solar cell, its irradiance is reduced before reaching the absorber layer due to reflection on the front surface such as glass and transparent conducting oxide (TCO) and absorption in the window layer and TCO. These two losses are known as the optical losses. These losses influence the shape of SR curves of commercial PV devices. Therefore, it is not as perfect as the ideal SR curve as shown in Figure 2.20. Another factor influencing the shape of the SR curve is the electronic losses which occur due to recombination in the absorber layer [60]. These two types of losses can be distinguished from one another by measuring the spectral response of a solar cell at different voltage biases. Only electronic losses are affected with variations in the applied voltage bias.

SR curves of different PV technologies are shown in Figure 2.21.
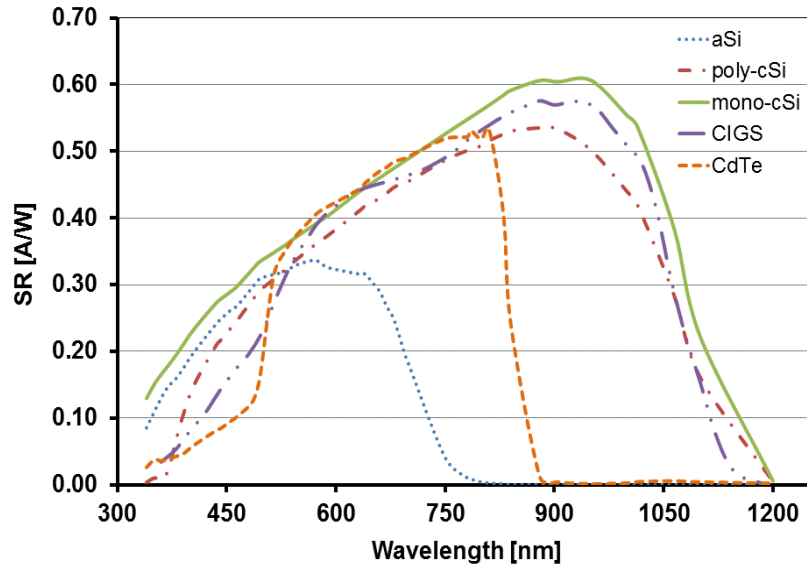
Figure 2.21: Spectral response curves of different PV devices

As shown in Figure 2.21, the cut-off at long wavelengths is specific for different PV technologies. These differences are related to the band gap energy of the absorber material used to fabricate a PV device.

Spectral response of a typical PV device is determined by illuminating the device under test with a series of different wavelength spectrum and concurrently measuring the short-circuit currents generated under the measured wavelength and their corresponding irradiances [47]. By dividing the currents to their corresponding irradiance at a given wavelength as shown in equation (2.20), SR of a tested PV device is determined. Another way to express the response of a PV device toward solar spectrum is using quantum efficiency (QE) which is a measure of collection efficiency of electron and holes generated from incoming photons as given in equation (2.21).

$$SR(\lambda) = \frac{I_{sc}(\lambda)}{P_{in}(\lambda)} \qquad (2.20)$$

$$QE(\lambda) = \frac{qSR(\lambda)}{\lambda hc} \qquad (2.21)$$

To obtain an accurate SR determination, the SR measurement must be performed under a controlled temperature condition (at 25°C in the IEC standard) [61], stable and uniform irradiance as stated in the standard IEC 60904-8 [47] and at the short-circuit current [59]. This is due to certain PV technologies, such as amorphous

51

silicon, exhibit temperature dependent spectral response behaviour [61]. Variations in these conditions introduce some uncertainties into the SR measurement as shown in [48]. Specific wavelength spectrum with certain bandwidth size can be provided by using different methods such as a grating monochromator system [58, 59], LED bias lighting system [62-65] filter based methods [56, 58, 66, 67] and using a tuneable laser system [68]. The monochromator system can produce high resolution of monochromatic wavelengths within 1 nm interval step. The narrow wavelengths produced from the filter system have a bandwidth larger than the monochromator system, within 20 nm to 50 nm. The LED system produces a monochromatic wavelength larger than that of the monochromator system, which results in higher beam intensity and wider beam size on the test area. As a consequence, a small-area PV device can be illuminated fully for the SR measurement. From different SR measurement methods, the filter method is widely used for determining the spectral response of PV devices. The layout of a typical SR measurement system using the filter-base method is shown in Figure 2.22.
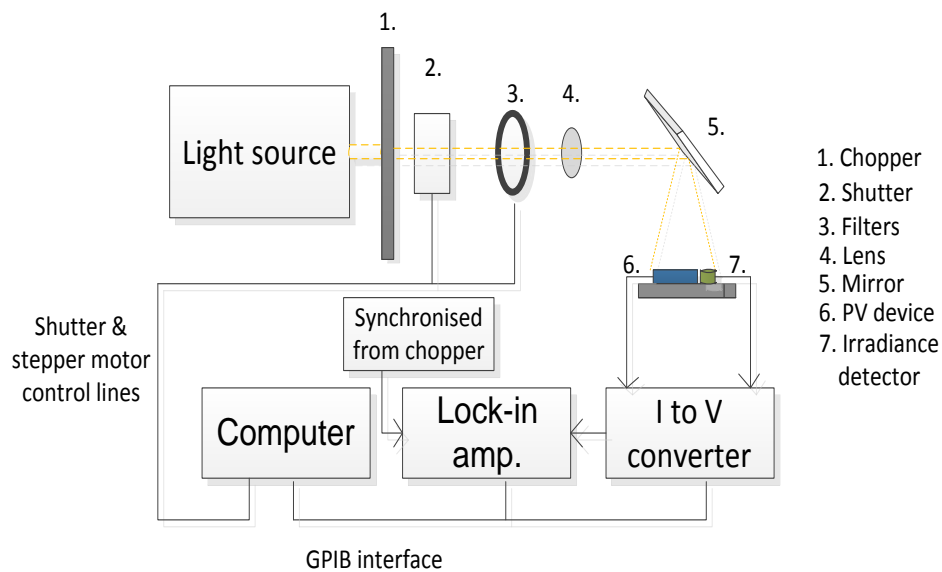
Figure 2.22: Diagram of a typical SR measurement system using a filter system

The photocurrent generated by the tested PV device is measured using the current to voltage converter method. A lock-in amplifier is used to detect the measured response signal by locking it into the specific frequency that is provided by a chopper [57]. This lock-in technique enables the measured voltage signal to be distinguished

from other signals produced from other light sources. The reference detector is used as an irradiance detector to measure irradiance falling onto the device under test. Finally, the spectral response of the tested solar cell is calculated by comparing two photocurrent signals generated by the tested solar cell and the calibrated reference solar cell as expressed in equation (2.22) [69].

$$SR_{DUT}(\lambda) = \frac{A_{ref}I_{sc,DUT}(\lambda)}{A_{DUT}I_{sc,ref}(\lambda)}SR_{ref}(\lambda) \qquad (2.22)$$

Certain PV devices exhibit a non-linear behaviour when they are exposed to low irradiance conditions [70] as a result of trapping of minority carriers in the junction layer and recombination. As a consequence, the current that is generated at low irradiance levels is not proportional to the irradiance level. To overcome the non-linearity problem and to eliminate errors in the spectral response measurement, bias lighting is applied for measuring spectral response of single-junction PV devices. The bias lighting is used to saturate defect states in the PV device under test to produce high minority carrier densities by injecting high irradiance power to the measured cell [71].

Measuring SR of a multi-junction PV device, which has individual sub-cells connected optically and electronically in series with only two output terminals, is slightly different from that of single-junction PV devices. Spectral response of each individual sub-cell must be determined separately as they have different spectral response toward the solar spectrum. Since there is no access to measure each sub-cell, the application of different colours of bias lighting and voltage bias are required to probe the measured sub-cell and to ensure the operating voltage of the limiting sub-cell at the short-circuit condition as the operating point of their I-V curve is dependent on each other [18, 72]. The bias lighting is used to saturate one sub-cell in order to measure other sub-cells. For example; to measure the spectral response of the top cell of a tandem solar cell, red light is applied to the tandem cell. In this way, the bottom cell will absorb most of the red light and becomes saturated. The blue light which is absorbed mostly by the top cell is applied to measure the spectral response of the bottom cell. If only blue light is given to saturate the top cell, the bottom cell produces almost zero current as the blue light is completely absorbed by

the top cell or vice versa. This will produce nearly no current from the tandem cell. As a result, there is no spectral response curve obtained from the measurement. Therefore, an adjustment in the intensity of the bias lighting is necessary in order to assure that the current of the limiting sub-cell can be measured. There is no a standardised rule describing how to apply appropriate colours of bias lighting to probe one measured sub-cell in the multi-junction structure [16, 17]. However, one approach which has been proposed by Burdick has been adopted for the application of bias lighting and voltage bias for measuring SR of different sub-cells in a MJ PV device as follows [18]:

$$I_{sc,meas-subcell} = 0.5 I_{sc,str-subcell} \qquad (2.23)$$

$$V_{bias} = ((n-1)/n) \cdot V_{oc,MJ} \qquad (2.24)$$

In those equations the intensity of the bias lighting should be regulated until the short-circuit current of the measured sub-cell ($I_{sc,meas-subcell}$) is equal to one half the short-circuit current of the unmeasured sub-cell ($I_{sc,str-subcell}$), while the application of voltage bias should be adjusted to the number of cells in series (n) and the total open-circuit voltage of the MJ cell as shown in equation (2.24).

Accuracy in the SR determinations depends on how far the error sources in the SR measurement can be eliminated. Errors in the SR measurement using the monochromatic filter method can be contributed from different sources: a finite photocurrent response time, bandwidth of the monochromatic light, waveform of the monochromatic light, the spatial uniformity of the monochromatic and bias lighting [59]. The magnitude of these errors depends on PV technologies, light source and measurement system. These error sources can be classified into two major contributors: the photocurrent measurement and the light power measurement [48]. Errors in the current measurement can be contributed by electrical instrumentation such as the current to voltage converter, the PV device under test, and the mechanical movement of the optics [59]. The errors in the irradiance measurement can be sourced from the fluctuation in the intensity of the light source, the stored calibration file, stray light, and the calibration of the detector's spectral response [59]. Errors associated with the application of monochromatic beams are the bandwidth, the filter defects, the polarisation variation with wavelength, the wavelength offset, the

wavelength variation with temperature, the beam wanders with wavelength, the beam larger than the tested device, and the beam smaller than the detector and device area [59].

The effects of the uncertainty in the current and irradiance measurements on the spectral response of a tested PV device can be analysed by varying their uncertainty levels at different wavelengths of the device's spectral interest as shown in Figure 2.23. The uncertainty in the irradiance measurement is represented by the uncertainty in the detector's current measurement as this device is used to measure the irradiance on the measurement plane.
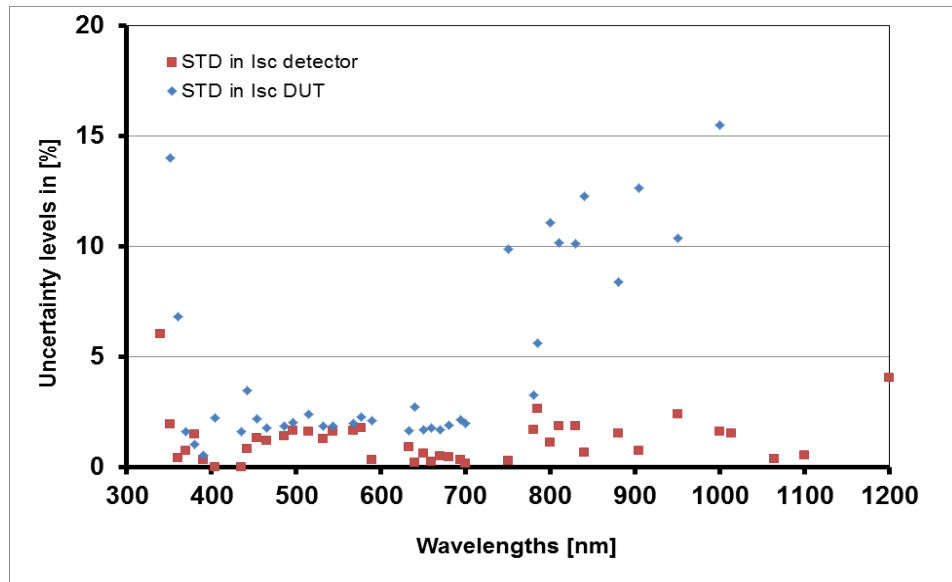
Figure 2.23: Uncertainty levels in the current measurements of a tested PV device and irradiance detector

The sensitivity of those uncertainty contributors to the total uncertainty of device's spectral response is analysed individually. Figure 2.24 shows the effects of the increase in the uncertainty levels of the device's current measurement on the spectral response curve of a tested PV device It is apparent that the spectral response curve of a tested PV device can be overestimated with the increase in the uncertainty levels of the device's current measurement particularly at the red end of the curve. The shift in the spectral response curve is significant up to 3% higher than its true SR curve when the uncertainty level in the device current measurement increases by 10 times from its initial uncertainty level.
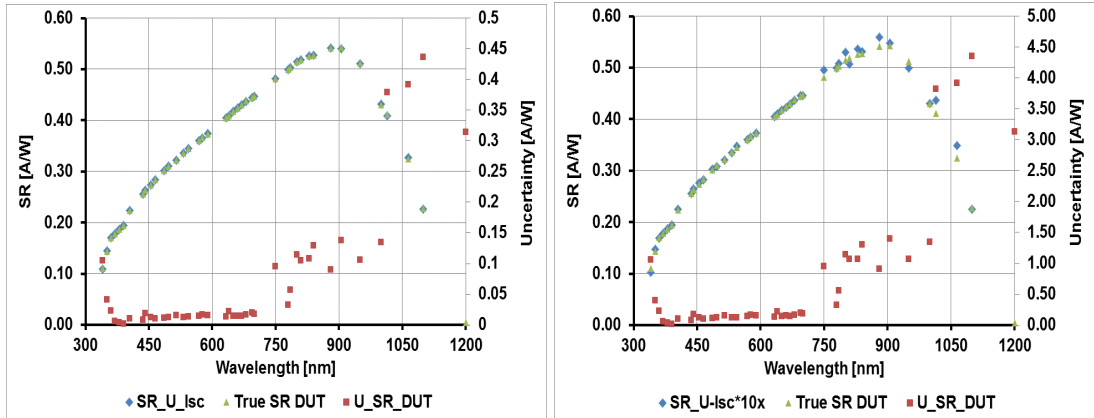
Figure 2.24: Impacts of uncertainty in the tested device's current measurements at a given monochromatic filter on the spectral response curve of a tested PV device

Similarly, the increase in the uncertainty levels of the detector's current measurement can also overestimate the spectral response curve of a tested PV device by approximately 2% at the red region when it is increased 10 times from its initial level as shown in Figure 2.25.
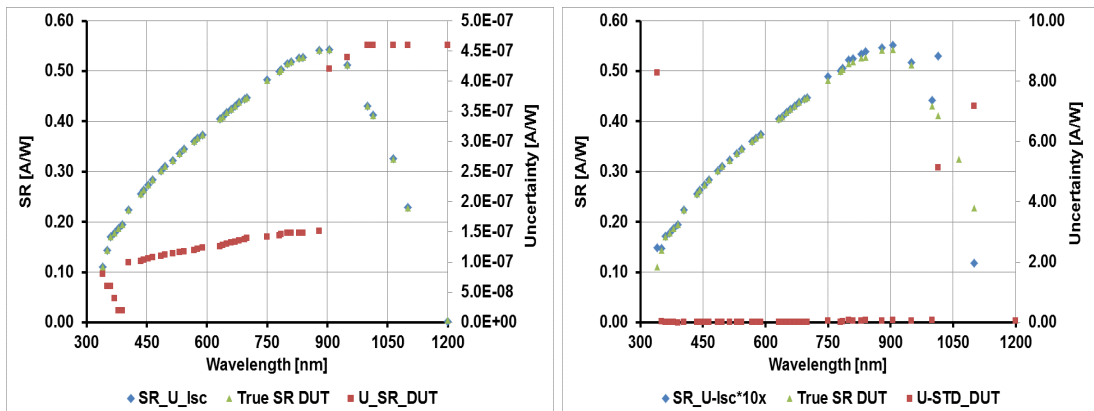
Figure 2.25: Impacts of uncertainty in the detector's current measurements at a given monochromatic filter on the spectral response curve of a tested PV device

An accurate spectral response determination is very important for calculating a precise spectral mismatch correction factor. Therefore, minimising uncertainty in the SR measurement is necessary such as by ensuring the non-uniformity of irradiance on the measurement plane should be less than ±2%, particularly when a tested PV device and a reference solar cell have different dimensions [4]. As the quality of the monochromatic beams which are produced from narrow band pass filters depends on their filter transmittances, special concerns should be given to their spectral

56

transmittances which should be checked periodically to identify any changes in their spectral bandwidth. To obtain accurate current measurements, the calibration of the resistors and their contact resistances also need to be checked periodically to ensure that it is still within its calibration value. Furthermore, the short-circuit current of a PV device should have a linear response with all irradiance levels at given wavelengths.

2.5. Conclusions

Since the short-circuit current of a PV device is one of important input parameters in the energy yield prediction method, measuring it under simulated sunlight using a solar simulator needs to be corrected for a spectral mismatch which is between the spectrum produced from a solar simulator and the reference spectrum. A reliable SR determination is essential for accurate spectral mismatch computation. Therefore errors associated with the SR measurement should be minimised. The significant error is contributed by lower irradiance of a typical monochromatic beam on a measurement plane. Therefore high irradiance is required to improve the signal strength of the tested PV device.

Having understood the fundamental knowledge about the characteristics of PV devices under different environmental conditions and their measurement techniques, the following chapter will explain specific problems related to the spectral response measurement of a PV device and introduce a new technique for measuring spectral response of a PV device.

Chapter 3

A New Spectral Response Measurement Approach

3.1. Introduction

This chapter introduces a new concept for determining the spectral response (SR) of a photovoltaic (PV) device. The approach is explained in detail in section 3.2 following a review of the different existing measurement techniques for obtaining spectral response. As the new approach requires a model of the spectral response, different existing mathematical models to represent spectral response are reviewed in section 3.3. The section also includes a newly-proposed model which exhibits some advantages over those existing. Section 3.4 explains the fitting algorithm required with the new proposed method. The types of filters and other hardware requirements of the new approach are discussed in section 3.5. To verify whether the proposed approach is feasible for its intended application, a software simulation is developed. These proof-of-concept results are presented in section 3.6. The chapter ends with the conclusions of the feasibility of the new approach.

3.2. A New Concept of SR Measurement Method

Currently, the measurement techniques for obtaining the spectral response of a PV device are broadly described in the international IEC standard 60904-8: Measurement of spectral response of a PV device [4]. The IEC standard only provides general procedures on how to perform an accurate spectral response measurement. Its application is limited to measuring the spectral response of single-junction PV devices. According to the IEC standard, beams of the light source projected onto a PV device under test (DUT) should have a narrow bandwidth of

wavelengths. These monochromatic beams must cover the entire range of spectral interest of the DUT with a wavelength step less than 50 nm. The crucial requirements for the monochromatic beams are their intensity, uniformity and stability during the spectral response measurement period. The non-uniform illumination of the monochromatic beams can lead to a systematic error in the spectral response determination as different levels of irradiances produce different responses [73]. Based on these provisions, the IEC standard describes two types of spectral response monochromatic measurement techniques. These are the grating monochromator and the filter-based method, as have been described in the previous chapter.

The benefit of using a grating monochromator system for spectral response measurement is that a high wavelength resolution can be achieved. However, there are some significant challenges encountered: low beam intensities, small beam size on the measurement plane; poor beam uniformity, and polarisation effects [57]. The small beam size is only able to illuminate a tiny spot on the active area of a tested PV device. Enlarging the beam size using optics does not increase the signal strength but can reduce the homogeneity of illumination on the measurement plane. As a result, the signal-to-noise ratios are still low and this contributes to high measurement uncertainty. Therefore, the grating-based method is only suitable for measuring spectral response of small-area PV devices.

The filter-based method can provide a larger beam size over a measurement plane, higher beam intensities and better uniformity than the grating-based method. Hence, it can be used to measure spectral response of larger-area PV devices. However, there are some problems associated with the application of optical filters, such as stray light, shape and width errors [74] and inflexibility in choosing a specific wavelength of interest [57]. The width errors are produced when narrow band pass filters with asymmetric transmittances around the centre wavelength are used, particularly around the lamp emission peaks as shown in Figure 3.1.
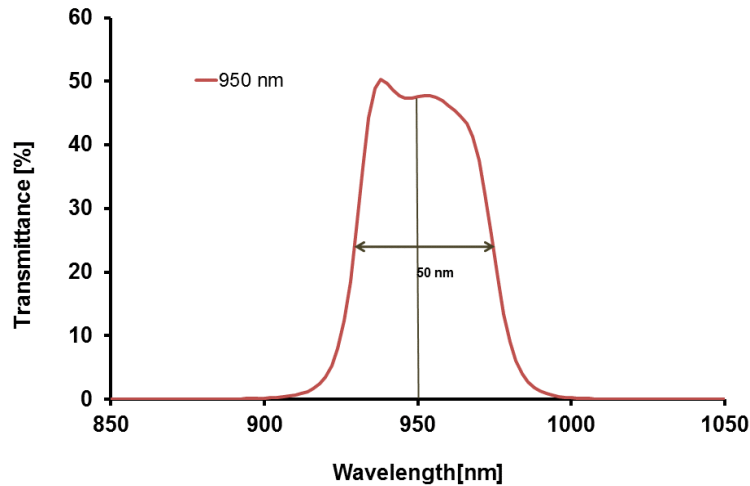
Figure 3.1: Asymmetric shape of the spectral transmittance of a narrow band pass filter with a bandwidth of 50 nm at FWHM

In such conditions, the response signal is not representative of the given wavelength (the centre wavelength of the measured filter). The effect of these width errors becomes prominent if the bandwidth of the asymmetric filter is greater than 10 nm [74]. Reducing the bandwidth of the monochromatic light reduces these errors, but also decreases the irradiance transmitted by the filter. If a filter with a narrow bandwidth is used in the ultraviolet (UV) or near infrared ranges, where the response signal generated by the DUT is very weak, the response signal becomes difficult to be detected even by a lock-in amplifier, due to the very low signal-to-noise ratio.

Stability problems can be also exhibited as a consequence of extended exposure to the UV radiation from the light source and environmental stress (temperature and humidity), resulting in deviation of the centre wavelength of the filter transmittance [57]. The filters also have a finite transmittance in the spectral region outside the transmittance peak and may yield variations in the angle of incidence of the monochromatic beam projected onto the tested PV device [58, 75, 76]. Overall, typical uncertainty levels in the spectral response determination are shown in Figure 3.2.
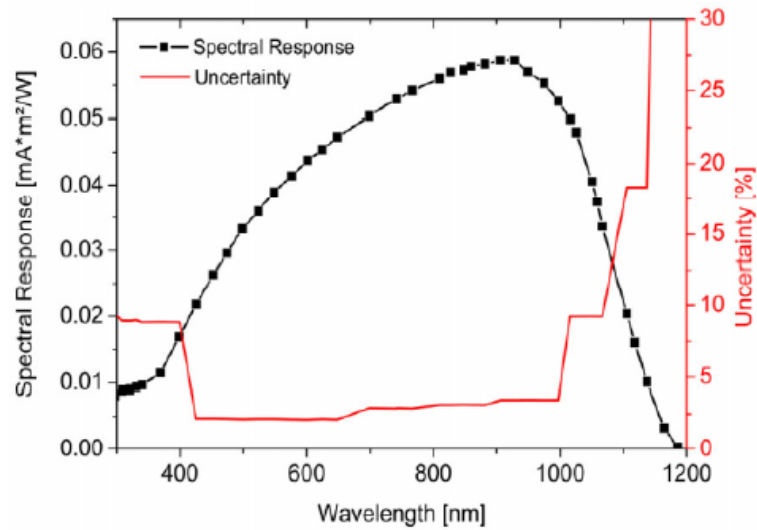
Figure 3.2: Uncertainty in spectral response determination using the filter-based method [77]

Methods of SR determinations based on the light emitting diodes (LEDs) have been developed as an alternative to spectral filtering of a broad band light source [62, 64, 65, 78]. Due to the limited variations of the centre wavelengths of LEDs [62] and the broad spectral bands [79], the spectral response of a tested PV device cannot be determined directly as for the truly monochromatic methods. The complete spectral response of a tested PV device must be obtained through a fitting process, by tuning a theoretical photocurrent formula to the measured currents. The current calculation requires a suitable spectral response model and spectra. Problems encountered using the LED-based method are the inhomogeneity, weak intensity and broad spectral bandwidth of their output. Despite this, interest in using LEDs for a solar simulator is increasing [79].

The last option for spectral response measurement is using electroluminescence (EL) spectroscopy [80]. In this method, spectral response of a PV device is measured by injecting current with a certain intensity level to a tested PV device whilst recording the light emission generated from the tested PV device by using spectrograph. Therefore, the EL technique requires a high precision current source for electrical excitation; as well as temperature controller and spectro-radiometer to collect and analyse the emitted luminescence. An issue related to this measurement technique is the poor quality of the EL signal at high current injection.

Of the existing spectral response measurement methods, the filter-based method is the most widely used. This is due to the intensity and uniformity of the monochromatic beams being much better than that of other methods. However, there are some problems associating with this spectral response method as have been mentioned earlier that are summarised in the following table.

SR measurement method	Strengths	Weaknesses	Applications
Monochromator system	- High wavelength resolution up to 1 nm - Continuous change in incident wavelength - Flexible wavelength selection	- Low beam intensity - Small beam size - Poor beam uniformity - Polarisation effect	Small-area PV devices
Filter-based system	- Larger beam size (10-50 nm) - Higher beam intensity and better uniformity than the monochromator system	- Stray light - Shape and width errors - Low signal to noise ratio at certain wavelength regions	Small-area and large-area PV devices
LED system	- A wavelength scan without requiring a filter or monochromator - No mechanical chopper - Irradiance throughput can be easily increased by adding more LED in the same type	- Lack of available LEDs at some wavelength range - Weak intensity - Inhomogeneity - Broad spectral range (50 nm to 150 nm)	Small area PV devices

Table 3.1: Different spectral response determination methods

To obtain highly accurate SR determinations, an ideal spectral response measurement system should have the following features:

1. Large beam size which is enough to cover the entire surface of any size of PV devices from small with a dimension less than approximately 100 by 100 mm^2 up to 2 m,

2. High spatial uniformity of the beam on the measurement plane with the non-uniformity of ±2% (Class A) [47, 49, 81],

3. High irradiance (greater than 100 Watt/m^2) radiating on the measurement plane [61],

4. High accuracy in the current measurement with uncertainty ±0.2% [47],

5. Stable device temperature at 25±0.5°C [47]

6. The mounting plane should be perpendicular to the beam direction with angle of incidence within ±10°[47].

Therefore, aiming to improve the accuracy of the filter-based method and to fulfil the features of the ideal spectral response measurement system, a new spectral response measurement technique is introduced here: the **polychromatic spectral response fitting method** or in short, '**the polychromatic method**'. The proposed spectral response method utilises polychromatic filters instead of monochromatic filters to provide higher irradiance and larger beam size on the measurement plane. As a consequence, the response signal produced by the tested PV device becomes higher and can be detected easily by any high precision current measurement devices. Hence, the lock-in technique is not necessary and the bias lighting can be eliminated for single-junction device measurements. This makes the spectral response measurement system simple.

The proposed method requires spectral variations of the light source. The variations are not monochromatic, but must affect different wavelength regions of the response band of the device being tested. Spectral variations can be obtained by using coloured filters with different broad spectral bandwidths. The advantages of using these types of filters are that the output beam intensity is much higher than that of using the narrow band filters and problems associated with the width and shape errors are no longer relevant. The new method offers a much simplified measurement setup for measuring the spectral response. To do this, it needs a precision current meter to measure the current produced by the device under illumination by a given

filtered spectrum; a high-accuracy spectro-radiometer to record the spectral irradiance transmitted by a given filter; polychromatic filters to provide different spectra; and a broadband and stable light source of reasonable intensity, ideally meeting solar simulator classification.

The proposed method draws on the photocurrent formula as shown in equation (3.1).

$$I_{sc} = A \int_{\lambda_1}^{\lambda_2} SR\,(\lambda) \cdot E(\lambda)d\lambda \qquad\qquad (3.1)$$

Knowledge of the measured currents generated by the PV device and the corresponding spectral irradiance, the spectral response of the tested PV device can be determined. Although it cannot be directly calculated by rearranging the short-circuit current formula above, it can be determined by representing the spectral response with a model and tuning the coefficients to minimise overall deviations between the modelled and measured data set. By assuming there is no change in the spectral response (due to varying irradiance and temperature during the spectral response characterisation test), the fitting process works iteratively to find the appropriate coefficients of a chosen spectral response model by fitting the measured short-circuit currents to the calculated short-circuit currents under different spectra. The success of the approach depends significantly on the chosen spectral response model and the fitting algorithm. Selection of a suitable model for representing the spectral response of different PV technologies is discussed in the following section.

3.3.   Selecting a Suitable Spectral Response Model

The spectral response model plays a central role in the polychromatic spectral response fitting method. If the model is unsuitable, the spectral response cannot be obtained accurately. The suitability of the model is determined based on the *goodness-of–fit* tests which represent how well the model fits the measured data points, and their compatibility for fitting the spectral response curves of a range of different PV technologies.

The complexity of published spectral response models varies from simple empirical shape fitting to physics-based opto-electrical models that require many input

parameters and knowledge of device structure. Of these, Schade et al. [82] developed a model for calculating quantum efficiency of an amorphous silicon device based on the cell geometry and materials. This model is used to optimise optical designs of amorphous silicon solar cells. The model requires knowledge of optical properties of all layers in the solar cell such as absorption parameters and film thicknesses. The quantum efficiency is modelled by assuming that every photon that is absorbed in the i-layer generates a carrier. The incident photons that are absorbed in other layers in the solar cell are counted as lost. The spectral response is derived from the modelled quantum efficiency (QE) as written in equation (3.2).

$$QE(\lambda) = [1 - A_{CTO}(\lambda)][1 - A_p(\lambda)][A_i(\lambda)] \qquad (3.2)$$

Where $A(\lambda)$ is the absorbance of different layers in a PV device. It is defined as:

$$A(\lambda) = 1 - exp[-\alpha(\lambda)d] \qquad (3.3)$$

As seen in equation (3.2), the model requires information on the absorption characteristics and thicknesses of different layers in the device. The advantage of using a physical model is that the effect of modifying these layers on the cell performance can be assessed. However, these properties are rarely available in practice and so such a model is not easily applied for the purpose of spectral response determination of an unknown device.

A spectral response model based on device structure has been adopted also by Koyanagi et al. from TUAT [63] to improve the spectral response determination of a crystalline silicon solar cell obtained from their LED-based experimental method. The model requires knowledge of internal reflection and absorption features of different layers in a mono-crystalline PV device such as glass and ethylene vinyl acetate (EVA), n-layer, p-layer, depletion layer and back surface reflection. The transmission, reflection or current response of each layer at a given wavelength λ is modelled as shown in equation (3.4):

$$f(\lambda) = 1 - \frac{1}{1 + e^{\frac{\lambda - \lambda_0}{a}}} \qquad (3.4)$$

Where $f(\lambda)$ is function of absorption, a is the rate of change, λ is centre wavelength of absorption.

The total spectral response is then determined by adding the spectral response of all different active layers which is determined by integrating their individual's function of absorption as shown in Figure 3.3.
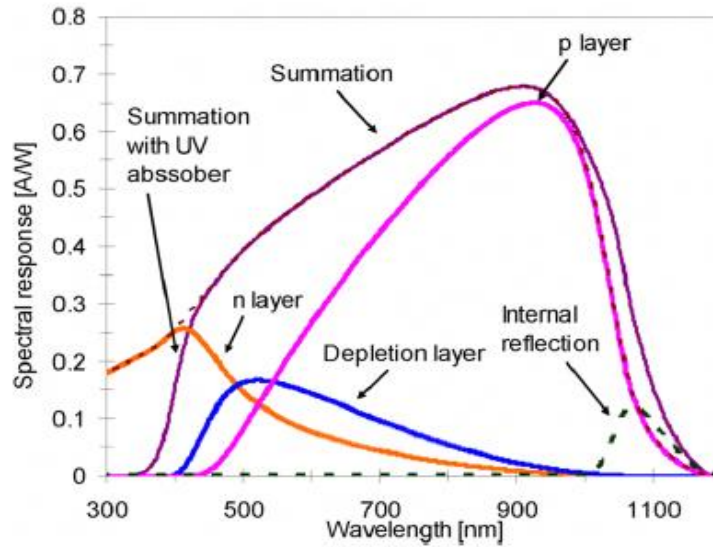
Figure 3.3: Summation of spectral response of each layer using the absorption feature spectral response model [64]

Again, if an absorption feature model is used to determine a spectral response curve of other PV technologies, prior knowledge of the device structure and cell parameters is needed in order to formulate the total photocurrent generated. As a result, different PV devices require different absorption feature models and this is undesirable for the proposed spectral response method, for which a generic, simple and robust model is desired.

Inspired by the absorption feature model, a simplified **exponential quantum efficiency** (EQE) model was developed by Bliss from CREST [65]. The model consists of seven unknown parameters. In this model, a PV device is considered as a package containing a glass layer, ethylene vinyl acetate (EVA), and an absorber layer. The total EQE of a PV device is modelled in equation (3.5).

$$EQE(\lambda) = \frac{1}{P_1 + exp\left(\frac{\lambda - P_2}{P_3}\right)} \cdot \left[\frac{1}{1 + exp\left(\frac{\lambda - P_4}{P_5}\right)} - \frac{1}{1 + exp\left(\frac{\lambda - P_6}{P_7}\right)}\right] \qquad (3.5)$$

It is considered as an empirical based model where P_1 to P_3 are the absorption and reflection losses at the front glass and encapsulation layer and P_4 to P_7 are the absorption curve in the active layer. The SR curve of a tested PV device is determined by fitting the measured photocurrent to the currents which are calculated using the EQE and measured spectra. How well this model works for finding SR curves of any types of PV devices will be discussed further in the following section.

A **fourth order polynomial** model was used by Zaid et al. [79] to correct the error due to the broad spectral bandwidth of the light sources in order to obtain accurate spectral response measurements using an LED-based integrating sphere source. The mathematical function of the fourth order polynomial model is shown in equation (3.6) with 'a' as the coefficients. This model is purely empirical. Its compatibility for spectral response curve representation of any type of PV devices is tested in the following section.

$$SR(\lambda) = a_1 + a_2\lambda + a_3\lambda^2 + a_4\lambda^3 + a_5\lambda^4 \qquad (3.6)$$

A novel spectral response model based on empirical fits is introduced as part of this work. Its aim is to obtain the spectral response without requiring prior knowledge of device structure and physical parameters. The model is only required to describe an accurate shape of the spectral response curve and therefore needs to be general enough to be applicable for any PV technologies. The approach used is similar to that shown in Figure 3.3. In that case, several curves representing specific absorption features in the PV device were added together to form a complete spectral response curve. In the new approach, each curve is represented using a Gaussian distribution function as expressed in equation (3.7), which breaks the link to the absorption physics but adds highly adaptable shape fitting capability.

$$F(x) = a * exp\left[-\left(\frac{x-b}{c}\right)^2\right] \qquad (3.7)$$

Where a, b and c are the coefficients. 'a' represents the amplitude of the curve, 'b' determines the shape of the curve and 'c' controls the bandwidth of the curve.

A curve generated using a Gaussian function model has a form like a bell shape as shown in Figure 3.4.
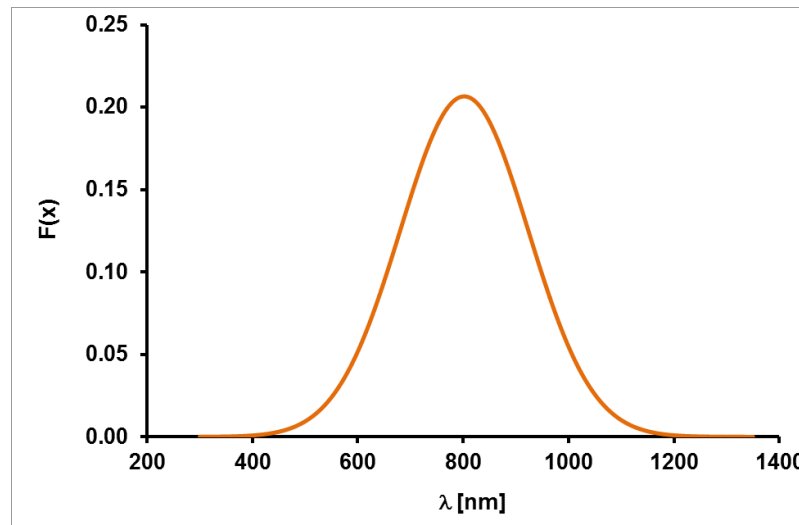
Figure 3.4: A typical shape of a Gaussian function model

As apparent in Figure 3.4, using only one order of Gaussian function is inadequate for obtaining an accurate spectral response curve. Its coefficients cannot produce a typical spectral response curve of a PV device. However, several Gaussian curves may be summed to form an accurate spectral response curve of a PV device. A preliminary test was conducted to determine the number of Gaussian functions required to match a measured spectral response curve. The number of Gaussian functions is varied and the coefficients of each fitted to the target (monochromatically-measured) spectral response curve, observing the goodness of fit. The results of this fitting test process are shown in Figure 3.5.
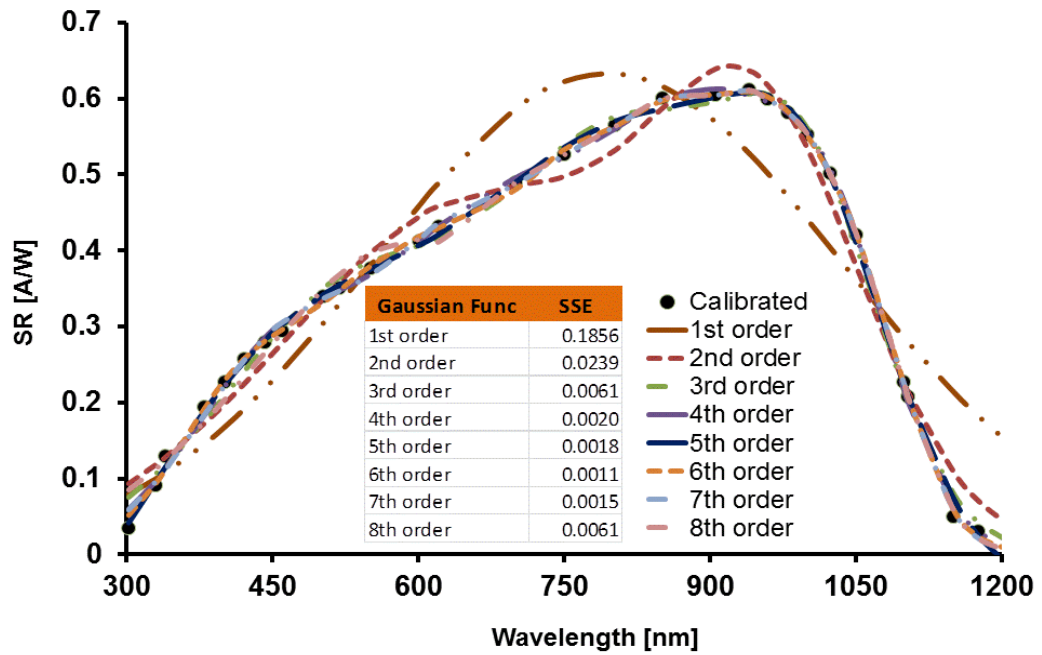
Figure 3.5: The goodness of fits of the fitted SR curves using different orders of the Gaussian distribution functions

As shown in Figure 3.5, increasing the number of Gaussian functions, that are summed together, improves the spectral response curve generated. A well-matched spectral response curve is produced from the higher order Gaussian functions, from forth order onwards. The *goodness-of-fit* used in the fitting algorithm is the sum of squared due to errors (SSE) which measures the total deviations of the points in the fitted curve to the measurement points. Based on the SSE values, the forth and the fifth order Gaussian functions were selected for further investigation. These selected Gaussian functions contain four and five sets of Gaussian functions as expressed in equations (3.7). A complete spectral response curve obtained using the fifth order Gaussian function is shown in Figure 3.6.
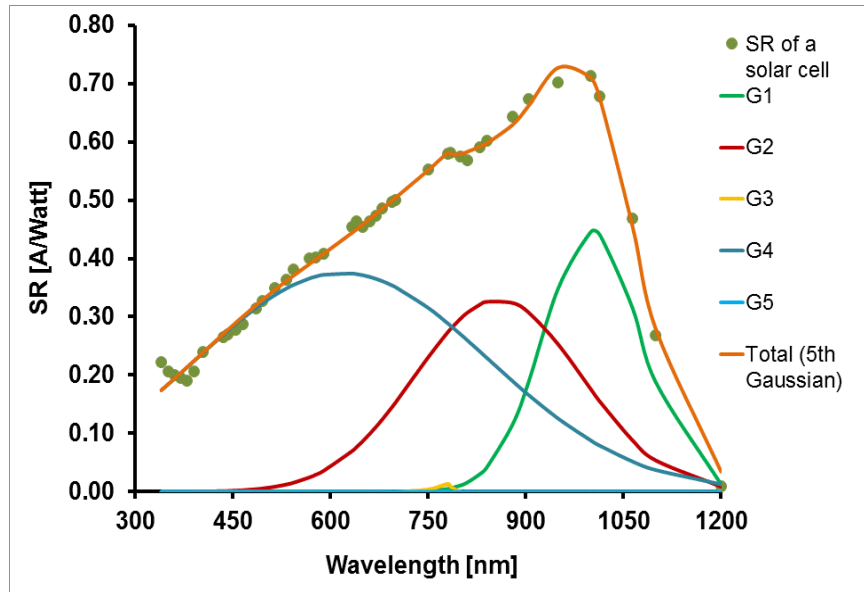
Figure 3.6: The fifth order Gaussian function as a summation of five sets of Gaussian function with different coefficient functions

Higher order Gaussian functions also show a very good agreement, however, they are not considered as the incremental improvements do not justify the many additional coefficients that need to be fitted. The number of coefficients in the Gaussian model needs to be limited as they can increase the uncertainty in the proposed spectral response method. The capability of the fourth- and fifth-order to fit different types of PV devices will be tested along with other selected spectral response models, as described below.

As the requirement for the model is to accurately describe only the shape of the spectral response curve of different PV devices, additional empirical models are selected for further examination. The aim of empirical modelling is that an accurate shape of a spectral response curve can be found without requiring prior detailed knowledge of device structures.

As the fourth polynomial model has been applied for fitting a spectral response curve of a PV device [79], its capability to fit spectral response curves of different PV technologies is examined together with the sixth polynomial function as a new SR model. Therefore, five empirical models are selected for examination: fourth- and sixth-order polynomial functions, the exponential EQE model, and fourth- and fifth-order Gaussian functions. Their suitability is examined individually to fit selected

spectral response curves from different PV technologies. A suitable model is selected based on the goodness of fit as defined in equation (3.8).

$$\chi^2(a) = \sum_{i=0}^{N-1} \left[\frac{y_i - y(x_i|a)}{\sigma_i} \right]^2 \qquad (3.8)$$

$$\sigma_i^2 = \sum_{i=0}^{N-1} (y_i - y(x_i))^2 / (N - M) \qquad (3.9)$$

The most appropriate model to represent a SR curve is chosen based on the lowest SSE value. The overall procedure for selecting the most appropriate model is shown in Figure 3.7.
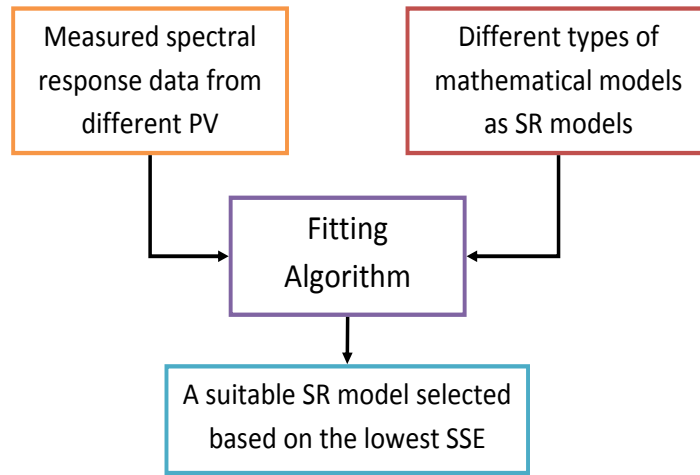
Figure 3.7: Procedure for selecting a suitable SR model

Results of the spectral response model selection are presented in Figure 3.8 and summarised in Table 3.2.

PV devices	Exponential EQE	4th Gaussian	5th Gaussian	4th Polynomial	6th polynomial
Mono-cSi	0.088478	0.001169	0.000725	0.011071	0.001078
aSi	0.00143	0.000429	0.000219	0.07543	0.025918
PolycSi	0.063409	0.002423	0.002438	0.014499	0.002975

Table 3.2: SSE values of selected SR models in fitting SR of the selected PV devices
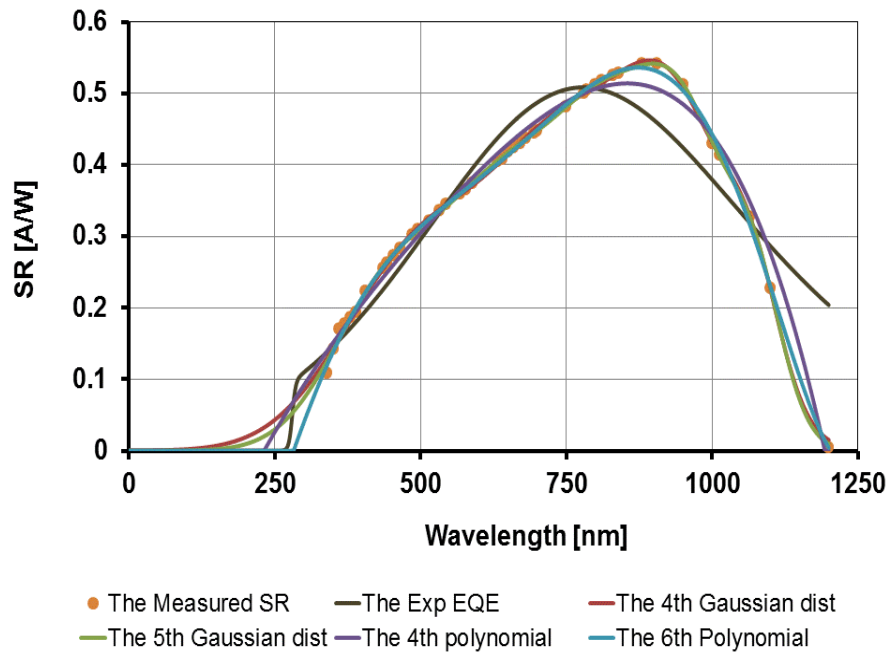
a. Mono-crystalline silicon cell
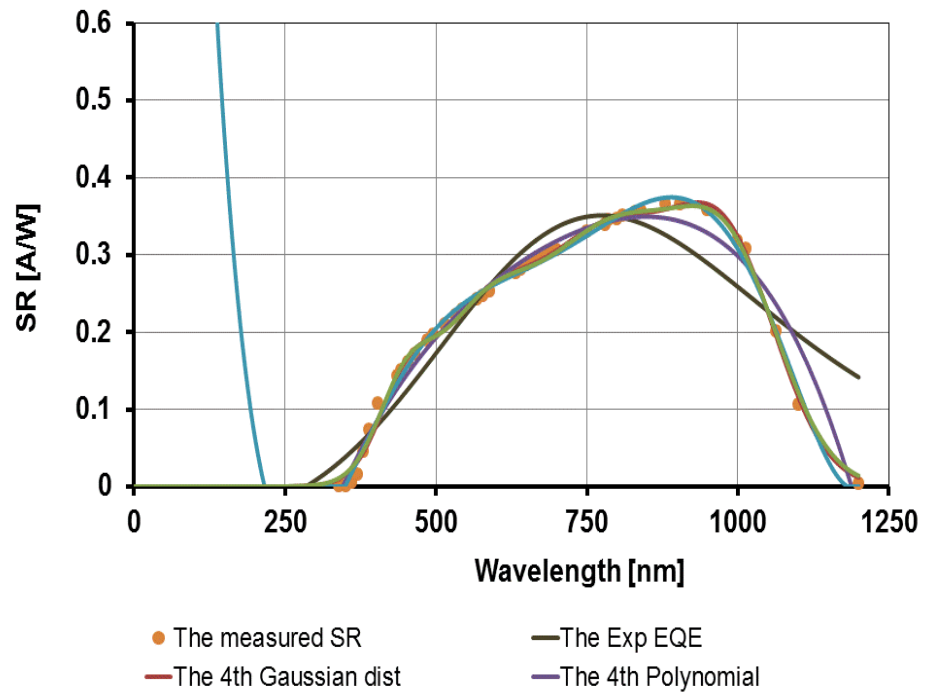
b. Poly-crystalline silicon cell
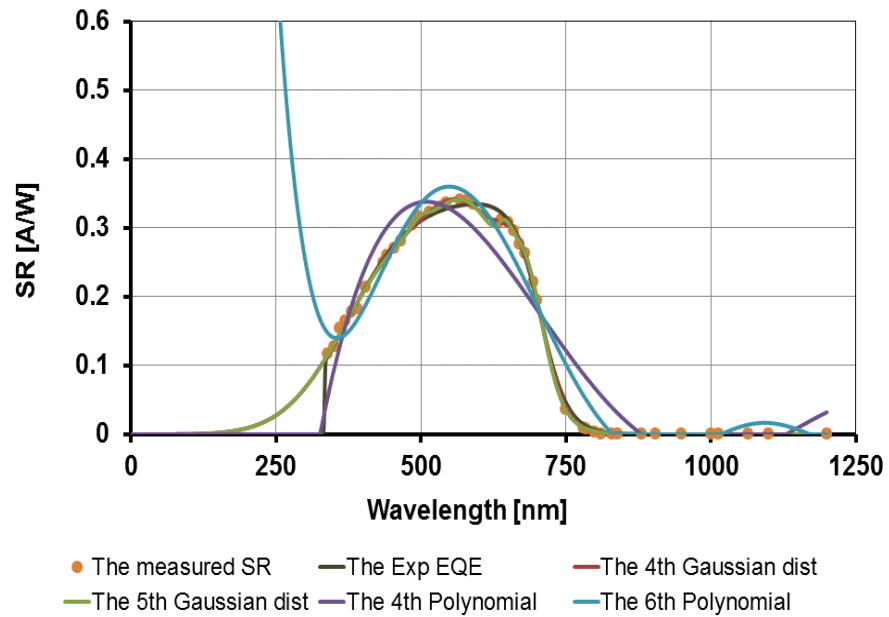
c. Amorphous silicon cell

Figure 3.8: Application of the four SR models to fit measured spectral response of selected PV devices

As shown in the three figures, neither the fourth- nor the sixth-order polynomial functions fit the measured spectral response curves accurately. The exponential EQE model only works well for fitting the amorphous silicon device. The model does not precisely fit spectral response curves of crystalline PV devices. This shows that the model is unsuitable for fitting the spectral response of the crystalline PV device. In terms of the SSE value, the fourth- and fifth-order Gaussian functions produce the lowest error compared to other models, demonstrating that they are compatible to fit correctly the spectral response curves of all devices tested here [83]. Considering the requirements for an accurate spectral response curve and providing flexibility for application to different devices, the fifth-order Gaussian function has been chosen and embedded in a new fitting algorithm that is specifically developed to fit the measured current data to the calculated current. The model can be switched to the fourth-order Gaussian as required, by inputting zero coefficients in the fifth term.

Deviations between the measured and modelled spectral response curves are shown in Figure 3.9. Compared to other models, the fourth- and fifth-order Gaussian functions have the smallest relative differences, within a range of ±2% across the response wavelength range of the selected PV devices.

73
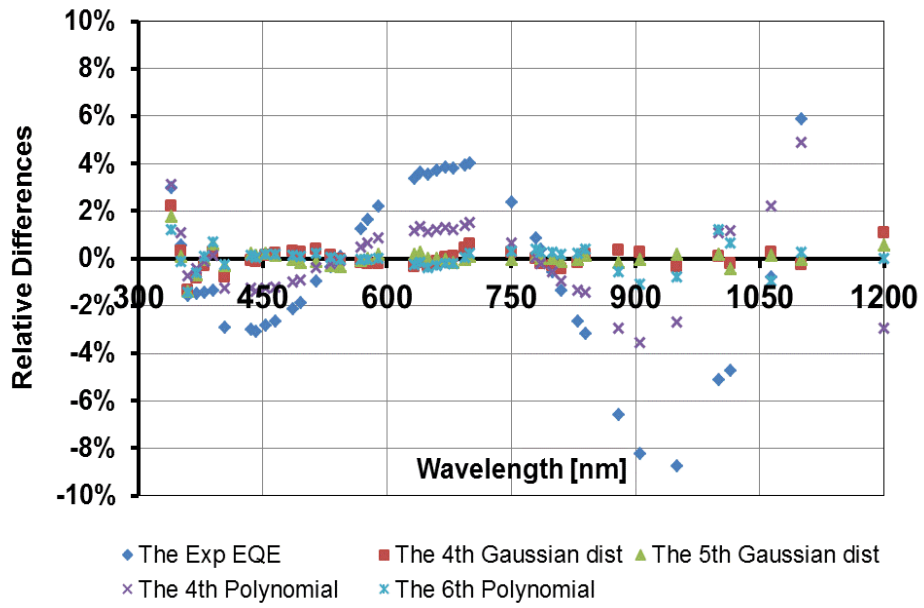
a. Amorphous silicon cell
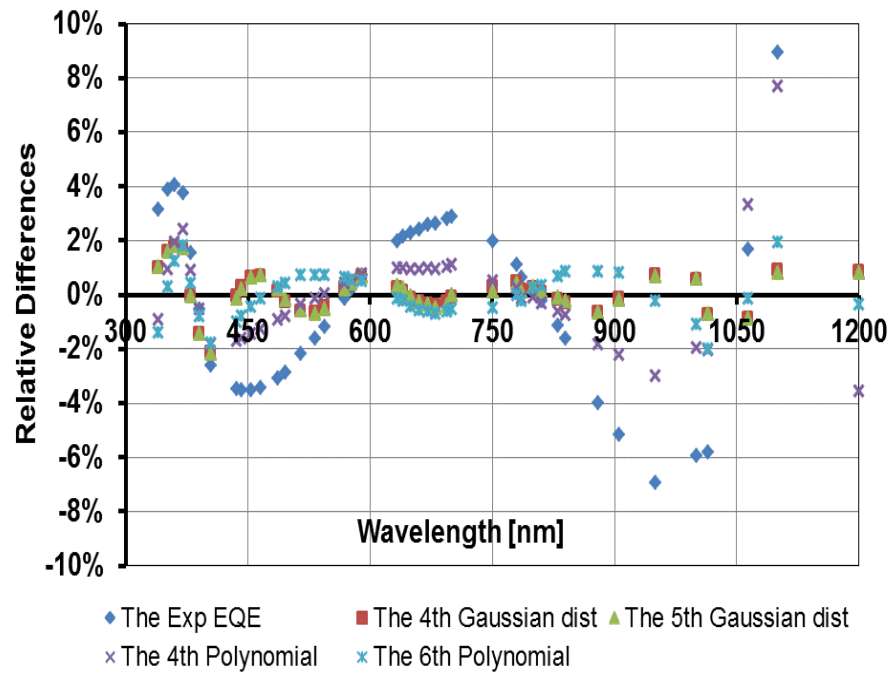
b. Poly-crystalline silicon cell
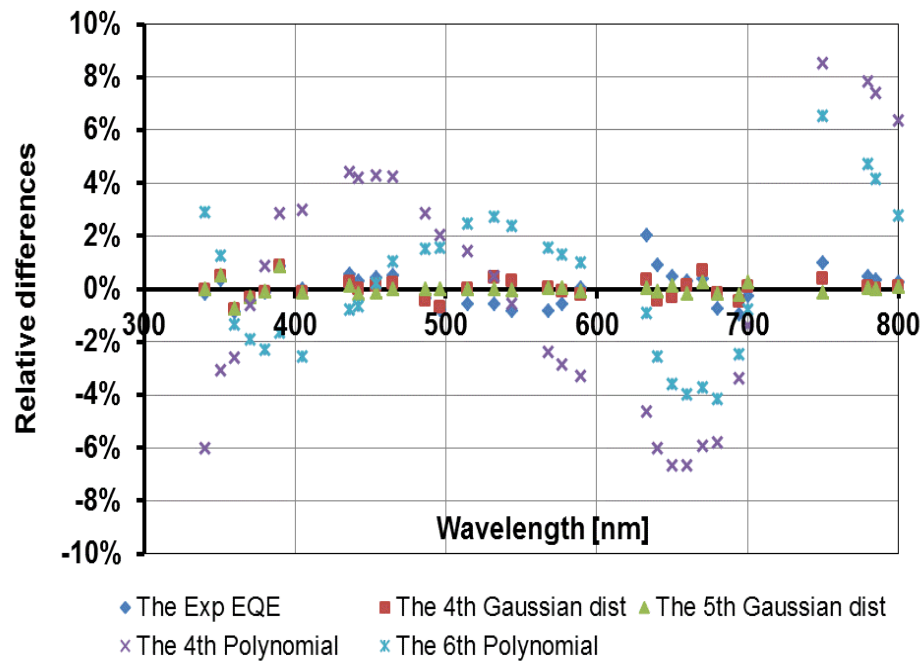
c. Amorphous silicon cell

Figure 3.9: Relative differences of the fitted SR curves obtained using the fifth order Gaussian function and the others to the measured SR curves of the selected PV devices

Based on comparison of the goodness of selected SR models, it can be concluded that the fifth order Gaussian function is more suitable to be used as an SR model.

3.4. Fitting Algorithm

The fitting algorithm is used as a means to obtain the appropriate fitted coefficients of the chosen spectral response model. It is developed based on the concept of photocurrent determination, as written in equation (3.1). The fitting algorithm functions to calculate the photocurrents from the spectral response model and set of irradiance spectra by tuning the coefficients of the model to match the measured currents. The process of fitting the coefficients differs from the standard fitting approach where the unknown parameters of the chosen model can be determined directly from the input data (as in the comparison of models in the previous section). The normal fitting process cannot be performed for fitting the photocurrent due to the difference in measurement point numbers of its input data. For example, one

measured spectrum is given as an array of wavelengths and spectral irradiance values, which consists of 2013 measurement points in the case of the equipment used here. This spectrum corresponds to one measured current. To optimise the spectral response model coefficients, the fitting algorithm must be made to calculate the spectral response of the tested PV device, calculate the resulting photocurrents for different spectra and compare these to the measured currents. To do this, the fitting algorithm requires four input parameters (as shown in Figure 3.10):

- A set of short-circuit currents of a tested PV device measured under different spectral conditions,
- A set of corresponding spectra under which the short-circuit currents are measured,
- A suitable spectral response model, and
- A set of initial values for the coefficients of the model.

To enable the fitting process, initial values must be given for the coefficients of the chosen spectral response model. These initial values are technology dependent. The values for the pre-set coefficients are determined from fitting the known spectral response curves of different PV technologies.

Having all the required input data, the fitting algorithm works iteratively to calculate the photocurrents from the measured spectral data and the spectral response model. The tuning of calculated currents to the measured currents is done by adjusting the coefficients of the spectral response model until the pre-set stopping condition is fulfilled. Once the stopping condition is met, the next step is to feed the optimised coefficients back to the chosen spectral response model in order to generate the final spectral response curve for the tested PV device.

Set of measured photocurrents

Set of measured irradiance spectra

Spectral response model with initialised coefficients

Set of modelled photocurrents

Fitting algorithm (compares currents)

Best fit?

No

Yes

Revised coefficients for spectral response model

Spectral response model with optimised coefficients
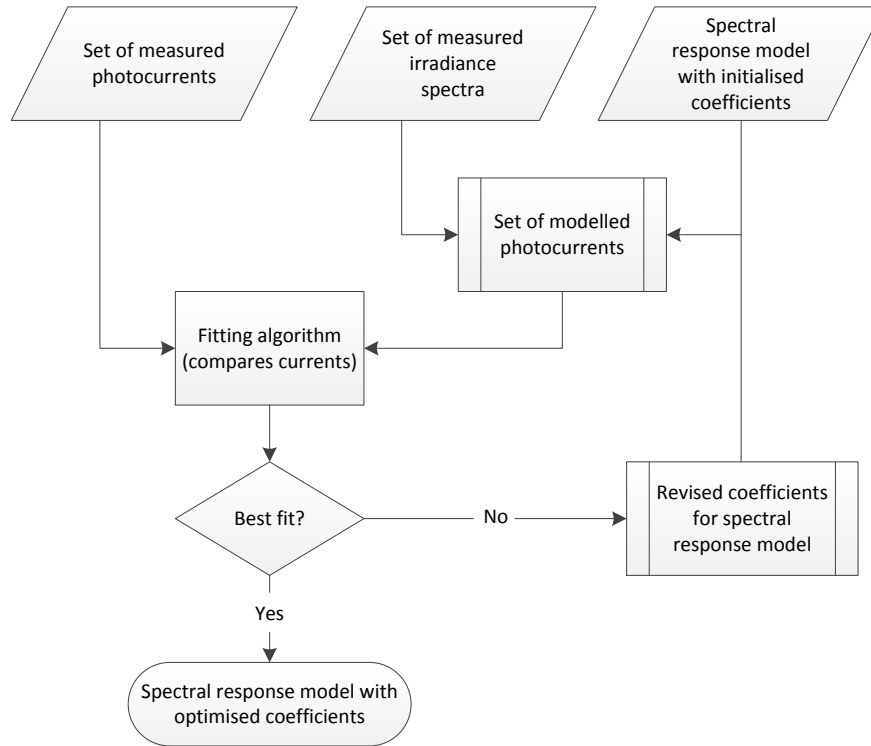
Figure 3.10: SR determination using a polychromatic SR fitting approach

As the measured short-circuit current and spectral irradiance data contain some degree of measurement uncertainty, the spectral response model cannot be fitted precisely to the data. To compensate for this error in the fitting process, it is necessary to apply weighting to the error criterion with the standard deviation of the measured data as shown in equation (3.8). This allows calculation of the accuracy of the fitted parameters [84].

3.5. Choosing Appropriate Filters

To find the appropriate coefficients for the chosen SR model, the fitting algorithm requires a wide range of spectral variations across the wavelength spectrum which is enough to cover the range of spectral interest of different PV devices. Therefore, the polychromatic filters that are employed in this SR measurement method should have specific spectral transmittances that are able to produce different throughputs across the entire wavelength spectrum. In addition, they should also possess a high operating temperature characteristic as the filter will be exposed to high temperature condition. The polychromatic filters used in this work are translucent coloured

polymeric materials with a thickness approximately 0.13 mm as shown in Figure 3.11.

Figure 3.11: Lighting gel filters used for polychromatic SR method

They are used industrially for different applications such as to tone light in theatre, photography, videography and cinematography and for colour correction. As the gel filters will be employed in the small-area SR measurement system, they will be exposed directly to a high temperature condition which is generated by a continuous xenon arc lamp. Therefore, a simple heat resistance test has been performed using a lab hotplate to observe the melting point of the filters. Samples of filter were put on the metal hotplate for about an hour at different temperature conditions. The results show that the proposed filters can withstand temperatures up to 200°C for this time period. Relating this result to the normal operating temperature of the small area spectral response measurement system which is about 25-27°C, employing the lighting gel filters in the measurement system will not lead the filters to failure. Another interesting feature of the lighting gel filters is that large variations in the shape of their spectral transmittances. This provides a wider flexibility in the filter selection. In addition, they are really cost-effective compared to specialist optical filters made from glass materials. As the cost of the spectral response measurement

system is dominated by the filter cost (the second greatest after the light source), employing lighting gel filters can significantly reduce the cost of the spectral response measurement system.

Appropriate lighting gel filters for the polychromatic spectral response fitting method are chosen based on the shape of their spectral transmittances and their capability to obtain a well-matched spectral response curve of different PV technologies. Prior to the selection, the spectral transmittances of the lighting gel filters are measured using a Varian Cary 5000 Spectrophotometer in the CREST lab and shown in Figure 3.12.
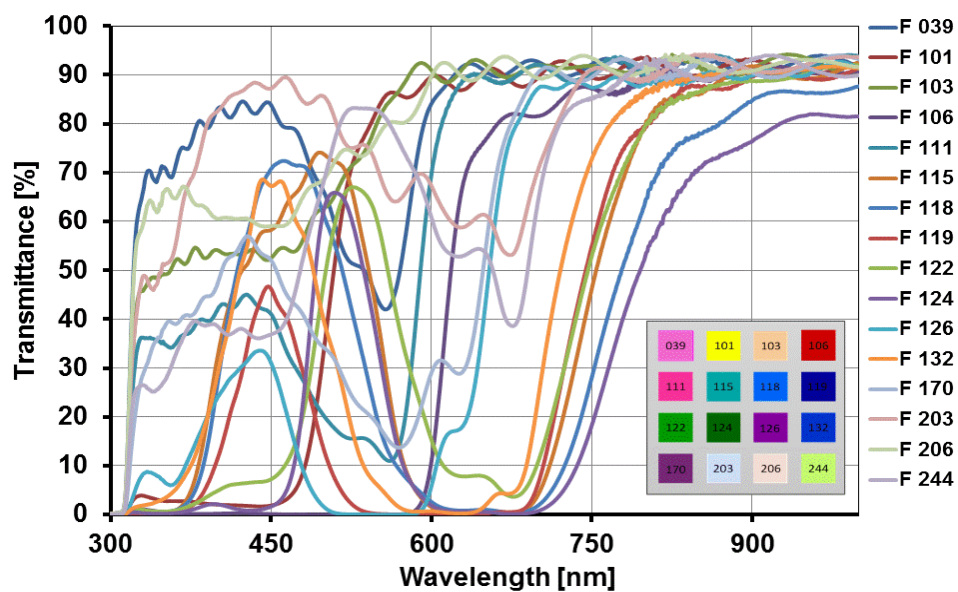
Figure 3.12: Transmittances of lighting gel filters employed in the polychromatic SR fitting method

As can be seen in Figure 3.12, each filter has a unique spectral transmittance. Their spectral throughputs vary according to a broad wavelength range. However, all the available gel filters have approximately 90% transmittance at wavelengths above 800 nm. This means that there are no variations in the spectral output of the gel filters above this wavelength. For certain types of PV devices with a range of spectral interest up to 1200 nm or even higher, spectral variations in those ranges are necessary in order to have different responses from tested PV devices. Therefore, to have spectral variations beyond 800 nm, a small number of other types of filters must be applied. Other types of filters with broad spectral bandwidths are added to the

79

selected gel filters to provide specific spectra at certain wavelength regions. The spectral transmittances of these additional filters are shown in Figure 3.13.
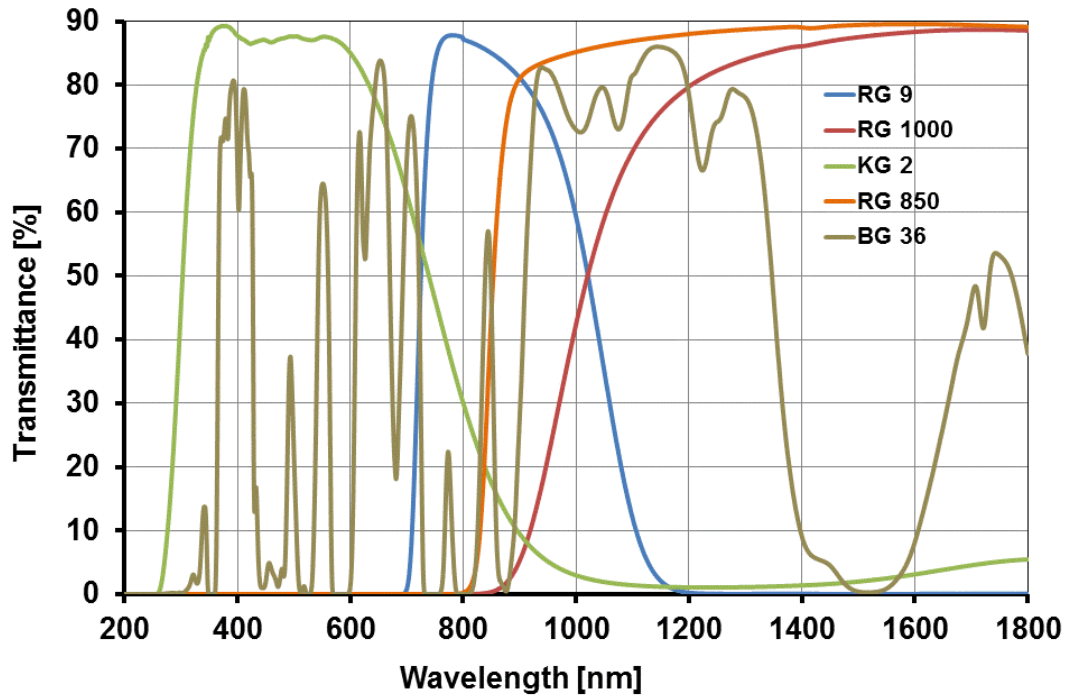
Figure 3.13: Transmittances of glass filters employed in the polychromatic SR method

To acquire the optimum number of the polychromatic filters which will be employed in the SR measurement system, all the filters' spectral transmittances are inputted into the fitting algorithm along with the spectral irradiance of the light source: the xenon arc lamp. The fitting algorithm calculates the appropriate coefficients for the SR model. From these results, the spectral response of a PV device is simulated and compared to the device's measured spectral response. The fitting process is repeated until it reaches to the minimum number of the filters where the simulated spectral response of the tested PV device is still matched to the measured one. Based on this test, there are 15 polychromatic filters selected for the final filter combination and their corresponding spectral transmittances are shown in Figure 3.14.
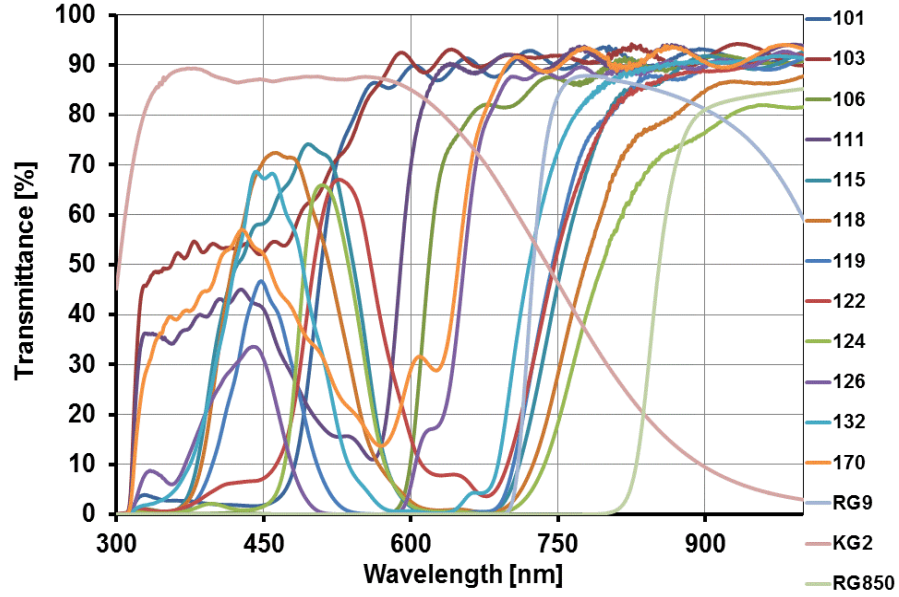
Figure 3.14: Transmittances of selected polychromatic filters in the final design of the proposed SR fitting method

3.6. Simulating the Spectral Response Determination

The feasibility of the polychromatic fitting concept for spectral response determination is examined by simulating the overall measurement and fitting process using the MATLAB environment. The processes are divided into two parts. The first part is to simulate the measurement of the short-circuit currents generated from a tested PV device under different irradiance spectra. The inputs for this simulation are the spectrum of the unfiltered light source, known spectral response of the PV device (from standard monochromatic measurements conducted at CREST and other laboratories) and the spectral transmittances of the filters

$$I_{sc\_measured} = A \int_{\lambda_1}^{\lambda_2} SR\,(\lambda) \cdot T(\lambda) \cdot E_{light\ source}(\lambda) d\lambda \qquad (3.8)$$

Where T is the filter transmittance.

The short-circuit currents calculated from this simulation are treated as the measured short-circuit currents of the tested PV devices.

The second part of the simulation is the spectral response fitting process. Inputs for this simulation are the 'measured' short-circuit currents that have been calculated in the first part and again the spectrum of the unfiltered light source and the transmittances of the filters. The 'measured' spectral irradiance at the measurement plane is calculated by multiplying the light source spectrum by the transmittance of each filter. The entire simulation process of the method is shown in Figure 3.15. The polychromatic fitting concept is verified for spectral response determinations for different single- and double-junction devices, in two different measurement systems: one for small-area measurements and one for large-area (full module size).
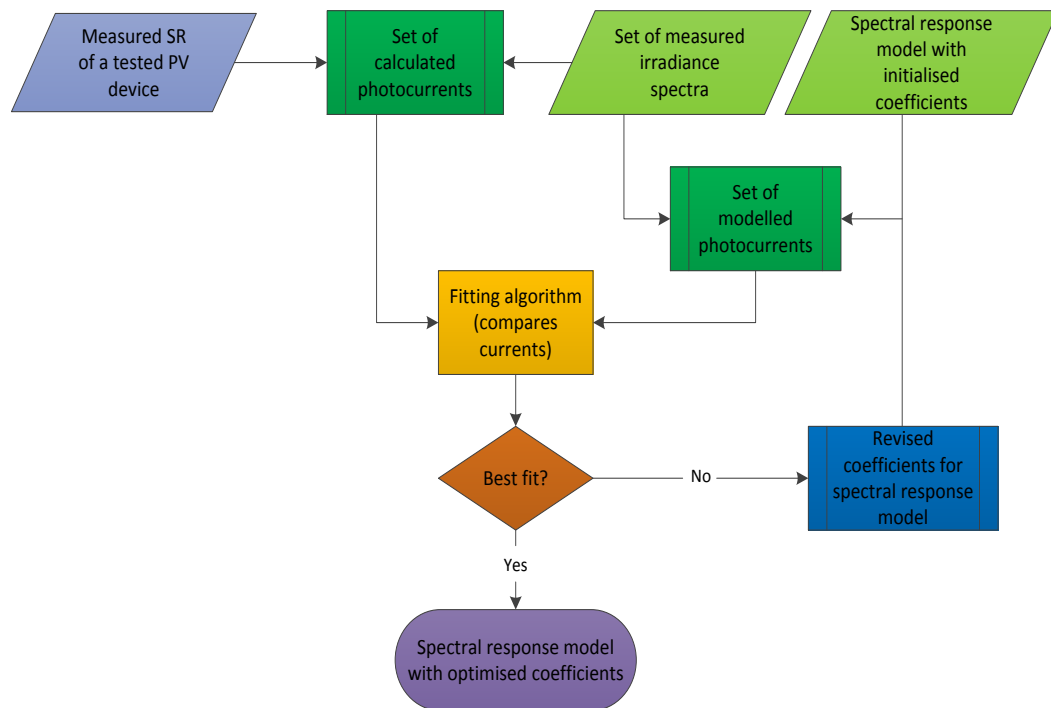
Figure 3.15: Simulation process of polychromatic SR fitting method

3.6.1 Small-area SR Measurement

Limited by the size of the illuminated area and the light homogeneity, only small area PV devices can be measured in the CREST spectral response measurement system. The maximum size of a PV device that can be measured is 10 cm by 10 cm. The spectral response measurement system consists of a dual-lamp light source to provide strong light output from 300 nm to 1200 nm. Lamps with different spectral shapes are employed: one 150 Watt continuous xenon arc lamp provides light from

300 nm to 750 nm and one 100 Watt halogen lamp provides light from 750 nm to 1200 nm. By employing a halogen lamp, higher variations in the irradiance due to the emission peaks in the unfiltered xenon spectrum can be eliminated. This makes the total spectrum produced from the two lamps quite smooth. The light spectra of these two lamps are shown in Figure 3.16.
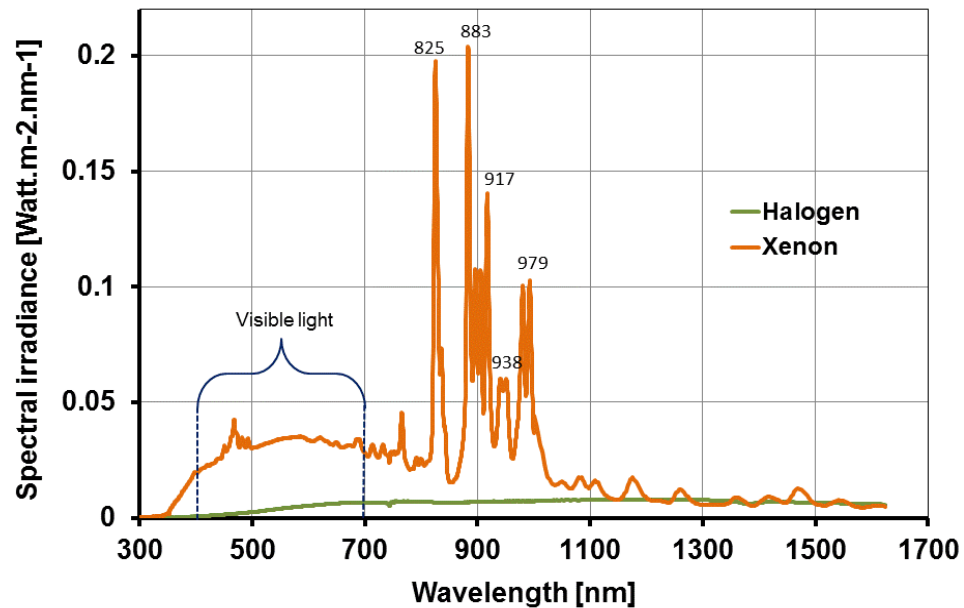
Figure 3.16: Spectral irradiance of xenon and halogen lamps in the small-area SR measurement system at CREST

The light source used in the spectral response fitting method must provide a range of wavelengths which accommodates the spectral response bands of different PV technologies. As shown in Figure 3.16, the spectral range of a xenon lamp can fulfil this requirement and so it is used as the source in the simulation of the method. Large variations in the irradiance due to the spikes in the xenon spectrum can be tolerated as the proposed spectral response fitting method only requires variations in the spectral output.

The spectral response curves obtained from the simulation of the polychromatic method for small-area devices are shown in Figure 3.17. The results are compared to the (monochromatically) measured spectral response curves in order to examine the level of agreement.
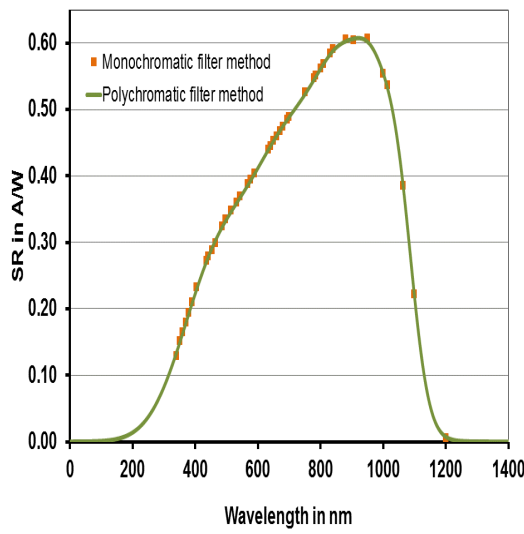
a. Mono-crystalline silicon
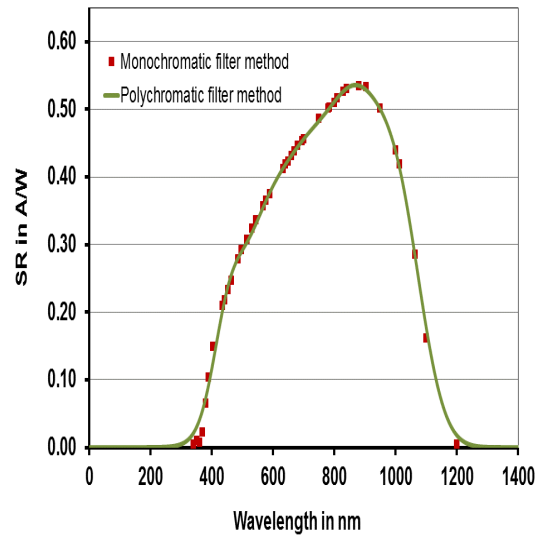
b. Poly-crystalline silicon
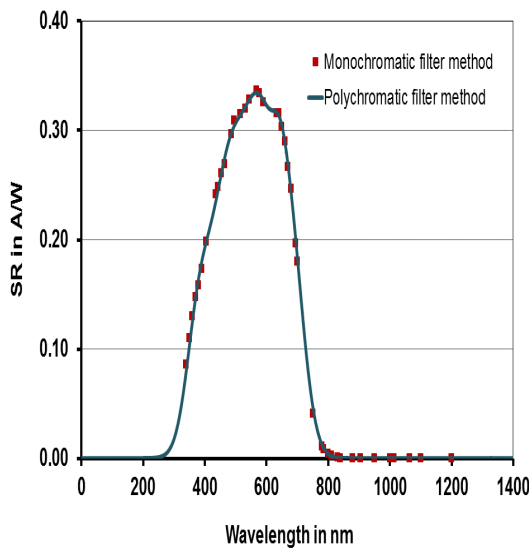
c. Amorphous silicon (a-Si)
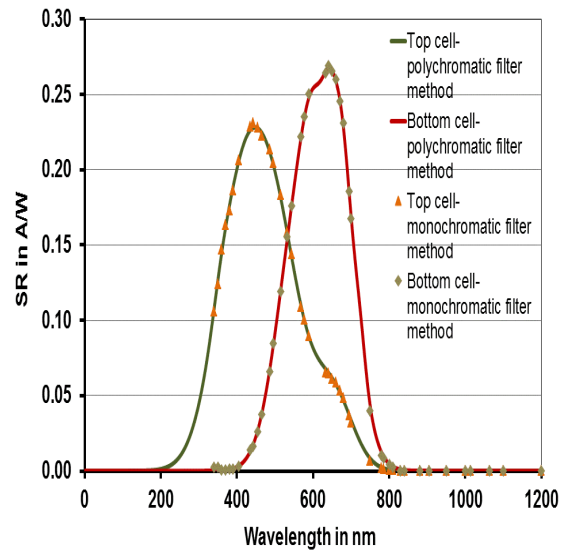
d. Tandem a-Si

Figure 3.17: Comparison of monochromatically-measured SR curves and process simulation of polychromatic SR determination for small-areas

As shown in Figure 3.17, the simulated spectral response curves for the selected PV devices are almost indistinguishable from the measured spectral response curves. This includes a double-junction PV device as shown in Figure 3.17d. This agreement

is quantified in terms of the percentage relative deviation by wavelengths as shown in Figure 3.18.
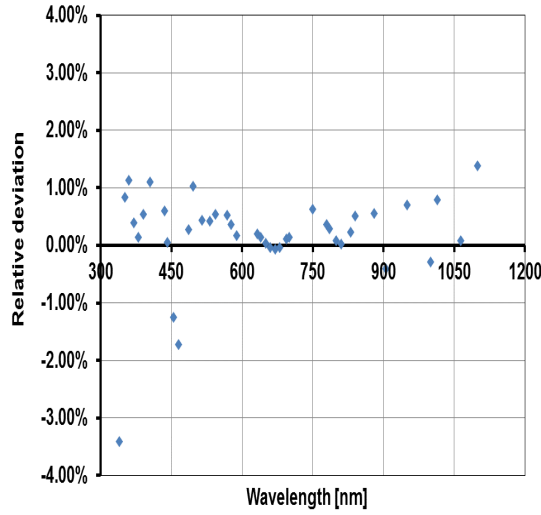
a. Mono-crystalline silicon
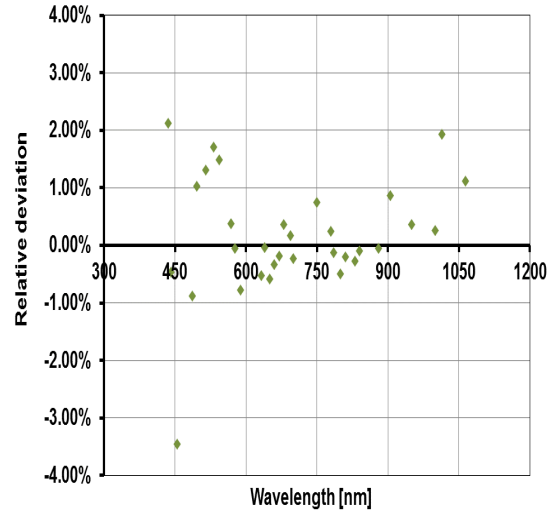
b. Polycrystalline silicon
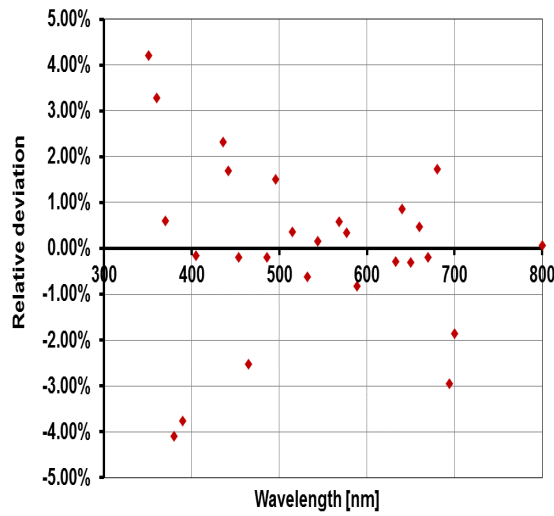
c. Amorphous silicon (a-Si)
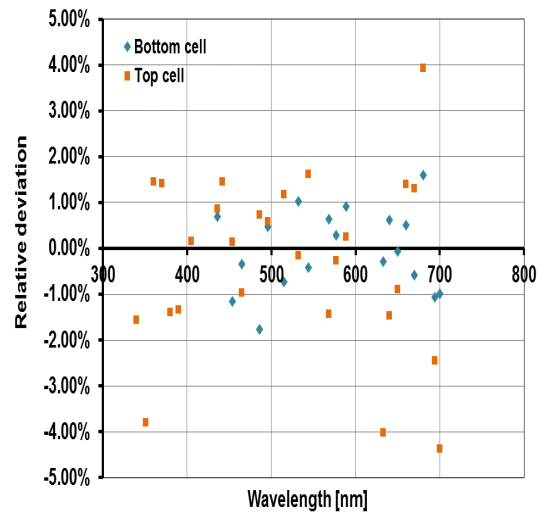
d. Tandem a-Si

Figure 3.18: Relative deviations of simulated and measured SR curves of selected PV devices

The agreement between the measured and the simulated spectral response curves is largely within a range ±2%. However, there is higher divergence in the ultraviolet

and infrared ranges. This is caused by low signal-to-noise levels in these measurement ranges.

3.6.2 Large-area SR Measurement

The large-area measurement system in use at CREST can be used to measure I-V characteristic curves at different irradiances, temperatures and angles of incidence. It is a single-flash PASAN Sun Simulator 3b with an illumination area of 2.5 by 2.3 m. The light source is a set of four xenon lamps with class A spectral irradiance as shown in Figure 3.19.
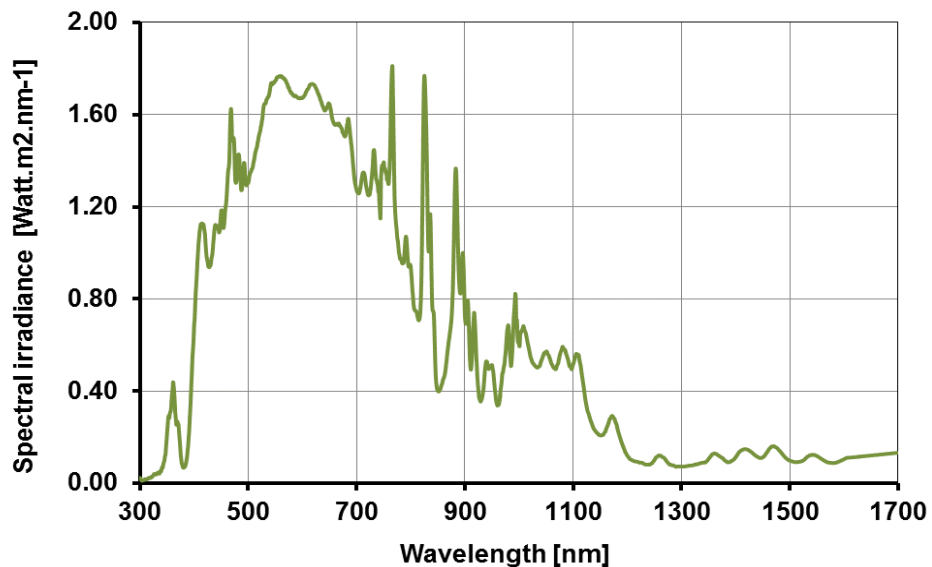
Figure 3.19: Filtered xenon spectrum in the PASAN solar simulator at CREST

Since there is a requirement for a reliable spectral mismatch correction for large-area measurements, the PASAN simulator needs to be upgraded to facilitate spectral response measurement by integrating the proposed polychromatic SR fitting method into its measurement system. As has been mentioned in the previous section, this SR measurement method is able to provide high irradiance on the measurement plane, which is significantly important for strengthening the response signal produced by a tested PV device and lowering uncertainty in the SR determination. Therefore, the feasibility of this proposed SR method for a large-area SR determination is examined by simulating its measurement process. Inputs for this simulation are similar to that

of the small-area measurement, including the same set of polychromatic filters. This time however, the light source spectrum is replaced by that shown in Figure 3.19. For the purpose of verification, the same selected PV devices are employed again. In this way, the correlation between the measured spectral response and the calculated one can be proven .Results of the simulation outputs are shown in Figure 3.20.
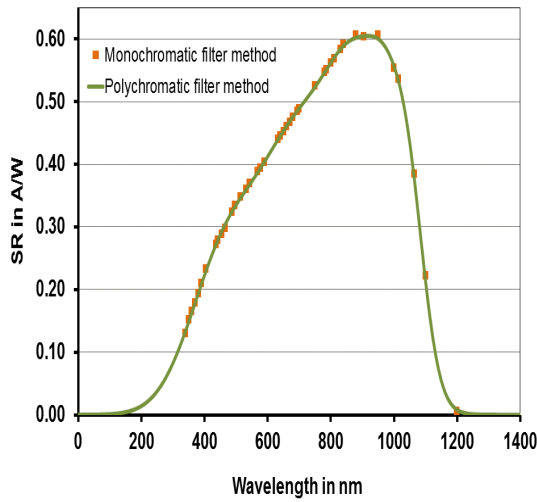
a. Mono-crystalline silicon   b. Polycrystalline silicon
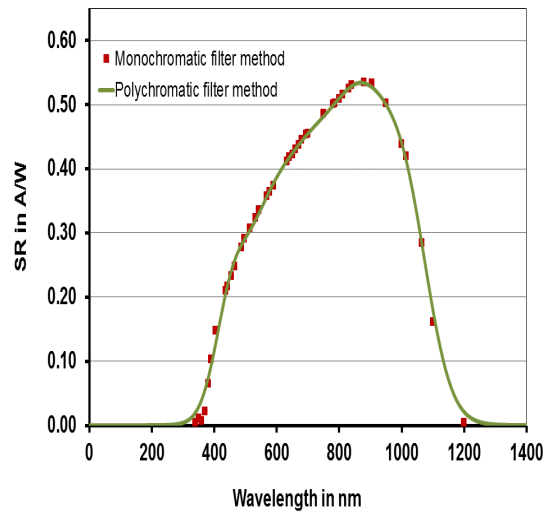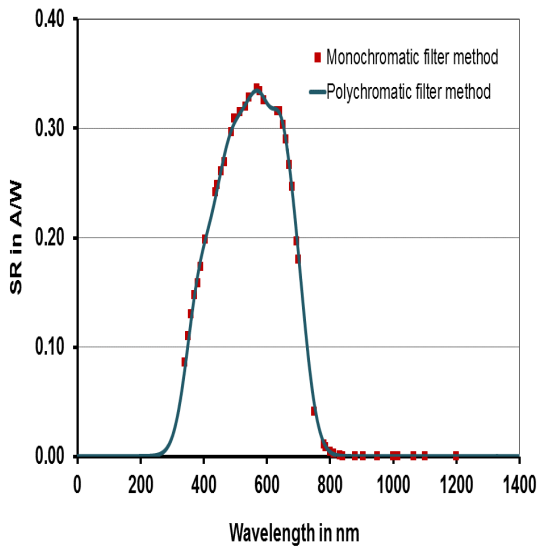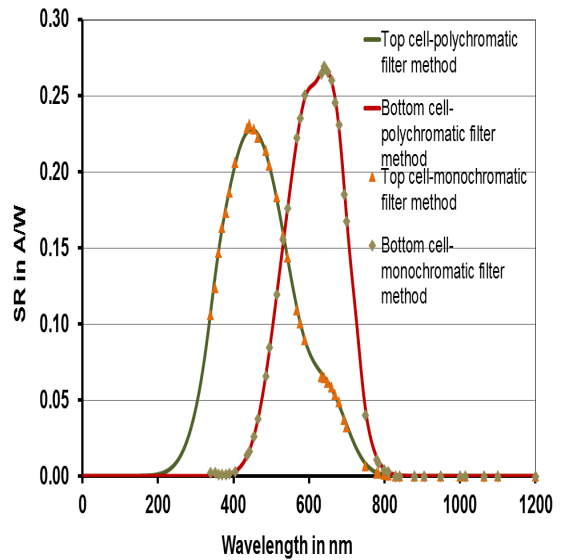
c. Amorphous silicon (aSi)   d. Tandem aSi

Figure 3.20: Comparison of monochromatically-measured SR curves and process simulation of polychromatic SR determination for large areas

The average difference between the measured and the simulated spectral response curves are also within a range of ±2%. The results of the simulations have proved that the proposed polychromatic spectral response fitting method is feasible to be implemented for both small-area and large-area spectral response measurement systems.

As shown in the above figures, the simulated and measured SR curves are qualitatively well-fitted for all selected PV devices. This is quantified in Figure 3.21.
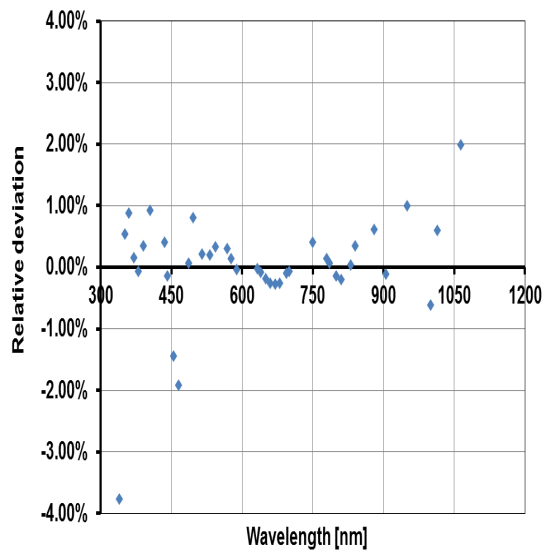
a. Mono-crystalline silicon   b. Polycrystalline silicon
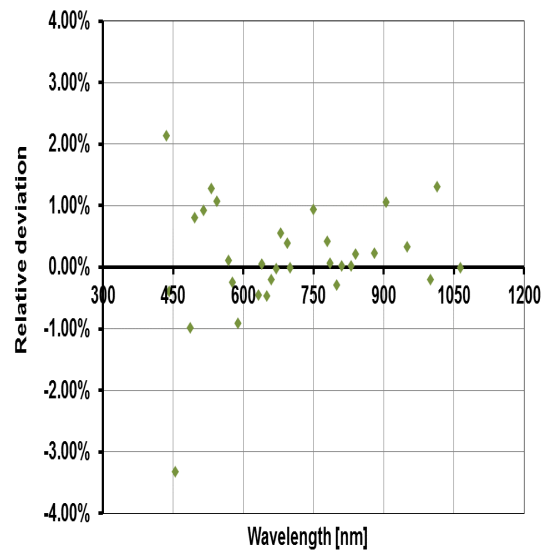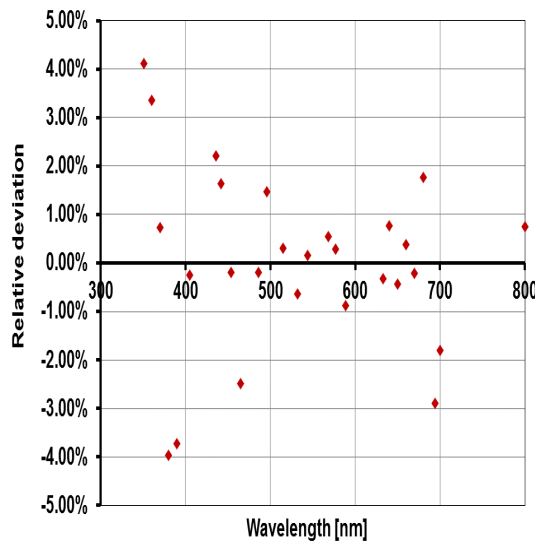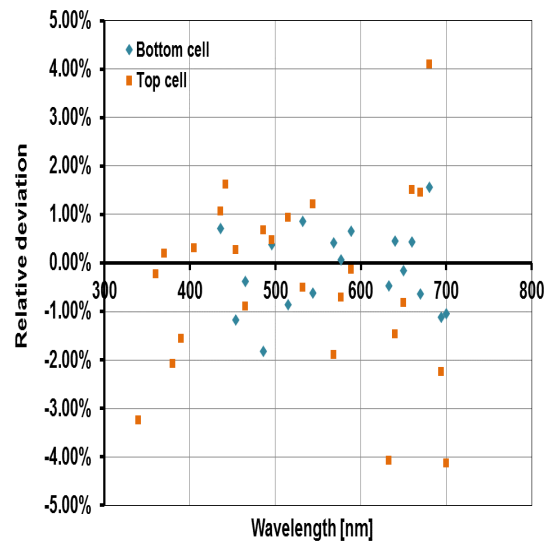
c. Amorphous silicon   d. Tandem a-Si

Figure 3.21: Relative deviation of simulated and measured SR curves of selected PV devices

The average difference between the measured and the simulated SR curves are also within a range of ±2%. The results of the simulations have proved that the proposed polychromatic SR fitting method is feasible to be implemented for a small-area and large-area spectral response measurement.

3.7. Conclusions

A new concept for determining the spectral response curve of a PV device has been proposed. The proposed concept is based on fitting a set of short-circuit currents measured under different spectral conditions to the short-circuit current calculated using the photocurrent formula. Filters with broad spectral bandwidths are employed to have different spectral conditions. An accurate spectral response determination can be obtained if the spectral outputs of the selected filters have variations in different regions of the spectrum. Therefore choosing appropriate polychromatic filters is important for accurate spectral response determinations.

A new empirical model has been introduced and is able to produce spectral response curves for different PV technologies. The measurement process of the proposed

polychromatic spectral response fitting method has been simulated for two measurement systems to be developed in the following experimental chapters. The results of the simulations show that the proposed spectral response fitting method produces spectral response curves of different PV devices with a relative deviation about 2% over the whole range of spectral interest, when compared to the spectral response curves measured using the monochromatic filter method. The simulation is performed under ideal conditions with assumptions that the spectrum illuminating the tested PV device is perfectly homogeneous and stable and that temperature controlled conditions are met as prescribed in the standard IEC 60904-8. If these conditions can be fulfilled in practice, it is confirmed that the spectral response fitting method is feasible for determining the spectral response curve of any size of PV device up to full modules. As real experimental conditions differ from such an ideal, the practical verification of the concept is required. This verification, and the related practical challenges, forms the basis of the following chapters.

Chapter 4

Spectral Response of Small-Area PV Devices

4.1. Introduction

This chapter contains the experimental validation of the fitting concept for determining the spectral response of a PV device, building on the proof-of-concept simulation work presented in Chapter 3. The experimental setup of the monochromatic and polychromatic filter method is described in section 4.2 and section 4.3. It includes the measurement procedure as well as the fitting approach. Validation of the polychromatic filter method for spectral response determination and sensitivity analysis of its input parameters are presented in section 4.4 and section 4.5. Lastly the feasibility of the proposed polychromatic method is concluded in section 4.6.

4.2. Spectral Response Measurement using Conventional Monochromatic Light Method

To enable a direct comparison to be made with the conventional monochromatic filter method, the hardware elements of the method have first been added to the existing CREST (filter-based) monochromatic spectral response measurement system. The system can now be switched between the standard and the polychromatic modes and this allows experimental validation of the new method to be performed on small-area PV devices. This has been done for different technologies: mono- and poly-crystalline silicon and amorphous silicon, the latter of single (SJ)- and double (DJ)-junction structures. A detailed description of the selected PV devices is given in Table 4. The mono-crystalline cell is a reference cell

that has been calibrated at an accredited photovoltaic calibration laboratory at the *Fraunhofer ISE* (CalLab)

PV devices	Type of technology	Manufacturer	Voc	Isc	Pmax	Size	Number of cell in series
			Volt	mA	mW	mm	
Monocrystalline PV devices	SJ PV device	ISE-Fraunhofer,	0.651	137.73	73267.7	20x20	1
Amorphous Silicon PV device	SJ PV device	Sanyo	2.684	91.959	130.008	42x44.8	3
Polycrystalline PV devices	SJ PV device	Select solar	4.840	109.361	402.546	53x52	8
aSi-aSi tandem PV devices	DJ PV device	Sanyo	8.814	39.414	245.974	50x61	5

Table 4.1: PV devices used for validating the proposed SR determination method measured at STC

Prior to implementing the proposed method, the spectral responses of the selected PV devices were measured using a conventional method based on the application of monochromatic beams, as explained in the international standard IEC 60904-8: Measurement of the Spectral Response of a Photovoltaic (PV) Device [4]. Here, the method is referred to as the '**monochromatic filter method**'. These standard measurements are then used to verify the validity of the proposed concept for spectral response measurement.

The spectral response measurement system employs 44 narrow band-pass optical filters as shown in Figure 4.1. It has a dual-lamp source of xenon and halogen lamps to provide a full spectral range for a tested PV device. A calibrated reference photodiode is used as the irradiance detector. A chopper with a frequency of 175 Hz provides the reference frequency for two lock-in amplifiers which measure the monochromatic photocurrent response signal produced by the PV device under test and the reference solar cell with a calibrated spectral response. Also included is an LED-based background bias lighting system with total intensity of approximately 400 W.
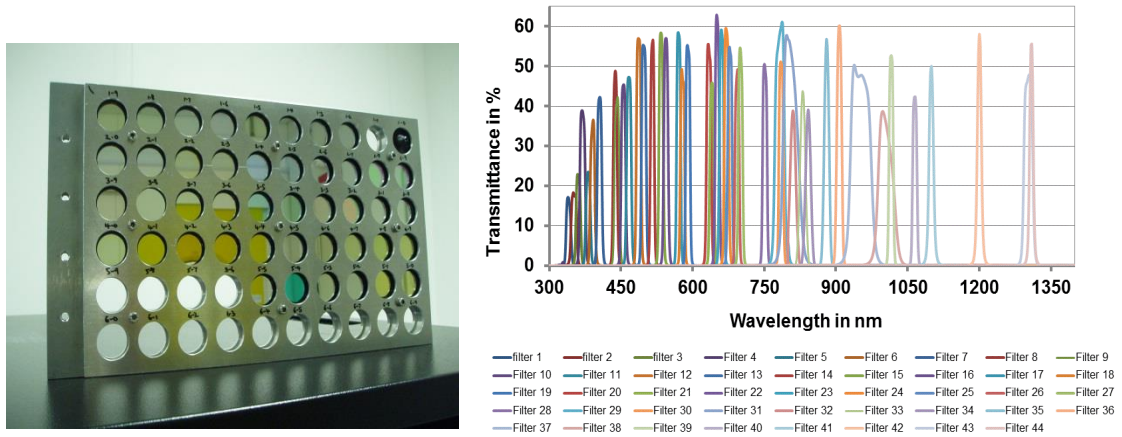
Figure 4.1: Monochromatic filters and their correlating transmittance as employed in the CREST spectral response measurement system

A schematic overview of the spectral response measurement setup in use at CREST using the conventional filter method is shown in Figure 4.2.

1. Monochromatic Filters
2. Shutter
3. Chopper
4. Homogeneiser
5. Mirror
6. Photodiode
7. Bias lighting
8. Tested PV device
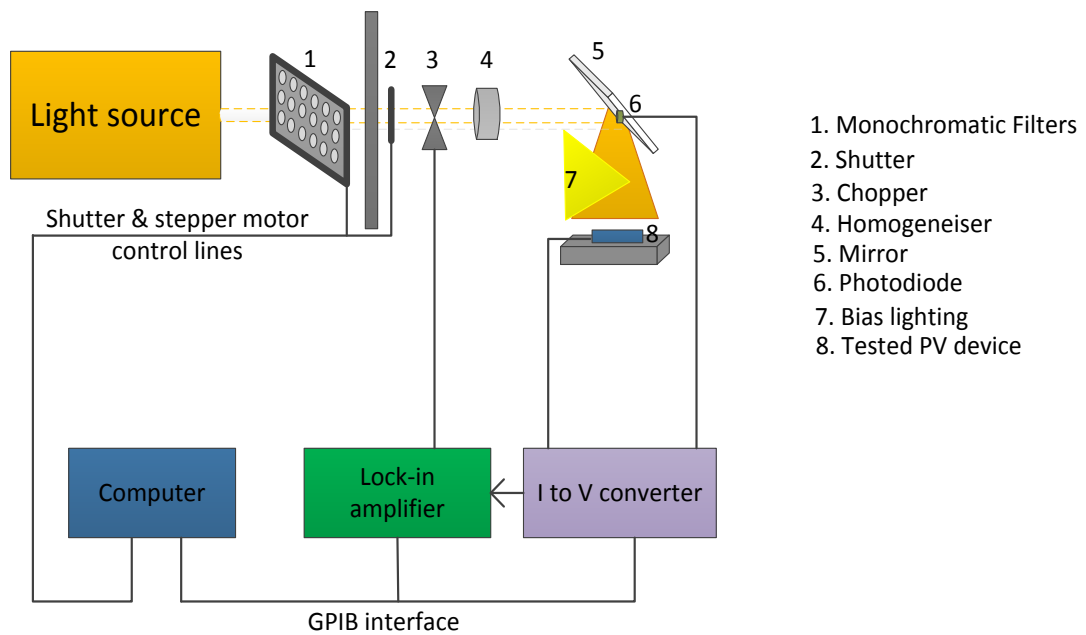
Figure 4.2: Spectral response measurement setup in use at CREST using the monochromatic filter method

The spectral response measurement is performed by illuminating the PV device under test (DUT) with a series of monochromatic beams at different wavelengths. These monochromatic beams are provided by filtering the spectrum of the light source using different narrow band-pass (monochromatic) filters. The PV device is placed horizontally on the measurement plane and a four-wire connection is used to

connect the tested PV device to the current measurement unit and to a separate voltage source which is used to bias the device at zero volts. To accurately measure the irradiance produced from a monochromatic beam, the reference photodiode is positioned in line with the monochromatic filter set in the measurement system. In such way, it can detect accurately the irradiance throughput of a given monochromatic filter without being mixed with the irradiance produced from the bias lighting system. As mentioned in the previous chapter in section 3.2, even a single-junction measurement requires bias lighting in order to overcome any nonlinear current response [70]. Therefore white bias lighting is applied for all single-junction spectral response measurements. Different colours of bias lighting are provided for measurements of double-junction devices [18] in such a way that one sub-cell can be measured in a current-limiting mode by saturating the other unmeasured sub-cells. The photocurrents generated by the tested PV device and photodiode are converted into voltage signals through $1\ \Omega$ precision shunt resistors. As weak response signals are produced from both the tested PV device and the photodiode, they are connected to different lock-in amplifiers. Thus, the actual current generated from a given wavelength can be distinguished from the background noise (other signals produced from other light sources). The amplified signals and their corresponding irradiances are fed into a Data Acquisition (DAQ) measurement card for recording. The spectral response of a tested PV device is determined by comparing the photocurrent signals generated by the tested PV device to that of the calibrated photodiode at a given wavelength as it is expressed in equation (4.1).

$$SR_{DUT}(\lambda) = \frac{A_{photodiode}}{A_{DUT}} \cdot \frac{I_{sc,DUT}(\lambda)}{I_{sc,photodiode}(\lambda)} SR_{photodiode}(\lambda) \qquad (4.1)$$

The measurement result is presented in a plot of the external quantum efficiency versus wavelength. As the photodiode detector is not placed in the same measurement plane as the tested PV device, the measured spectral response of the tested PV device needs to be corrected with certain scaling factors at given wavelengths. The scaling factors are obtained by measuring the spectral response of a calibrated reference solar cell directly after finishing the device's spectral response measurement. To eliminate any errors during the measurement, the reference solar cell is mounted in the same position and height as the tested PV device on the

measurement plane. The same measurement process is repeated to determine the spectral response of the reference solar cell. The spectral response determinations of this measurement are compared to its calibrated values. The differences in the spectral response at given wavelengths are used as scaling factors to correct the spectral response of the tested PV device.

The spectral response curves of the selected PV devices that are measured using the monochromatic filter method are shown in Figure 4.3.
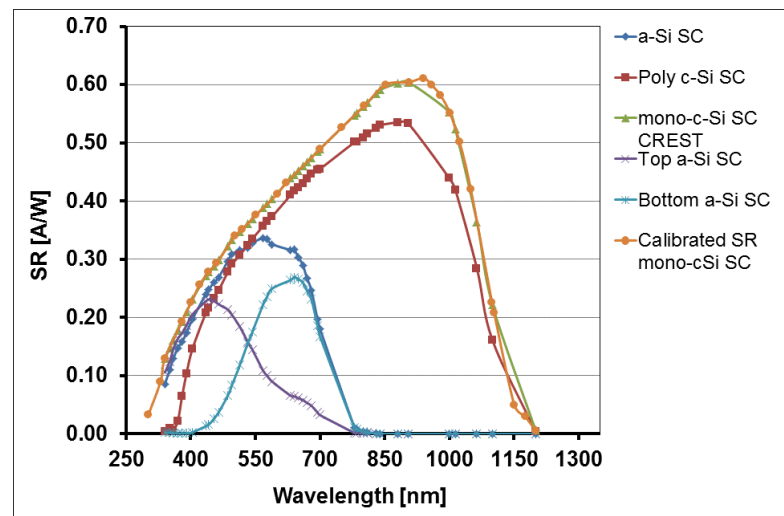
Figure 4.3: Spectral response of selected PV devices measured using the monochromatic filter method

Determining the spectral response of multi-junction (MJ) PV devices is quite different from that of the single-junction devices. The challenge is found in the isolation of the sub-cell to be measured. The individual sub-cells are usually inaccessible due to monolithic series connection between them. As a consequence, if one sub-cell is probed, other sub-cells will affect the measurement [17]. Therefore, to measure the spectral response of a specific sub-cell, it needs to be the current-limiting sub-cell in the MJ structure. Appropriate bias lighting is required to saturate the unmeasured sub-cells and to make the measured sub-cell the limiting one. The level of bias lighting intensity needs to be higher than that of the monochromatic beams illuminating the DUT. However, there is no standard definition regulating how to provide the bias lighting intensity for MJ spectral response measurement.

Conventionally, the application of bias lighting intensity must make the short-circuit current of the measured sub-cell at most one-half of that of the unmeasured sub-cells [18]. To shift the operating voltage of the limiting current sub-cell to its short-circuit condition, it needs to be biased at a voltage approximately one-half the total open-circuit voltage of the overall device. Once the current-limiting sub-cell has been forced through the application of the bias lighting, it is ready for spectral response measurement. The procedure of the spectral response measurement is similar to that of the single-junction PV device from this point onwards.

The MJ PV devices used in this work are double-junction amorphous silicon. They have an open-circuit voltage (V_{oc}) of 7.5 volts and consist of five cells in series. The spectral response determinations of the top and bottom cells which are measured using the narrow band pass filter method are shown in Figure 4.3. To ensure that each sub-cell produce a limiting current at about one-half the short-circuit current of the other sub-cell, the top cell is measured under amber bias light intensity at 80% and ultraviolet at 5% and the bottom cell is measured at amber intensity 5% and ultraviolet 80%. The bias voltage applied is at 3.75 volts. How to apply the bias lighting and voltage bias to measure the spectral response of a tandem solar cell can be found in [18].

4.3. Spectral Response Measurement using Polychromatic Filter Method

The validation of the new spectral response fitting method in the small-area spectral response measurement rig is realised by changing the set of filters from the narrow band pass filter set to one of polychromatic filters. As have been shown in Figure 3.10, the spectral response fitting method requires some variations in the measured current and spectral data as inputs for the fitting algorithm. A spectro-radiometer is used for measuring the spectrum of a given filter and the current generated is measured using a Keithley source-meter unit (Figure 4.4). Some alterations are made to the arrangement of the measurement units in the small spectral response measurement system. The major changes are replacing the chopper and lock-in

amplifier used in the monochromatic filter method with a Keithley source-meter unit and spectro-radiometer.
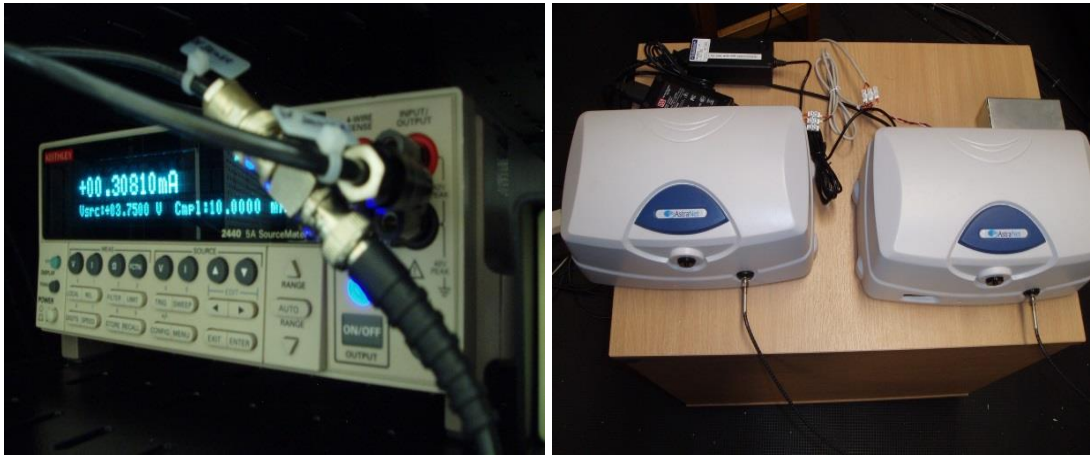
a. Keithley source-meter unit   b. AstraNet spectro-radiometer

Figure 4.4: Instruments used in the polychromatic filter method

The arrangement of these instruments and procedure of how to perform spectral response measurements using the polychromatic filter method are explained in the following section.

4.3.1. Experimental Setup for a Small-area System

The experimental setup of the polychromatic filter method consists of a light source, a set of polychromatic filters, a source meter unit, a spectro-radiometer unit and a computer to control the measurement and log data. A schematic of the spectral response setup using the polychromatic filter method is shown in Figure 4.5.

1. Polychromatic Filters
2. Shutter
3. Homogeneiser
4. Mirror
5. Photodiode
6. a tested PV device
7. Diffuser
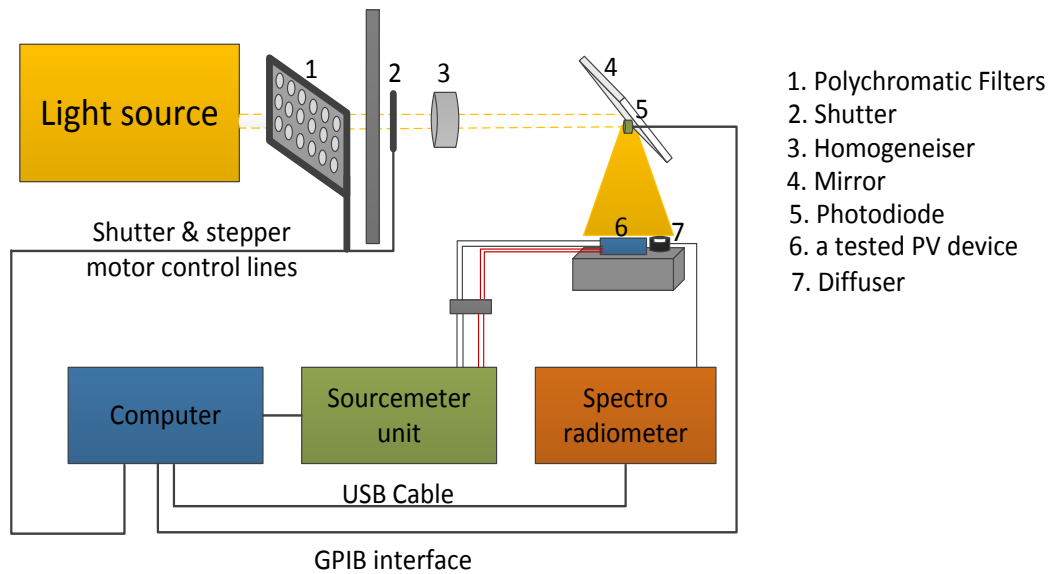
Figure 4.5: A schematic of SR setup using a polychromatic method

The same light sources, i.e. a 150 W continuous xenon arc lamp and 100 W halogen lamp as used in the monochromatic method are employed in the polychromatic method. However, only the xenon arc lamp is used to provide a spectral irradiance from the visible to the near infrared (300 nm to 1200 nm) ranges with an acceptable intensity. The tested PV device is placed horizontally in the centre of the illumination area of the measurement plane as shown in Figure 4.6.
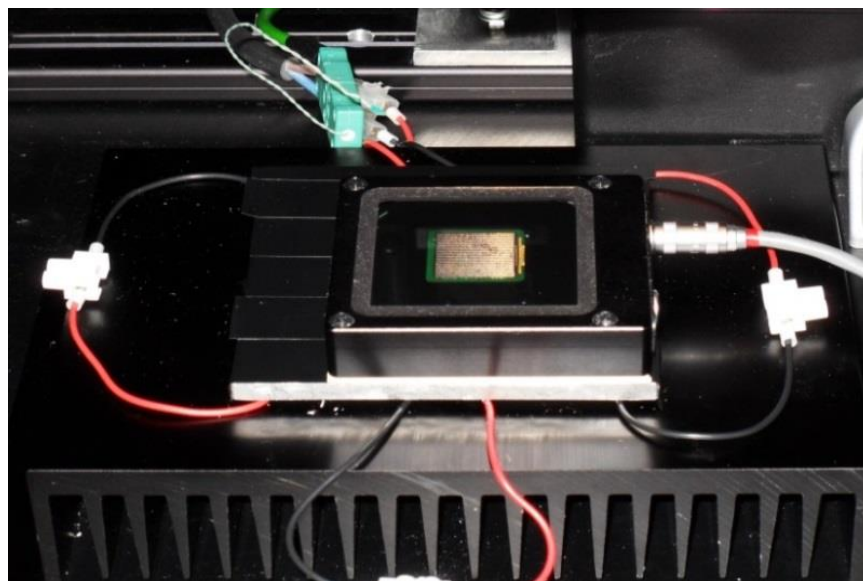
Figure 4.6: Arrangement of the tested PV device for small-area spectral response measurement

The tested PV device is directly connected to the Keithley 2440 source meter unit using a 4-wire connection as shown in Figure 4.7 for current measurement and voltage biasing. The advantage of the 4-wire connection is to eliminate errors associated with voltage drop in the connection cable. This connection increases accuracy in the measurement and ensures that the response current signal from the device is measured at a short-circuit condition (0 volts).
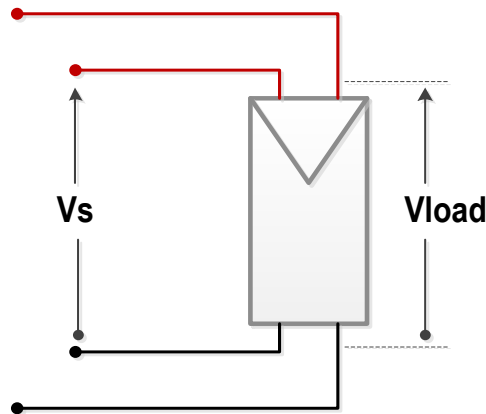
Figure 4.7: A schematic of the 4-wire measurement, Vs = Vload

The spectral irradiance throughput of a given polychromatic filter is detected via a diffuser-covered optical input and transmitted directly to the AstraNet spectro-radiometer using a fibre optic cable. This spectro-radiometer is equipped with charge coupled device (CCD) array detectors. It can be used to measure the spectral irradiance from 300 nm to 1700 nm. The advantage of using a CCD spectro-radiometer is that it can acquire an absolute spectral irradiance measurement within short measurement time. It is connected to a control PC via USB. The instruments are equipped with different irradiance sensors. One spectro-radiometer uses a Si detector to measure spectral irradiance in a visible range from 243 nm to 1028 nm and another spectro-radiometer uses InGaAs detector for detecting spectrum in the near infrared range from 623 nm to 1787 nm. The two spectro-radiometers are connected together using a diffuser detector with a dual optical fibre. To regulate the detectors' temperature evenly at their normal operating conditions, each instrument is equipped with a Peltier cooling element. Before starting the spectral measurement, both spectro-radiometers have been calibrated indoor using a Newport calibrated quartz tungsten halogen standard lamp.

The polychromatic filters comprises of three glass filters and 12 lighting gel filters, which are the same selected filters used for proving the concept in previous chapter in section 3.5. These filters are arranged sequentially in a square filter frame with a size of 337x192 mm^2 as shown in Figure 4.8 and placed in the same chamber as the light source. Each filter can be accessed easily for the measurement, as the filter frame is mounted on an x-y movement stage as shown in Figure 4.8.
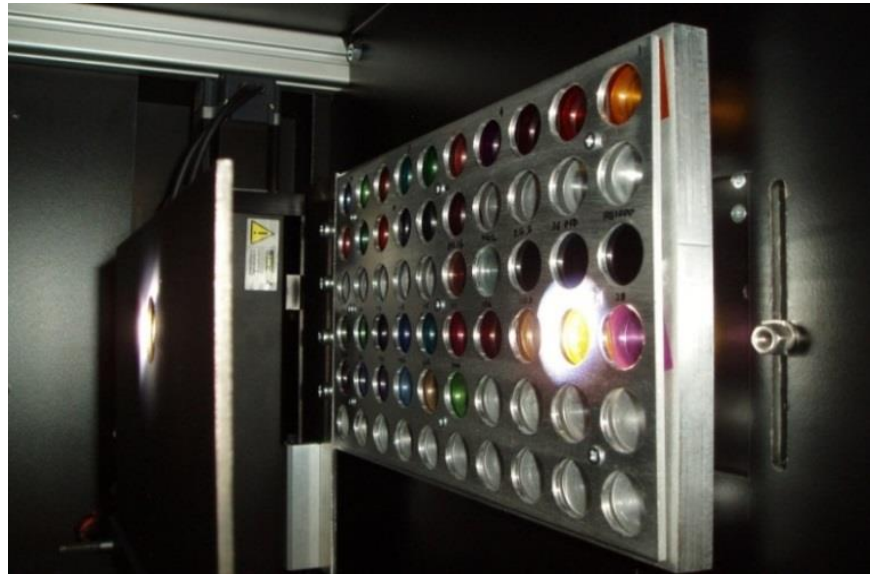
Figure 4.8: Arrangement of polychromatic filters in their filter holder

4.3.2 Measurement Procedures

The intensity of the beam transmitted through each polychromatic filter is sufficient to generate a response signal from a tested PV device, measurable directly by the source-meter unit. As a result, bias lighting is unnecessary for measuring single-junction PV devices. The current generated at each specific spectrum is measured directly under dark and light conditions in order to obtain high accuracy in the current measurement. Accordingly, the actual measured current is determined by subtracting the current measured at dark conditions from that measured at light conditions.

Due to the non-perfect uniformity of illumination at the measurement plane and small illumination area, placing a tested PV device side by side and coplanar with the diffuser of the spectro-radiometer is not possible. Therefore, the output spectra of the

selected polychromatic filters must be measured separately from the current measurements as shown in Figure 4.9a. A photodiode is used to detect changes in the total irradiance of the measured spectra. Its position is aligned with the filters and facing the opening slit (Figure 4.9b). Both the diffuser and tested PV device are positioned at the same height on the measurement plane. This ensures that both devices receive the same intensity under illumination by each polychromatic filter.
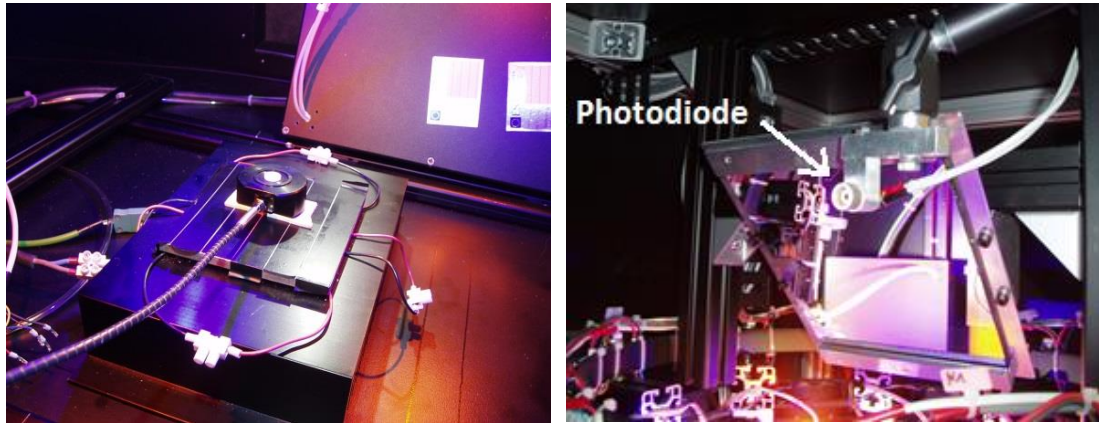
a. Diffuser of spectro-radiometer   b. Photodiode monitor

Figure 4.9: Spectral measurement and position of photodiode solar cell in the SR measurement system

As the measurements taken with this particular spectro-radiometer are temperature dependent, the measurements are performed at 20°C, the calibration point of the spectro-radiometer. The spectral throughput of a given polychromatic filter is measured by illuminating the diffuser of spectro-radiometer at dark and light conditions. The dark condition is used to provide baseline zero for the measured spectrum at the light condition. During the spectral measurements, the output spectrum of each polychromatic filter is correlated to the photodiode current response (used later for comparison of lamp output stability). In this way, all the spectra produced with the polychromatic filters are measured only once. Any changes in the total irradiance of spectrum illuminating the PV device during the spectral response measurement will be detected by the photodiode. The measured spectra of all selected polychromatic filters and their correlating photodiode currents are stored in the fitting algorithm. To suit the format input of the fitting algorithm, these spectral data are interpolated from 300 nm to 1700 nm with a wavelength step

of 1 nm and stored as a regular array of wavelengths and correlating spectral irradiance values.

Having the measured spectra, the current produced from a tested PV device at each filter is measured, and at the same time the photodiode's current is recorded. The photodiode's currents obtained during the device current measurements and those during the spectral measurements are used as scaling factors to correct the measured spectra of a tested PV device. Thus the changes in the lamp output are accounted for. All the measured currents are inputted into the fitting algorithm to optimise the coefficients of the chosen spectral response model.

4.3.3 Fitting Approach

Referring to the schematic of the SR fitting approach (Figure 3.10 in Chapter 3), after obtaining the measured short-circuit currents and their correlating spectral irradiance data, the next step is to find the appropriate coefficients of the chosen SR model by fitting the measured currents to the calculated currents.

To function well, the fitting algorithm also requires other input data, i.e. device area and a set of initial values for the coefficients of the chosen SR model. The fitting algorithm works iteratively to tune the calculated currents to the measured currents. Once the fitting criterion is met, the best fitted coefficients for the chosen SR model are obtained. These coefficients are inputted back into the selected SR model to return the SR of the tested PV device.

4.4. Validation of Polychromatic SR Determination

This section presents experimental results of spectral response determination using the polychromatic filter method. Qualitatively, good agreement was found between the spectral response curves of the mono-crystalline silicon device obtained using the monochromatic and polychromatic filter methods as shown in Figure 4.10. To examine the effects of bias lighting on the spectral response determinations using the polychromatic method, the spectral response of the tested device is measured with and without applying the bias lighting to superimpose the polychromatic beams. The

bias lighting is provided from the same LED system that is used in the monochromatic filter method.
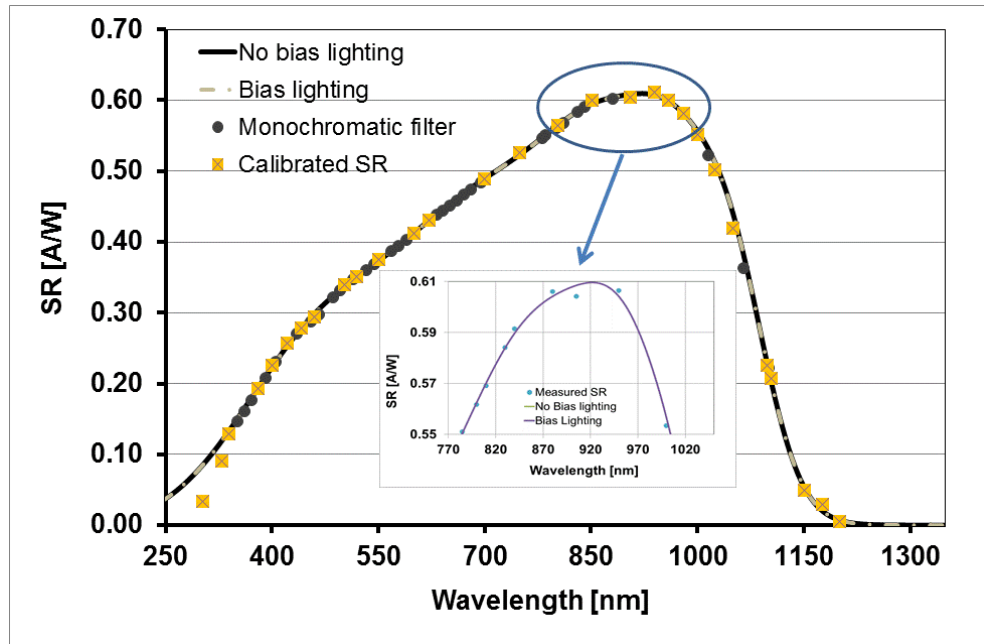
Figure 4.10: Comparison of two different methods for SR determination of mono-crystalline PV device

As shown in Figure 4.10, the application of the bias lighting does not have significant effects on the spectral response determinations of the mono-crystalline silicon device. This implies that the bias lighting is not required in the polychromatic filter method. It is also confirmed that the two spectral response curves obtained monochromatically from an accredited laboratory and at CREST, are aligned across the entire spectral response band. This verification provides additional assurance that the results obtained using the CREST spectral response measurement system is credible. The numerical agreement between the two different spectral response methods is shown in Figure 4.11.
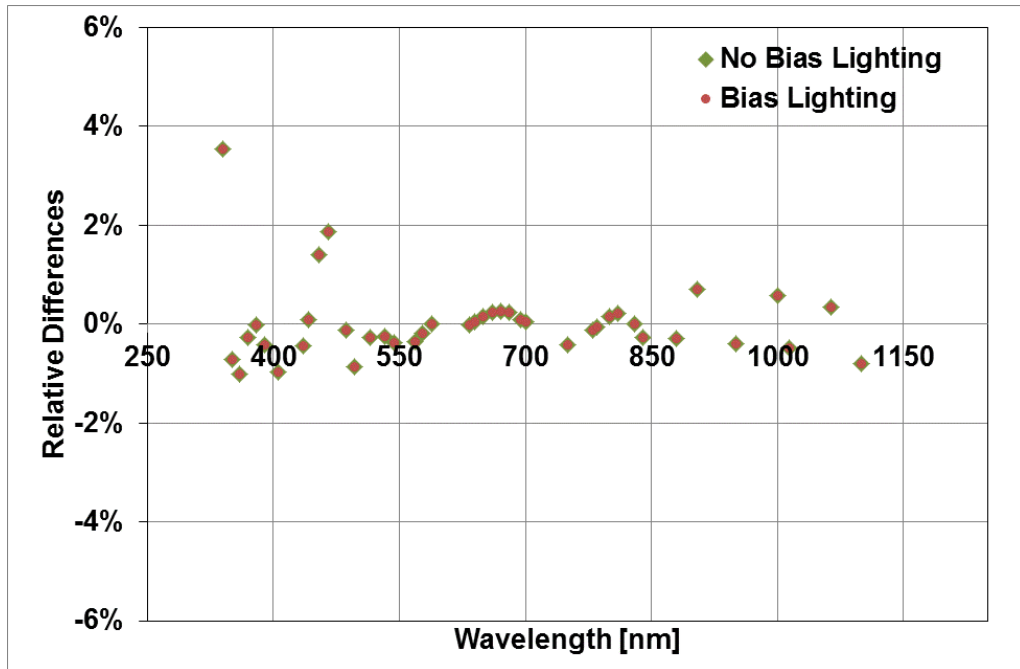
Figure 4.11: Deviations in the SR determination of mono-crystalline PV device using two different SR measurement methods

As shown in Figure 4.11, the deviations between the monochromatic filter and the polychromatic filter methods are less than ±2% across the entire spectral response band. The effect of applying bias lighting during the polychromatic method measurements is negligible.

To verify the general applicability of the proposed method, the method is used to obtain the spectral response of other selected PV devices: amorphous silicon, poly-crystalline silicon and tandem amorphous silicon PV devices. The determinations of their spectral response are also performed with and without the applications of the bias lighting. The results of these verifications are shown in Figure 4.12, Figure 4.14 and Figure 4.17. The differences in their spectral response determinations to those of using the monochromatic filter method are shown in Figure 4.13, Figure 4.15 and Figure 4.18.
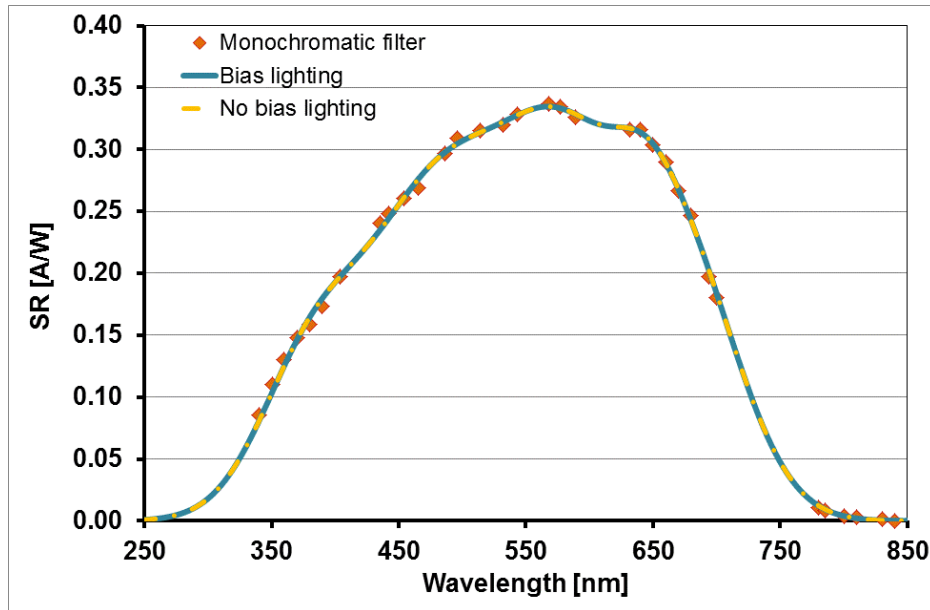
Figure 4.12: Comparison of two different methods for spectral response determination of the amorphous silicon device
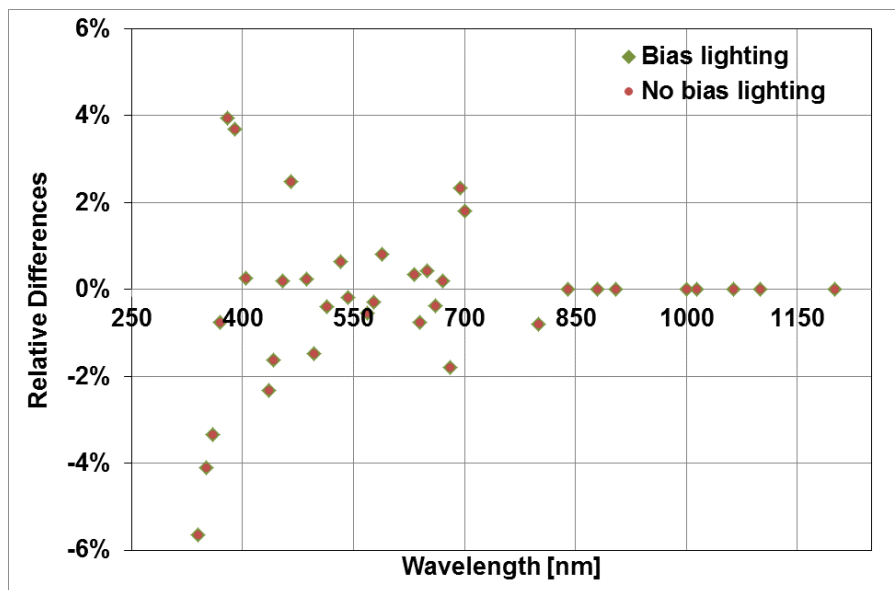
Figure 4.13: Deviations in the spectral response determination of amorphous silicon PV device using two different spectral response measurement methods

The agreement is not achieved well in the UV range as shown in Figure 4.13, where the deviations in the spectral response determinations rise to ±6%. Due to the nature of the intensity of the light spectrum in the UV range is very low and this light is only absorbed in the surface (emitter part) of a PV device, the device' response in this measurement range is very difficult to be detected. The measurement uncertainty

in this UV range becomes quite high as the signal to noise ratios (SNR) in this measurement range is extremely low (Figure 3.2). The measurement point produced by the polychromatic filter method in the UV range is very small. When this value is compared to the corresponding measurement point produced from the monochromatic filter method, it produces a large percentage deviation. However, this large deviation only occurs at an extremely weak part of the spectral response. Therefore it can be negligible. The agreement in other wavelengths (450 nm to 660 nm) is excellent with differences approximately ±2%. It also shows that the application of bias lighting is not required for measuring a-Si devices, even with their weak photocurrent density, as the light intensity illuminating the device is higher than for monochromatic measurements.

A good correlation between the two measurement methods is also demonstrated in the spectral response determination curves of a polycrystalline PV device as shown in Figure 4.14.
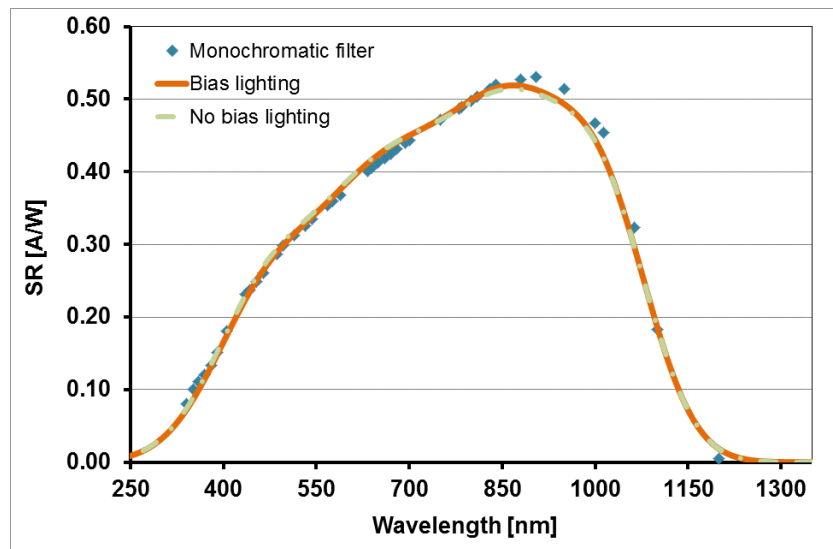
Figure 4.14: Comparison of two different methods for SR determinations of polycrystalline PV device

As it is shown in Figure 4.14, there is a slight difference between the spectral response curves with and without the application of bias lighting. However the impact of the application of the bias lighting is almost negligible particularly in the visible range compared to the spectral response curve obtained without the bias

lighting. Applying the bias lighting only brings the measurement points in the UV range closer about 3% to that of using the monochromatic filter method. The differences in the spectral response curves between the two measurement methods are still quite high in the UV and infrared ranges which are up to approximately 14% and 8% respectively. The large deviations in these measurement ranges have quite similar trends to the previous spectral response determination curves (Figure 4.11 and Figure 4.13) which occur in the extremely weak points in the spectral response curves. However, the differences in the visible range are quite impressive less than ±3%.
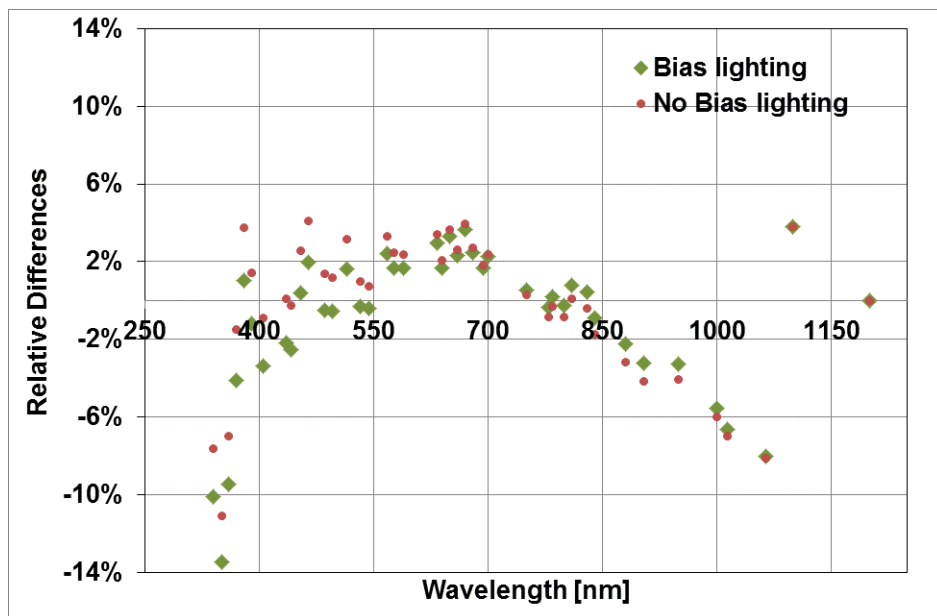
Figure 4.15: Deviations in the SR determination of polycrystalline PV device using two different SR measurement methods

The polychromatic filter method has also been tested on a multi-junction device (an amorphous silicon double-junction mini-module, as described in section 4.2. Prior to applying the polychromatic filter method, the monochromatic filter method was used to determine spectral response of the solar cell. To measure the top and bottom cells, different colours and intensity of bias lightings are applied as shown in Figure 4.16.
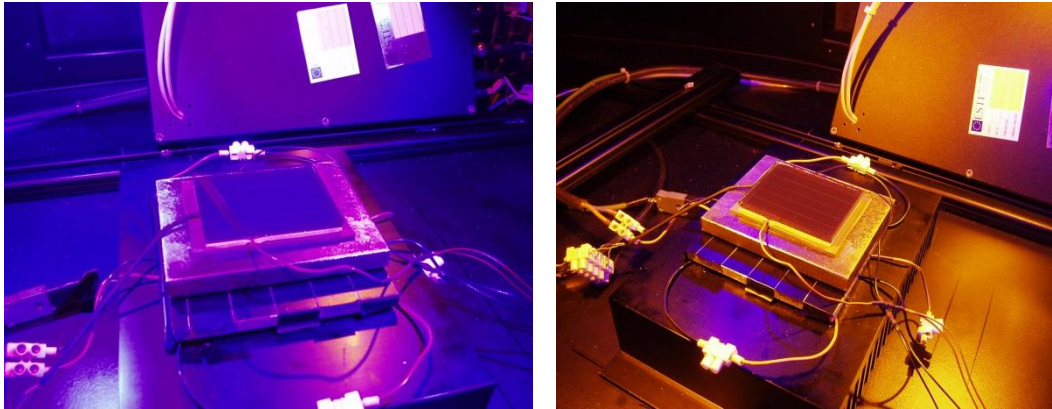
a. Top cell (UV=80%; Amber=5%)   b.Bottom cell (UV=5%; Amber=80%)

Figure 4.16: Different compositions of bias lightings for measuring top and bottom sub-cells of a double-junction solar cell

The same compositions of bias lighting are applied during the polychromatic filter method. The procedure for measuring one sub-cell is similar to that applied to measure a single-junction PV device. Results of the spectral response determinations are shown in Figure 4.17. As can be seen in the figure, the two spectral response curves obtained using the monochromatic and polychromatic filter methods are well-matched with deviations within ±2% across wavelength bands as shown in Figure 4.18. These findings reveal that the polychromatic filter method is also feasible for determining spectral response of double-junction PV devices.
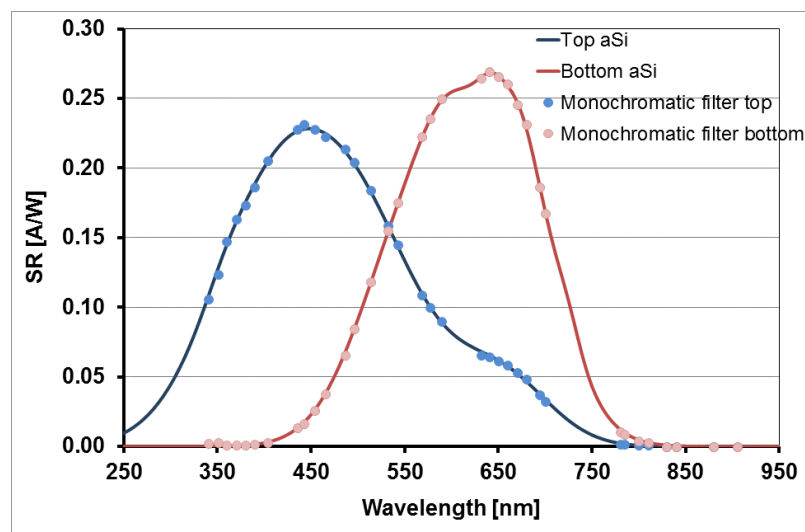
Figure 4.17: Comparison of two different methods for SR determinations of double junction amorphous silicon PV device
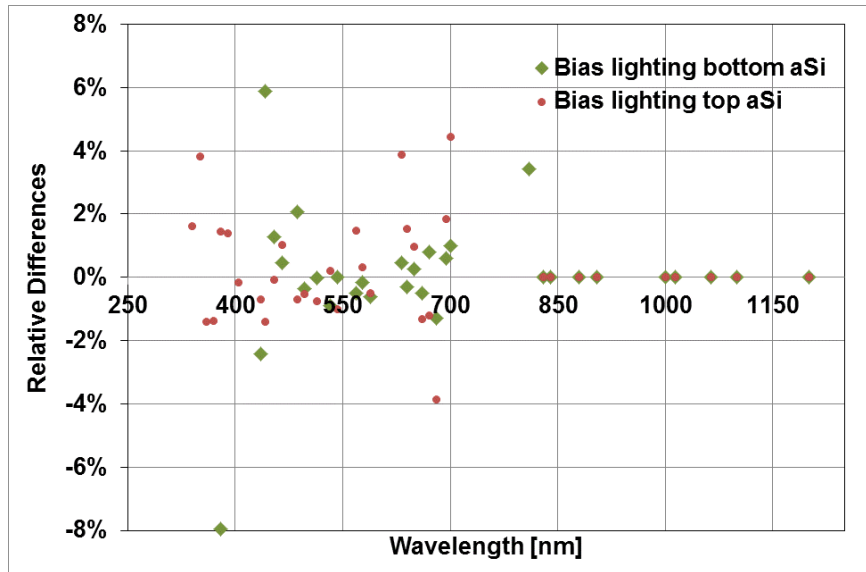
Figure 4.18: Deviations in the SR determination of double junction amorphous silicon PV device using two different SR measurement methods

4.5. Sensitivity analysis of the Spectral Response Fitting Method

As with all measurements, spectral response determinations using the polychromatic filter method contain some measurement uncertainties. The possible error sources contributing to the final uncertainty of the polychromatic filter method results are listed in Table 4.2. These uncertainty sources can be grouped into the measured currents, the measured spectra, and the choice of initial values of coefficients for the chosen spectral response model. Uncertainties in the measured spectra can be influenced by the stability of the light source, the homogeneity of spectral illumination on the measurement plane, temperature conditions and the precision of the spectro-radiometer.

Measurement	Fitting algorithms

• **Light source:**
  – Spatial uniformity of polychromatic beams
  – Stability/repeatability
• **Current measurement:**
  – Method of cable connection
  – Accuracy of the source meter unit
• **Spectral measurement:**
  – Device position (height)
  – Sensor position and orientation
  – Accuracy of spectral measurement unit
• **Ambient temperature** during measurement
• **Device linearity and area**
	• **Spectral response model**
	
	• **Initial values for the coefficients of the chosen SR model**
	
	• **Fitting functions and criteria**

Table 4.2: Error sources in the polychromatic filter method

The non-uniformity of the spectral output of xenon lamp varies with the illumination area. These variations are shown in Figure 4.19.
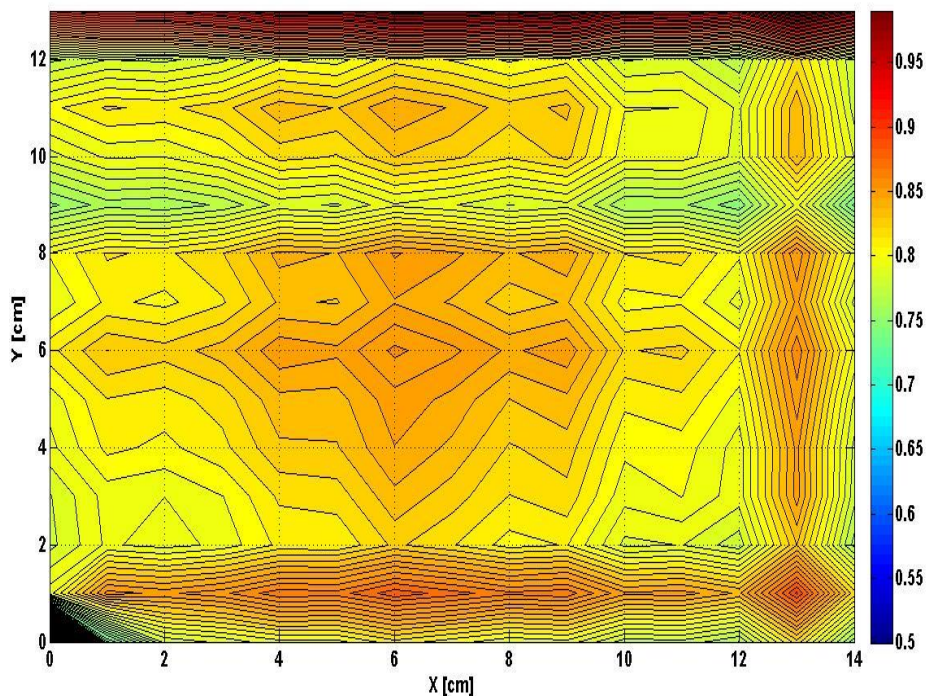
Figure 4.19: Non-uniformity of spectral output of Xenon arc lamp in the small-area SR measurement at CREST with an illumination area of 14 cm x 13 cm

As shown in Figure 4.19, the non-uniformity of irradiance on the measurement plane is very high at approximately 37.2%. This uniformity level is not suitable for the performance measurement test. To achieve the suitable uniformity level as has been prescribed in the international standard IEC 60904-9 [49], the area of the measurement plane needs to be minimized. After the reduction, the minimum level of the non-uniformity irradiance that can be reached on the measurement plane is at 8.5% for an illumination area of 12x10 cm^2. This non-uniformity level corresponds to Class B solar simulator and limits the size of PV device that can be measured in the small-area SR measurement system.

After knowing the information of homogeneity level of irradiance on the measurement plane, the stability of the xenon arc lamp that is used in the measurement system is measured and the results are shown in Figure 4.20.
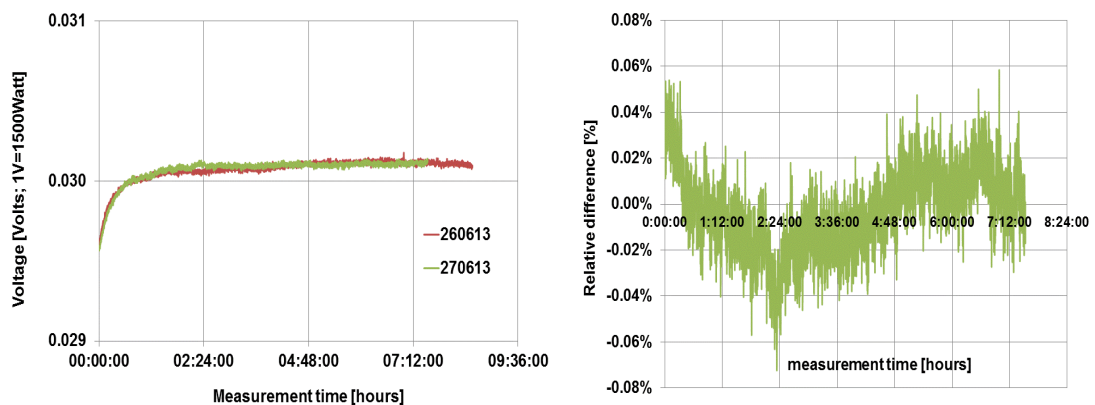
    a. Irradiance Versus time   b. Relative difference in irradiance

Figure 4.20: Stability of xenon arc lamp in the small-area SR measurement system at CREST

As shown in the figure, the intensity of the xenon lamp stabilises after 2 hours of operation time and it is repeatable with a relative difference of 0.02% between two consecutive days of measurements. The long-term instability of the xenon lamp is 1% [49]. From the non-uniformity and stability measurements, it is clear that the spectral response measurement system can only accommodate small-area PV devices with maximum dimensions of 100 mm by 100 mm and the spectral measurement generally cannot be done at the same time as the device current measurement

because of the limited space in the test plane. However, the lamp stability allows sequential measurements of current and spectrum, within a small, quantifiable uncertainty.

To determine to what extent the effects of individual input parameters (the current, spectra and initial values of the fitted coefficients) on the device spectral response results, their sensitivity is analysed using a Monte Carlo approach. In this technique, each input parameter is randomly varied within certain uncertainty levels, i.e. 2%, 3%, 4%, and 5%. For each uncertainty level, the numbers of the tested input parameter are generated randomly for 10000 measurement points using the Gaussian probability distribution functions. These measurement points are inputted into the fitting algorithm in order to derive the best fitted coefficients of the spectral response model and to obtain the spectral response curve of the tested device. To observe changes in the device spectral response curve due to the changes in the uncertainty level of the tested input parameters, the generated spectral response curves are averaged and compared to its true curve. The random numbers for the spectral measurement points are generated as a function of wavelengths at defined uncertainty levels. For the initial model coefficient values, their random numbers are made by varying a set of initial values that have been used in the fitting algorithm to produce a well-matched spectral response curve. When one input parameter is tested, the others are kept at their original values. Thus, the influence of individual parameters on the accuracy of the spectral response determinations can be determined. The results of sensitivity analyses of individual parameters to the spectral response determination are shown in the following figures.

Effects of uncertainty in the current measurement

Effects of uncertainties in the measured currents on the accuracy of the spectral response determinations can be seen in Figure 4.21. As it is shown in the figures, there are no significant changes in the device spectral response curve when the uncertainty in the current measurement is increased from about 2% to 3%. Deviations between the average and the true spectral response curves are observed particularly in the peak of the two curves (in the range of 700 nm to 1000 nm of the wavelength intervals) when the uncertainty level in the current measurement is

increased from 4% up to 5%. The increase in the uncertainty level of the current measurement by 4% to 5% has lowered the device spectral response curve by 4% to 5% from its true curve. This observation reveals that to obtain an accurate spectral response curve of a tested PV device, the uncertainty level in the current measurement should be less than 4%.
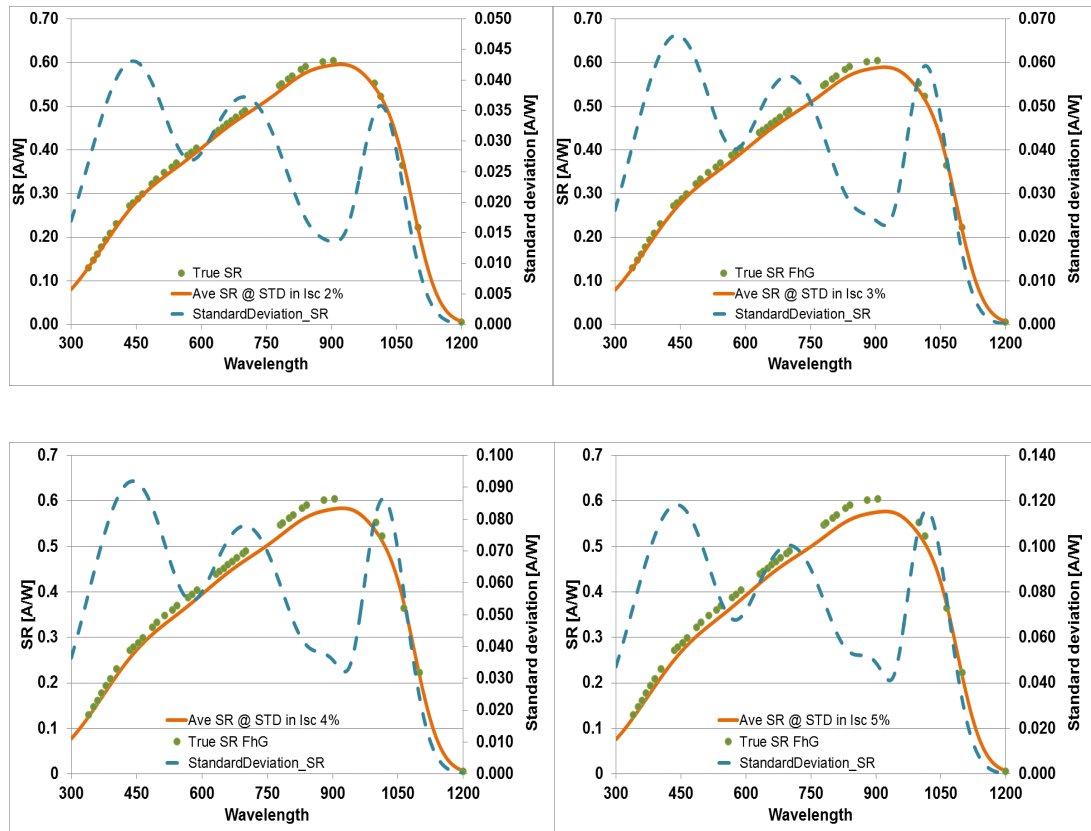
Figure 4.21: Effects of the uncertainty in the measured currents on the accuracy of SR determinations

Effects of uncertainty in spectral measurement

The accuracy of the measured spectra significantly influences the uncertainty in the device spectral response curve as shown in Figure 4.22. The effects of the increasing uncertainty in the measured spectra are detected in the orange range (633 nm) up to the infrared range (1000 nm) of the wavelength spectrum when the uncertainty in the measurement spectra is increased from 4% up to 5%. The deviations in the spectral response curves are clearly observed around the peak of the curves when the uncertainty in the measured spectra is increased up to 4%. This implies that to obtain

113

an accurate spectral response determination using the polychromatic spectral response fitting method, the spectro-radiometer that is used to measure the spectra illuminating the PV device under test must have measurement uncertainty less than 4%.
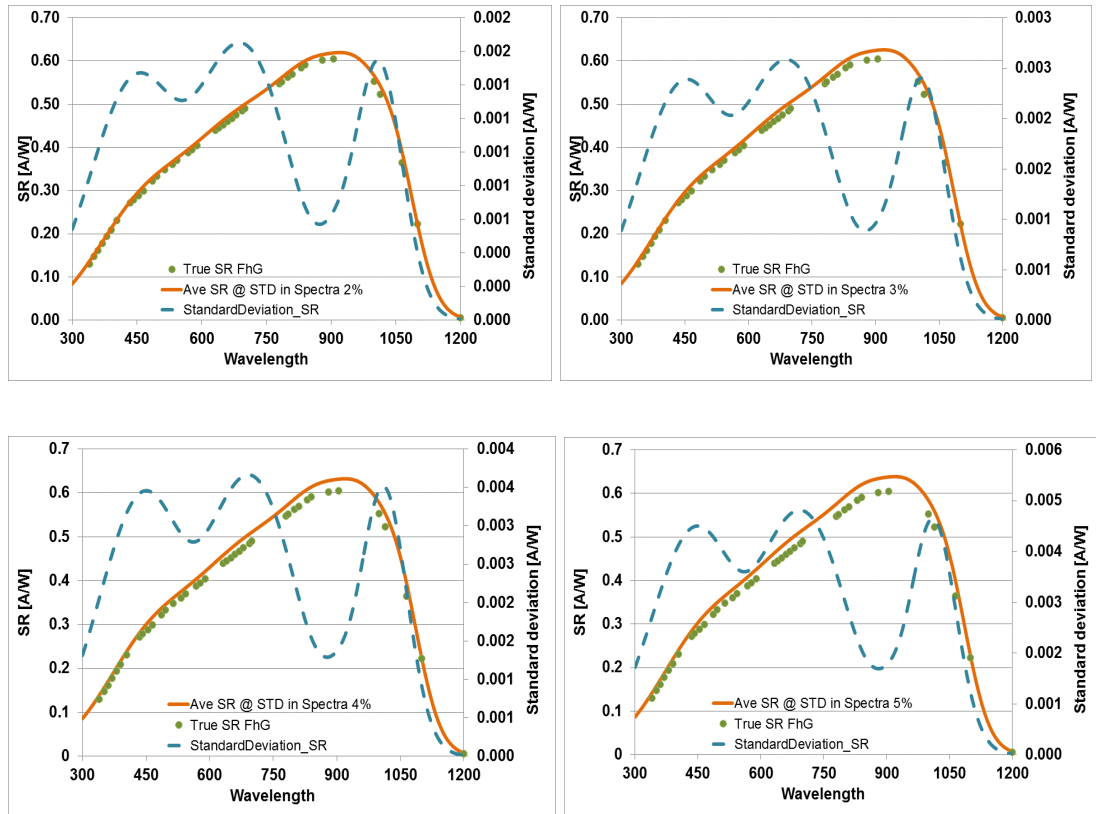
Figure 4.22: Effects of the uncertainty in the measured spectra on the accuracy of SR determinations

Effects of uncertainty in the initial values of the fitted coefficients

Choosing appropriate initial values for the coefficients of the chosen spectral response model is considerably important for the accuracy of the spectral response curve. This can be seen in Figure 4.23. The deviations in the shape of the device spectral response curve are clearly observed when the changes in the uncertainty level of the initial values are made even for 3%. This shows that choosing appropriate initial values for the chosen spectral response model is critical for the polychromatic filter method.
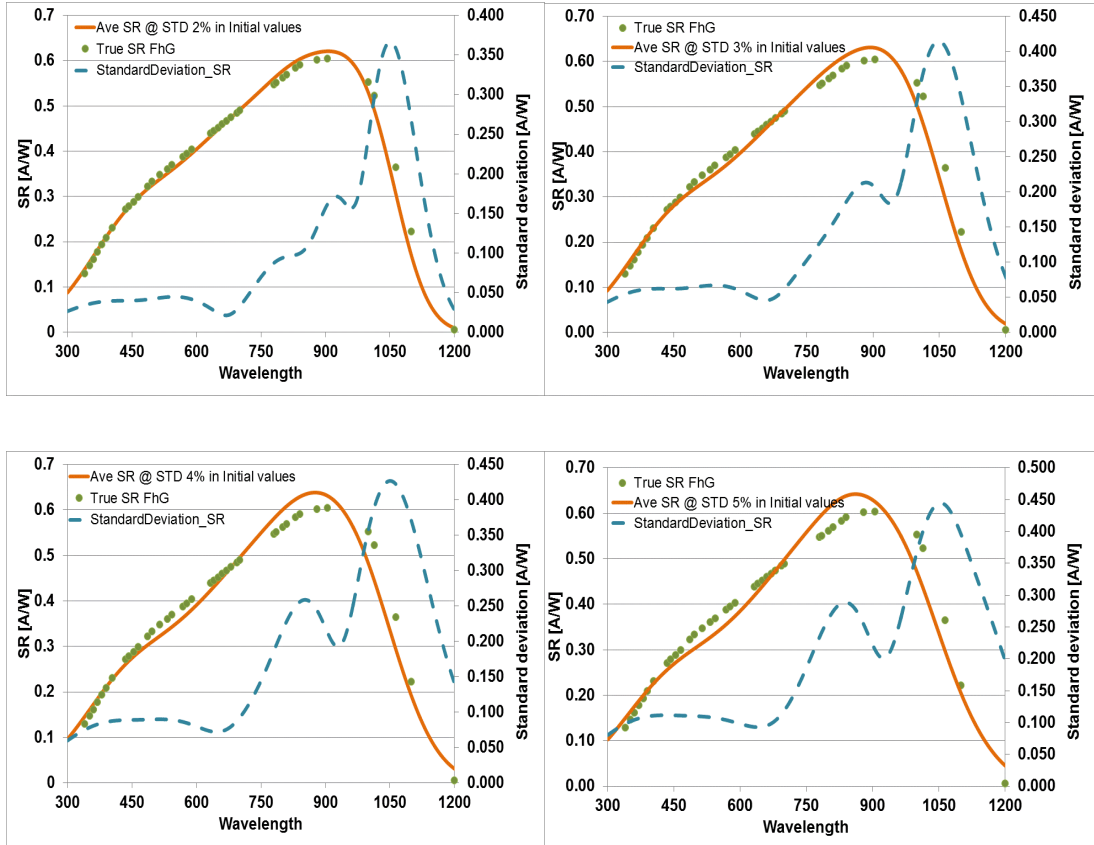
Figure 4.23: Effects of the uncertainty in the initial values for the coefficients of the chosen SR model on the accuracy of SR determinations

4.6. Conclusions

The concept of spectral response fitting method for spectral response determination, proved by simulation in the previous chapter has been validated experimentally. Using polychromatic filters for obtaining the spectral response of a tested PV device is not only feasible, but compares favourably with established methods. The key success of the proposed method is strongly dependent on the accuracy of its input parameters, particularly the initial values for the fitted coefficients of the chosen spectral response model and of the measured spectra. Implementing the proposed spectral response method as a new tool for spectral response determinations requires high precision and accuracy in the current and spectral measurements. Variations in the measured currents, spectra and the initial values of the chosen coefficients are intolerable in the fitting algorithm even up to 4% uncertainty.

As the need for a large-area spectral response measurement is inevitable, it is important to examine the feasibility of the fitting concept for a large-area spectral response measurement. This will be explored further in the following chapter.

Chapter 5

Spectral Response of Large-Area PV Devices

5.1. Introduction

Having demonstrated the spectral response fitting concept for determining spectral response curves of a selection of small-area PV devices, this chapter demonstrates the up-scaling of the method for measuring a large-area, full module-scale PV device. In the first section, different existing approaches for a large-area spectral response measurement are reviewed, including the challenges that have been encountered. Section 5.3 presents the experimental setup modifications to obtain the spectral response using the polychromatic fitting method. Section 5.4 addresses the validation of the polychromatic method for large-area spectral response measurements. Section 5.5 analyses the problems associated with the specific implementation of the polychromatic spectral response fitting method in the PASAN solar simulator system. The chapter ends with conclusions on the feasibility of using the polychromatic method for large-area spectral response measurements.

5.2. Approaches to Large-area Spectral Response Measurement

Due to series-connected PV devices, measuring spectral response of a large-area PV device (module size) becomes challenging because it requires a large beam size to fully illuminate the entire module uniformly and powerful beam intensity on the measurement plane. The beam intensity that is transmitted from a monochromatic filter is limited by the bandwidth of its spectral transmittance. This becomes the practical limit of the current signal strength produced. Increasing the size of monochromatic beam can reduce its intensity on the measurement plane and finally,

it can also reduce the signal strength produced from a tested PV device. To date, only few institutions are able to perform a spectral response measurement on full-sized PV modules: the National Renewable Energy Laboratory (NREL) in the USA [59], the PV calibration laboratory of Fraunhofer ISE (ISE CalLab) in Germany [76], the National Institute of Advanced Industrial Science and Technology (AIST) in Japan [66], the European Solar Test Installation (ESTI) of the European Commission in Italy [69], the University of Applied Sciences and Arts of Southern Switzerland (SUPSI-ISAAC) in Switzerland [85, 86] and the TUV Rheinland laboratory [87, 88] in Germany.

These institutions have applied quite similar measurement methods to obtain the spectral response of large-area PV devices, based on **the application of a series of monochromatic beams (the filter-based method)**. However, there are some differences in their approaches in terms of how the monochromatic beams are applied to the tested PV device, and the requirements for bias lighting and a lock-in technique for current measurements. Different techniques for measuring a large-area PV module proposed by different institutions are summarised in the following table.

Institution	Measurement technique	Target area of measurement
NREL [59]	- Filter-based method - Different intensity of bias lighting for the target cell and other cells in the module - Voltage bias - Lock-in technique	One cell in the module
Fraunhofer ISE [76]	- Filter-based method - Different bias lighting for the target cell and other cells in the module - Lock-in technique	One cell in the module, is separated optically from other cells using a square aluminium duct
AIST [66]	- Filter-based method - Different bias lighting for the target cell and other cells in the module - Lock-in technique - Voltage bias	One cell in the module
ESTI [69]	- Filter-based method - No bias lighting - No lock-in technique	The entire module is fully illuminated

TUV [87]	Adopting the AIST approach	One cell in the module
SUPSI, ISAAC [85, 86]	- Filter-based method - No lock-in technique	The entire module is fully illuminated

Table 5.1: The state of the art of the approaches for measuring a large-area spectral response of a PV device

Measuring the entire module area looks simple as there is no lock-in technique and bias lighting is required as have been implemented at ESTI and SUPSI. However, some problems are encountered in the measurement approach: the uniformity of monochromatic beams on the measurement plane as reported by NREL [59] and ESTI [69]. This makes different cells limiting at different wavelengths as a result of the non-uniform monochromatic beam incident on the tested PV device.

The non-uniform monochromatic beam is produced from the variations in the spectral transmittance of the filter and the spectral output of the xenon lamp as have been highlighted in Figure 3.1 in Chapter 3. The spectral response which is produced by different cells at different wavelengths cannot be used to represent the true spectral response of the module. This is because each individual cell has a different current response at any given wavelengths as a result of a different weight in the irradiance illuminating the entire module and the current-limiting cell does not then operate at its local short-circuit condition [59]. For certain PV devices such as an amorphous silicon module which exhibits voltage dependent spectral response, this condition significantly affect the accuracy of its spectral response determination. The spectral response of this PV device will be higher at the short-circuit voltage than at the maximum power point voltage [89]. To avoid this problem, a typical spectral response of a single-junction PV device should be measured at the short-circuit voltage by applying bias voltage at the output terminals of the tested module as have been described in the international standard IEC 60904-8 [4]. In this way, the operating voltage of the current limiting cell is ensured at the short-circuit condition. As the cells in a PV module behave like a multi-junction PV device, the application of the bias voltage is related to the measured open-circuit voltage (V_{oc}) of the module as written in the equation (5.1) [59].

$$V_{bias} = \frac{(n-1)}{n} \times V_{oc} \qquad (5.1)$$

Where n is the number of cells in series

119

One approach which is by partially illuminating one cell in the module has been suggested by NREL and AIST [59, 66] to ensure that only one cell limits the total current of the module at different wavelengths. This approach has been practiced at the TUV Rheinland laboratory for industrial applications [87]. To distinguish one measured cell from other cells in the module, the application of a proper bias lighting is required to make them current-limiting. Choosing appropriate bias lighting is considered significant for obtaining accurate spectral response determinations. For a single-junction spectral response measurement, white bias lighting with different intensity is applied to the target cell, while for a multi-junction spectral response measurement, different colours of bias lighting is applied to the target cell. A lock-in technique is still required to detect the measured current, to separate the monochromatic response from the bias light-induced response. This partial spectral response approach is not only practical for measuring crystalline silicon PV modules where each cell is separated spatially from other cells but also other PV technologies such as thin film PV devices. However, there is a problem encountered with the application of this partial approach, which is a very weak signal response produced from the target cell. This is due to low irradiance level of the monochromatic beam incident on the target cell as reported by Hishikawa [66]. To make the target cell limiting, high intensity of monochromatic beams is required.

The accuracy of the spectral response measurement using the monochromatic filter-based method is significantly influenced by the quality of the monochromatic beams illuminating the tested PV device as have been mentioned before in section 3.2. To avoid bandwidth error and to obtain high resolution of the spectral response determination curve, the bandwidth of a monochromatic beam should be narrowed to below approximately 10 nm [74]. In relation to the above, and depending on the light source, this sets a limit on the absolute power of the beam. As a result, an extremely weak current signal is produced which can introduce high measurement uncertainty as shown Figure 3.2. Another problem exists in the application of the band-pass filter is the spectral deviation of the centre wavelength of the quasi monochromatic filter [76]. This deviation is caused by the shift in the filter transmittance of the blocking region due to the relative shape of the lamp's spectrum and spectral response of the tested device. Due to this spectral deviation, the spectral response determination of a

tested PV device becomes inaccurate. As have elaborated in Chapter 2, the mounting position of the filter can also introduce stray light on the measurement plane due to high angle of incidence. Since a large number of monochromatic filters are required to produce accurate spectral response results, the cost for building such a spectral response measurement system becomes high. This can affect the testing cost for measuring the spectral response of a PV device as have been implemented at TUV Rheinland laboratory.

Aiming to improve the accuracy in a large-area spectral response measurement, the feasibility of up-scaling the spectral response fitting method using polychromatic filters is assessed. The potential advantage of this approach is that it can provide higher beam intensities and hence larger beam sizes onto the illumination plane without any problems related to bandwidth as found in the monochromatic filter method. As a result, the entire area of a tested PV device can be fully illuminated with uniform light of reasonably high intensity. The following section explains the experimental work required in the integration of the method into the industrial-standard, pulsed-light solar simulator in use at CREST for module I-V characterisation.

5.3.   Experimental Setup and Methodology

The validity of the polychromatic filter method for a large-area spectral response determination is testified using the PASAN solar simulator. This solar simulator can be used to measure a large-area PV module up to 2 m. It uses a pulsed xenon lamp as a light source with pulse duration of 10 ms. Since the polychromatic method requires spectral measurement, measuring the whole range of light spectrum within a such short time is quite challenging. A spectro-radiometer with a proper integration time is required to capture the entire range of wavelength spectrum within 10 ms. This short pulse duration also dictates the sweep time of the entire I-V scan of a PV device. If the pulse duration is made very fast for example at 2 ms and a tested PV module has an open-circuit voltage of 21.6 volts, the device must be biased at 10800 V/sec to obtain the entire I-V curve within 2 ms. Due to the capacitive effects which are present in the junction (depletion capacitance) and the bulk region (diffusion

capacitance) of a solar cell as shown in Figure 2.8 in Chapter 2, this short light pulse changes the concentration of the excess minority carriers instantaneously in the device's bulk regions as its capacitance is voltage and frequency dependent. As a result, a high capacitive current is produced from this bulk region and affects the accuracy of the photocurrent measurement either it is underestimated or overestimated from the true value. [11].

The pulsed-light solar simulator system in use at CREST (PASAN IIIb) consists of a capacitor bank as a power supply, an electronic load which is equipped with a set of data acquisition, a computer for controlling the entire measurement system and storing the measurement data, a monitor PV cell for measuring the irradiance produced from the xenon lamp, a temperature sensor for sensing a device temperature during the measurement, four pulsed-xenon lamps of the same type, a set of neutral density filters for reducing the level of irradiance on the measurement plane, a four-wire connection and a measurement rig for mounting a tested PV device which is placed at a distance of 8 meters from the light source. The connection of these devices in the PASAN measurement system is shown in Figure 5. 1.
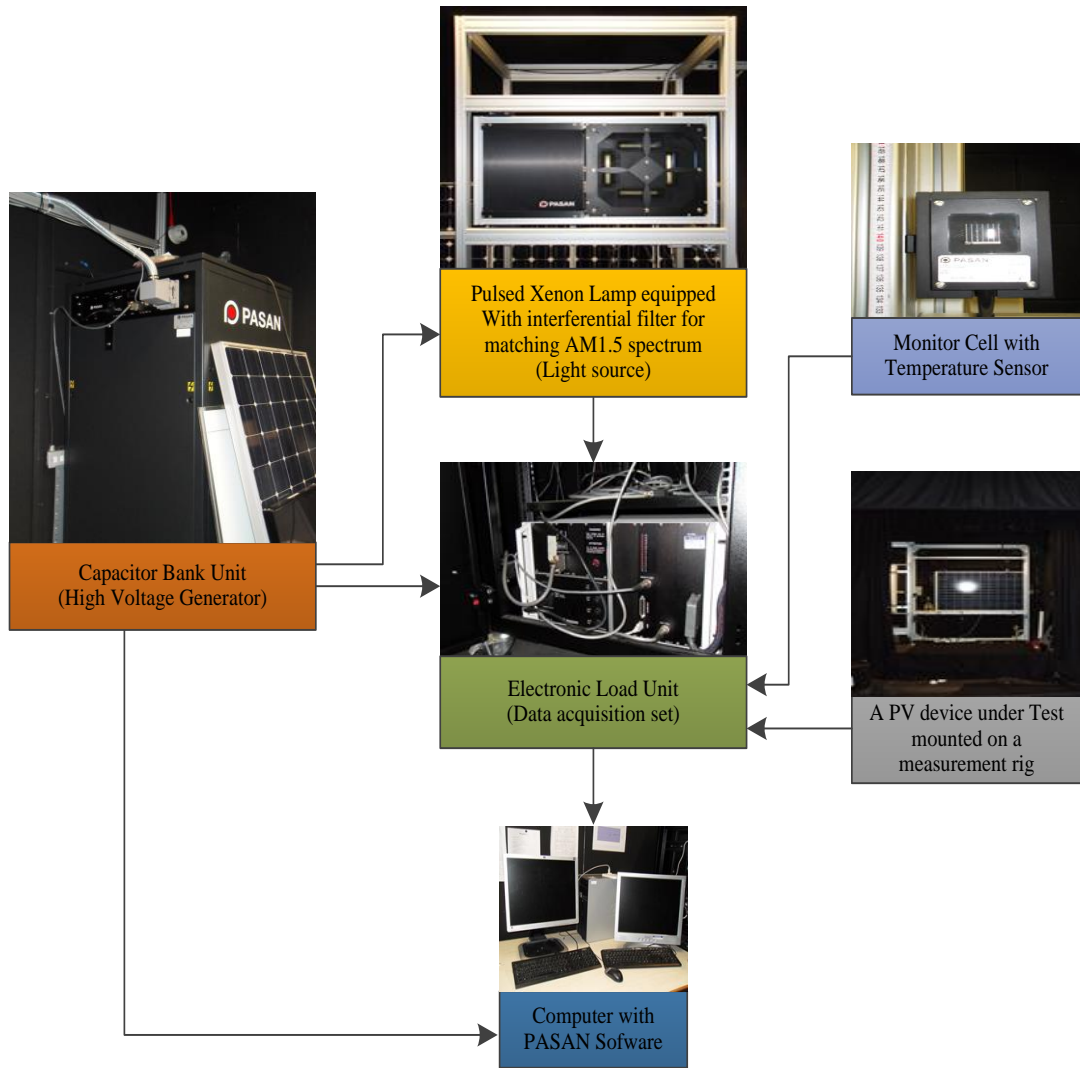
Figure 5. 1: A set of equipment composes a PASAN measurement system in use at CREST

So far, only current-voltage (I-V) characteristic measurements at different irradiances, temperatures and angles of incidence can be performed in the PASAN measurement system in use at CREST. As mentioned in Chapter 2, the I-V characteristic is influenced by the environmental conditions, therefore the device temperature needs to be monitored and kept stable during the I-V measurement. For this purpose, Pt1000 temperature sensors are attached at the back of the PV device under test. The irradiance incident on the target area is monitored by a 2x2 cm, calibrated PV cell. Both devices must be aligned in the measurement plane as described in IEC 60904-1 [47] in order to ensure that the same irradiance is received by the monitor cell and device under test. For the purpose of the I-V measurement at different irradiance conditions, a set of neutral-density filters are used in conjunction

with a small amount of electronic control. A fixed air mass 1.5 filter is used to bring the spectral output of the xenon flash lamps within class A and match to the standard AM1.5 reference spectrum [1]. The full current-voltage curve is obtained by programming a voltage profile output from a variable electronic source/load, typically a linear ramp from the short-circuit voltage to the open-circuit voltage, within the 10 ms duration of the flash. The current signal produced from a tested PV device at a given measurement point is measured by converting the current to voltage signal through an electronic load and loaded into the computer for further analyses. The flash unit triggering and device measurement are electronically controlled using the standard PASAN software, running on a PC.

The integration of the proposed spectral response measurement technique requires only the addition of a set of polychromatic filters for providing spectral variations and a spectro-radiometer for spectral irradiance measurements. The 15 selected polychromatic filters that have been used to validate the proposed polychromatic method in the small-area spectral response measurement system are reemployed to vary the spectral output of the light source in the large-area PASAN measurement system. However, their installations for the large-area spectral determinations are very different from that have been implemented in the small-area spectral response measurement system. To suit the layout of the existing xenon lamp in the light box, each polychromatic filter is assembled in a filter frame, as shown in Figure 5.2a. The frame is a square of side 390 mm. This frame dimension matches the size of the manufacturer-supplied filter frames holding the neutral-density filters. Each frame consists of four symmetrical rectangular holes with a dimension of 206 mm by 56 mm for the filter. These filter frames of the 15 selected polychromatic filters are housed in the original filter cassette of the PASAN measurement system as shown in Figure 5.2b. The same spectro-radiometer as that has been employed in the small-area spectral response measurement system is reused to measure the spectral output of the selected polychromatic filters.
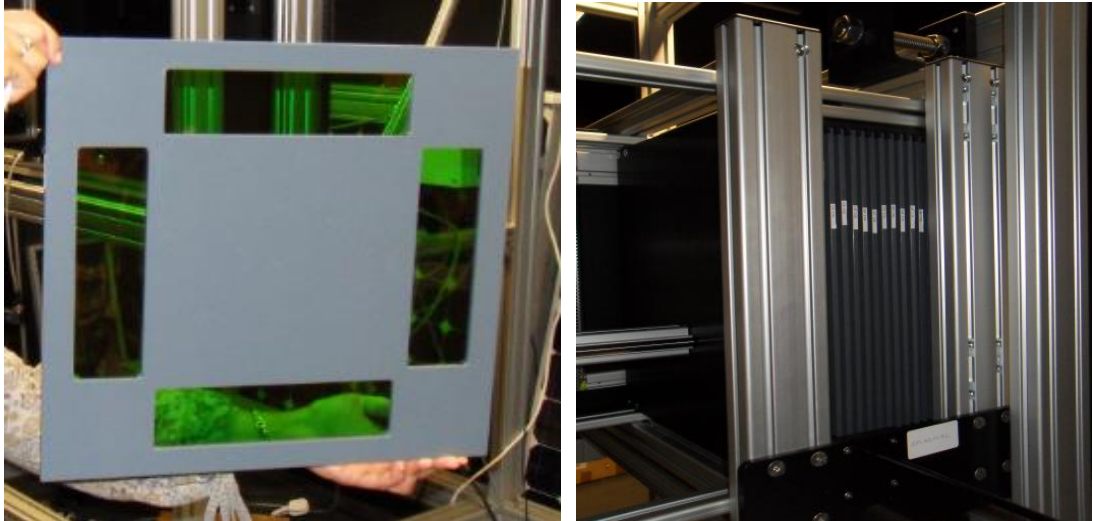
a. Individual Filter frame   b. Filter cassette

Figure 5.2: Arrangement of a set of polychromatic filters in a filter cassette in the PASAN solar simulator system

A schematic of the modified PASAN measurement system for the spectral response determination using the polychromatic method is shown in Figure 5.3.

1.Diffuser; 2. DUT; 3.Monitor cell; 4.Temperature sensor;
5.Xe lamp; 6.Polychromatic filters; 7.Filter cassette
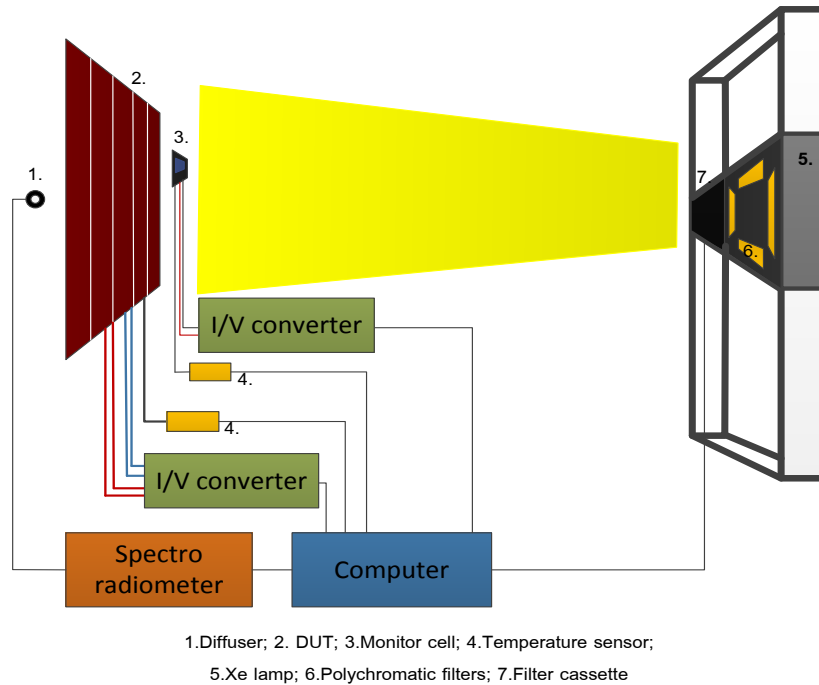
Figure 5.3: The experimental setup for a large-area SR measurement using a new polychromatic SR fitting method

The uniformity of the light output emitted by the xenon lamps without filters and with each polychromatic filter in place was assessed, as non-uniformity may significantly affect the accuracy of the spectral response determination. Therefore, its measurement results are used to inform the positioning of both the PV device under test and the input of the spectro-radiometer on the measurement plane. This is necessary in order that both devices receive the same irradiance level. For accurate device characterisation measurements, the non-uniformity of the irradiance output at the measurement plane should be approximately ±2% [49] as have been discussed in section 2.4.1, Chapter 2. The effect of the non-uniformity by 2% on the polychromatic spectral response fitting method is that there is a possibility that the incoming irradiance received by a tested PV device is higher or lower by 2% than that is detected by the spectro-radiometer if they are randomly placed at the measurement plane. A worst case is that if the non-uniformity of the irradiance output on the measurement plane is more than ±2%. This does not only affect the different irradiance detected between the device under test and the spectro-radiometer, but also it can lead to a mismatch between cells in a module. As a consequence, the current that can be produced from the device under test is not maximised. This ultimately produces an inaccurate current measurement from the tested device. Since the fitting algorithm tries to balance the calculated current to the measured current in order to produce the appropriate fitted coefficients for the chosen spectral response model, the fitting algorithm of the polychromatic method can overestimate the spectral response of a tested PV device by 2% if the measured spectra detected by the diffuser is lower by 2% than that is received by the tested PV device. The uncertainty in the spectral response measurement by 2% is highly acceptable for PV performance measurements as have been analysed in section 4.5. Therefore to reduce the uncertainty in the spectral response determination, the information of the non-uniformity of irradiance on the large-area measurement plane is necessary. However, the uncertainty in the spectral measurement is not only contributed by the non-uniformity of irradiance on the measurement plane but also other factors such as the uncertainty in the spectro-radiometer itself and the positioning of the spectro-radiometer and the tested device which must be aligned and placed in the same height on the measurement plane

The uniformity test is performed by measuring 22 irradiance sensors which are placed in a line along a movable bar at the measurement plane and one sensor is used as reference irradiance. Each sensor is separated by 100 mm from the next. The setup of the uniformity measurement rig is shown in Figure 5.4.
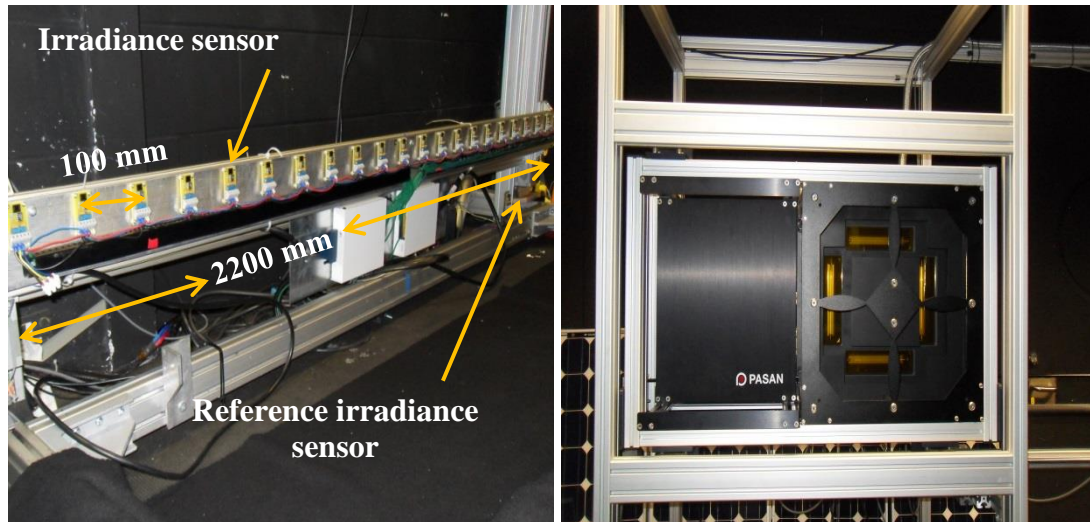
a. Position of irradiance sensors   b. Position of polychromatic filter

Figure 5.4: The layout of the homogeneity measurement setup in use at the PASAN measurement system

To start the homogeneity measurement, the irradiance sensor bar is placed at a reference position as shown in Figure 5.4a and the tested polychromatic filter is positioned at a distance of 15 mm in front of the light source in the light box as shown Figure 5.4b. The lamps are flashed and the response signals produced by all sensors are recorded. The bar is raised by 100 mm from the initial position in order to provide an equal size test area i.e. 100 mm by 100 mm and another flash is triggered. This process is repeated until the last height has been reached, 1800 mm from the reference position. Since the total irradiance produced by the solar simulator may not be stable during the measurement due to the total irradiance map built up from multiple flashes, the reference irradiance sensor is used to account for flash to flash variability and at the end to correct the measurements from the other sensors. For this reason, it is always put at a fixed position near the ground during the measurement. The non-uniformity of irradiance at the measurement plane is then determined by comparing the maximum and minimum irradiances as written in equation (2.19) in

Chapter 2. The spatial uniformity of the unfiltered xenon lamps and with one selected polychromatic filter are shown in Figure 5.5 and Figure 5.6.
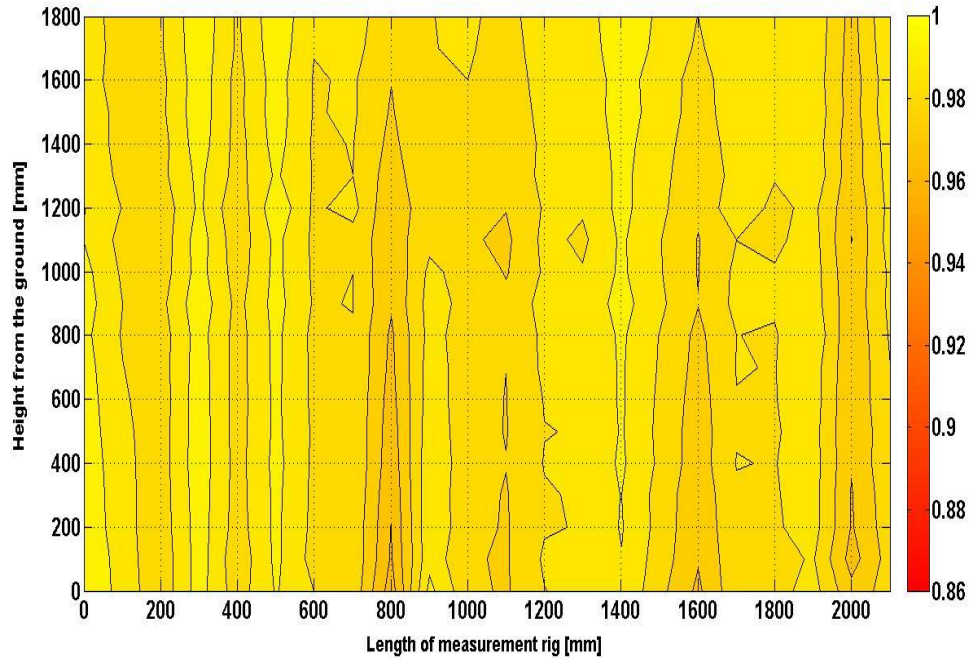
Figure 5.5: Spatial uniformity of irradiance produced by a pulsed xenon lamp at the tested area of PASAN measurement system with the non-uniformity of 1.9%

As shown in Figure 5.5, the spatial uniformity of irradiance produced from only the pulsed xenon lamp at a designated area of 2100 mm by 1800 mm varies within ±1.9% and is in compliance with class A as described in IEC 60904-9 [49]. However, once a polychromatic filter which is made from a polymeric material is put in front of the lamp as shown in Figure 5.4, the non-uniformity of irradiance increases considerably to ±8.3% as shown in Figure 5.6. Based on this figure, the throughput of the selected polychromatic filter has met class C spatial uniformity classification (±10%). The increase in the spatial non-uniformity is caused by the distortion in the filter material as can be seen in Figure 5.7.
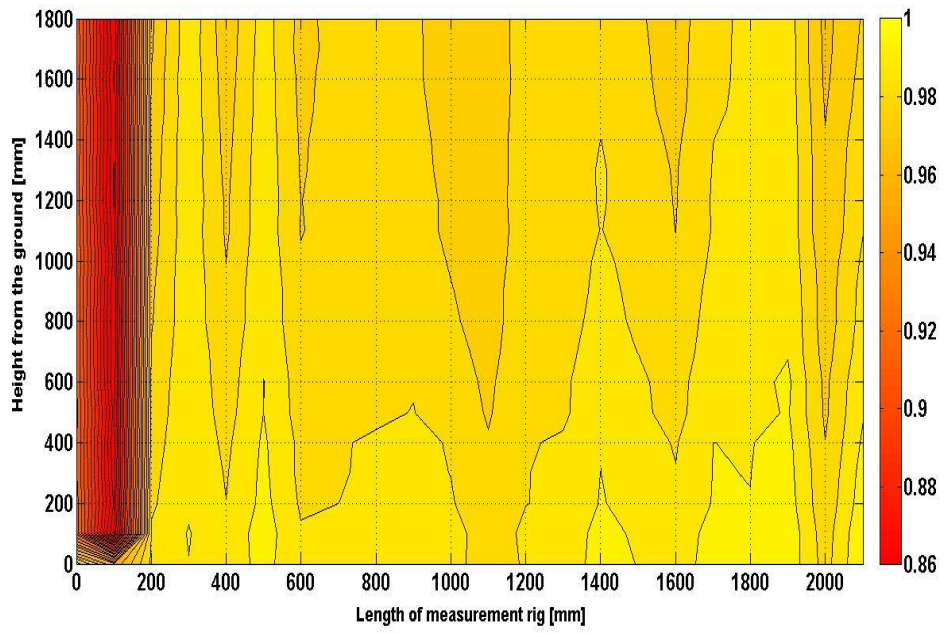
Figure 5.6: The spatial uniformity of irradiance throughput of one selected polychromatic filter (GF103) at the tested area of PASAN measurement with the non-uniformity of 8.3%
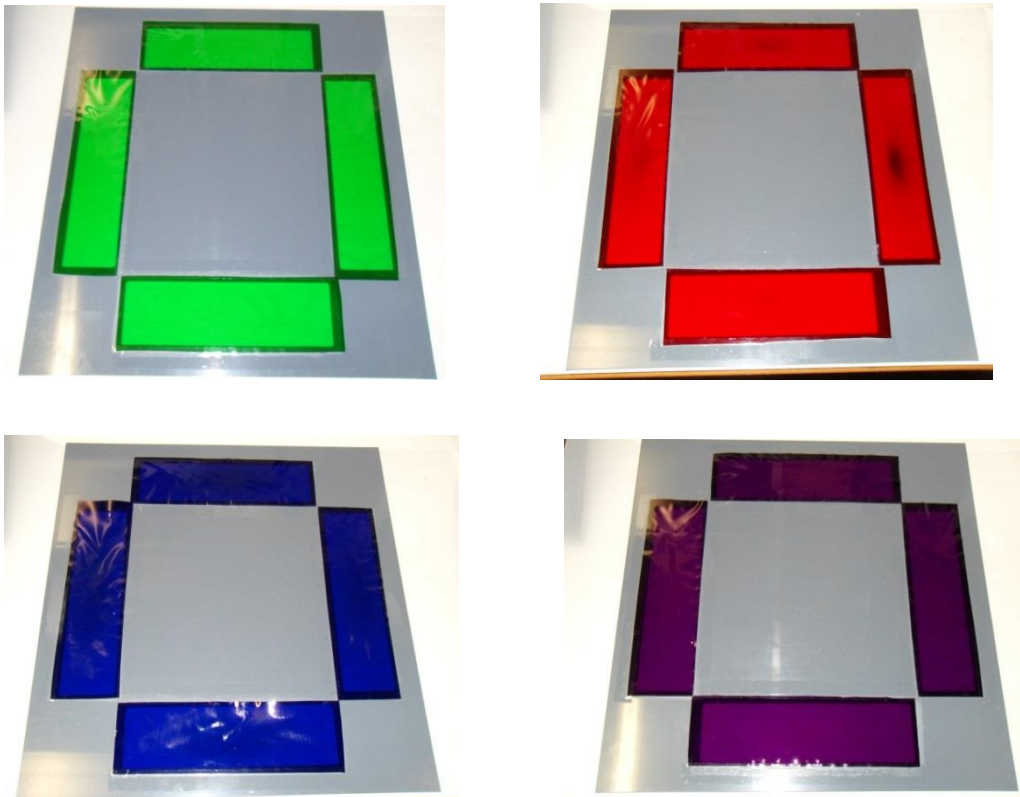
Figure 5.7: Performance of lighting gel filters after enduring 19 consecutive flashes under a 1000 watt/m^2 irradiance intensity

The low irradiance in the first 200 mm along the vertical axis of the measurement rig indicates that one of the four filters in the tested frame has been severely damaged as it is apparent in Figure 5.6. The degree of deformation is different for each polymeric filter depending on their transmittance. Filters which have blocking regions in the UV and blue range of spectrum have been most damaged. This is due to high irradiance exposure experienced by the filters at a distance of 15 mm as shown in Figure 5.8.
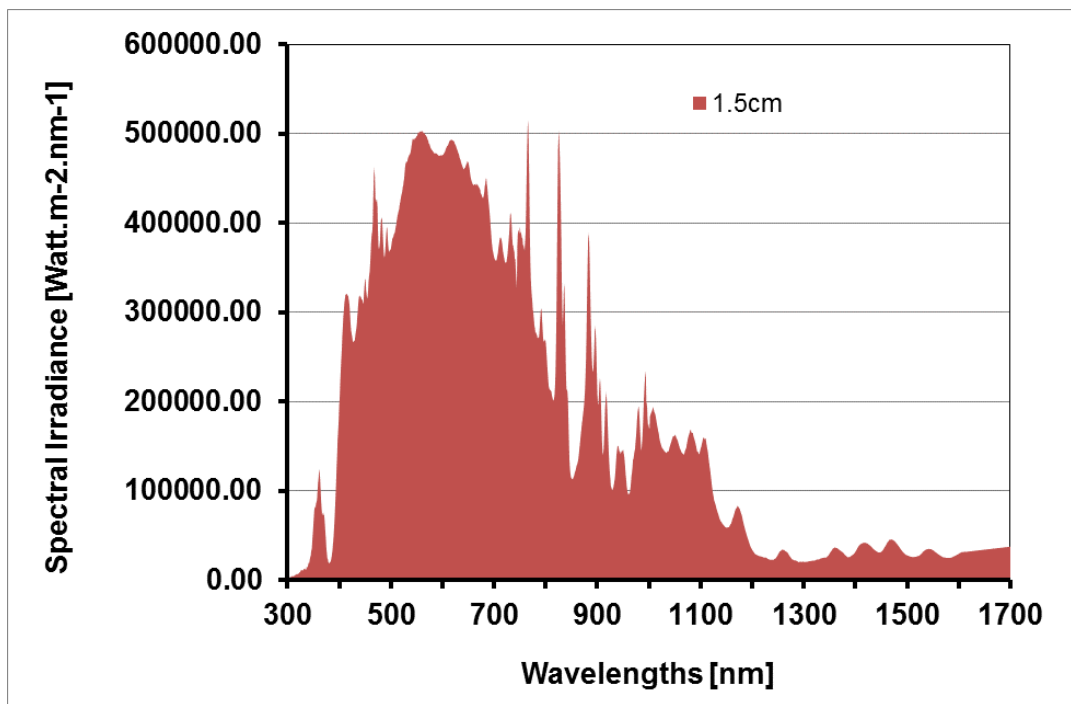
Figure 5.8: The spectral irradiance radiated by the xenon arc lamp at 15 mm distances (filter's position) calculated using the inverse of distance square relationship and its irradiance at 8 m

The filters absorb most of the irradiance at their blocking regions and convert them into heat. The energy per second absorbed by each filter material can be calculated using the Stefan's law as shown in equation (5.2)[39]:

$$P = A\sigma T^4 \qquad\qquad (5.2)$$

Where P is the power of energy per second in watts, A is the surface area of a black body in m^2, in this case the filter material, σ is the Stefan constant: 5.7×10^{-8} $W.m^{-2}K^{-4}$ and T is the temperature in Kelvin.

The following figure shows the total energy absorbed by each filter within 10 ms.
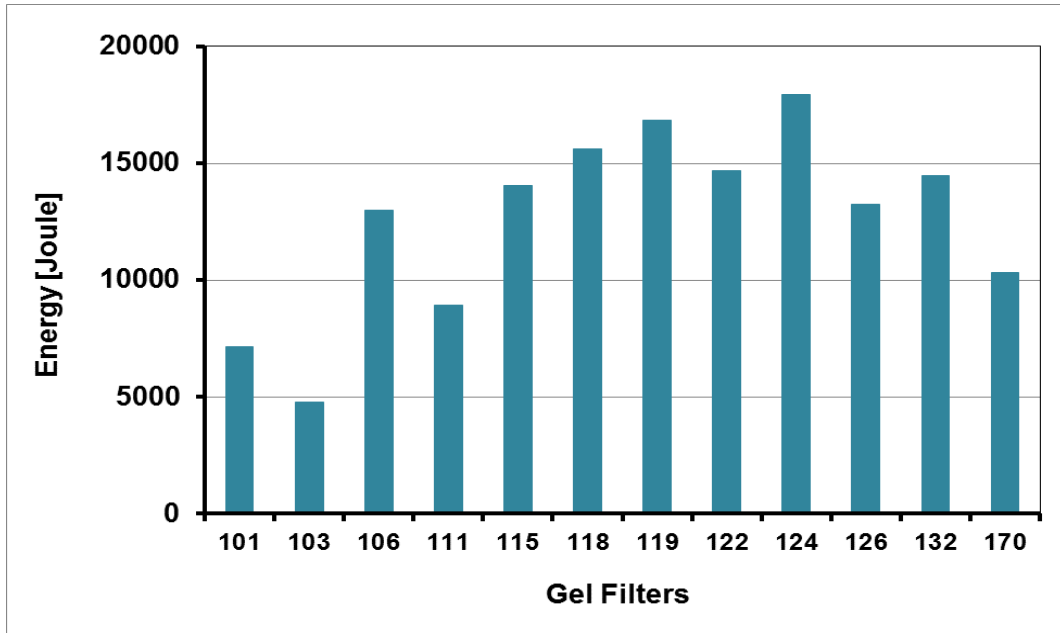
Figure 5.9: The total energy absorbed by each filter material within 10 ms

As shown in Figure 5.9, all of the lighting gel filters suffer from very high irradiance stress. This radiation has increased the temperature inside the filter materials as shown in Figure 5.10 and it heats the internal components of the filters.
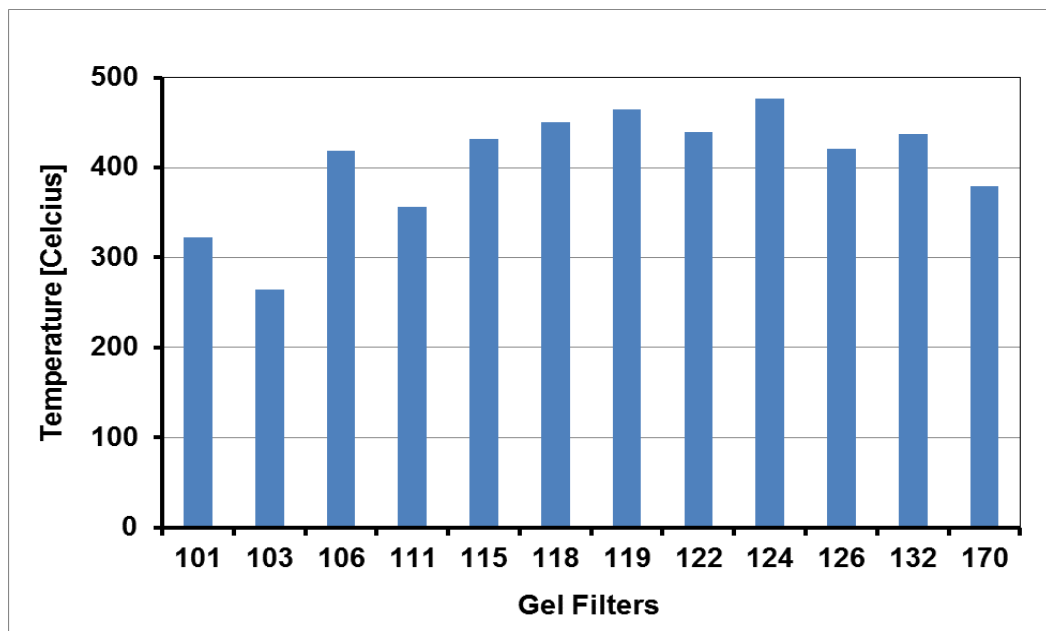
Figure 5.10: The increasing temperature inside the each filter material due to high irradiance stress produced from the short pulsed xenon lamp

As shown in Figure 5.10, the increasing internal temperature has gone beyond the limit of the filter tolerance temperature (200°C) as has been shown in section 3.5. This high temperature stress has deformed the filter material and shortened the lifetime of the polychromatic filters which are made from the polymeric materials. Based on this observation, it is clear that these polychromatic filters which are made from the polymeric materials cannot be used for large-area spectral response measurements in the PASAN measurement system. Other suitable materials need to be found to replace the polymeric materials such as glass with high heat and irradiance resistances.

Even though the lighting gel filters had failed to survive at the high irradiance exposure when they were put close to the lamps, the investigation was continued with a new identical set of lighting gel filters, but modifying the filter arrangement in the PASAN system. To reduce damage and sustain the filter life time, the filters were positioned approximately 26 cm from the xenon lamps, as shown in Figure 5.11This arrangement is possible as the size of one gel filter is 60 cm by 50 cm.
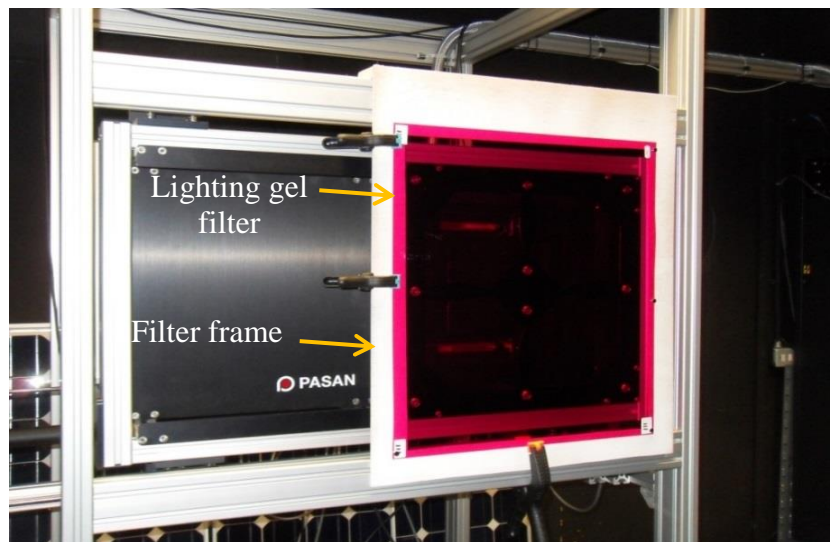
Figure 5.11: Lighting gel filters are arranged in front of four xenon lamp tubes

The lifetime of the filter in such a distance from the lamp was tested by giving several intermittent flashes as have been done in the homogeneity test and observing any physical damage afterward. From the test, it is observed that there is no physical damage found in the material of the selected filters. This implies that putting a tested

filter at a distance of 26 cm in front of the light source is feasible for carrying out the spectral response measurement.

For PV performance measurements, the spatial uniformity of irradiance at the measurement plane must meet at least class B classification which is ±5% [49]. To meet class A spatial uniformity classification, the size of the measurement plane has been reduced to 1800 mm by 1700 mm which is measured from 0 mm to 1800 mm vertically and from 200 mm to 2200 mm horizontally. This reduction produces a better spatial uniformity of irradiance at the measurement plane, 1.4% and at the same time, it also has restricted the capability of the polychromatic spectral response fitting method for measuring spectral response of any large-area PV devices with a size up to 1.6 m.

To cross validation between the large- and small-area spectral response measurements, the same selected small-area PV devices are re-used for comparison. As shown in Figure 3.12 in section 3.5, the spectral variations which are produced from the polymeric material filters are limited in the visible range, only amorphous silicon PV devices can be tested. Therefore, other three selected polychromatic filters which are made from glass materials need to be added to accommodate the spectral response determination of crystalline PV devices. These glass filters are RG850, KG2 and RG9 which are the same types as those glass filters that have been used in the small-area spectral response measurement. The glass filters have a square shape with a dimension of approximately 165 mm x 65 mm x 2 mm. Their arrangement in the filter frame is made similar to that of the lighting gel polychromatic filters, where each filter frame consists of four identical glass filters.

The spectral response measurement of a tested PV device on the measurement rig is made at a height of 130 mm from the ground. This position is considered good in terms of the uniformity of irradiance on the measurement plane as shown in Figure 5.12. The arrangement of the device under test and spectro-radiometer input at the measurement plane is shown in Figure 5.12. The device under test is connected to the measurement unit through a four-wire connection. The current and spectral measurements are performed at STC and recorded at the same time.
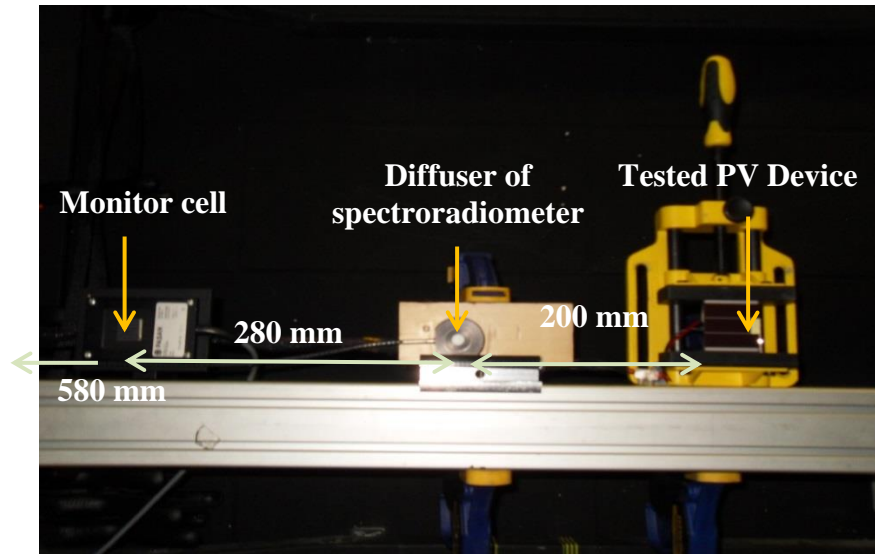
Figure 5.12: The arrangement of a tested PV device and the measurement units at the test area of the PASAN measurement system

When a selected polychromatic filter is placed in front of the lamp, the cooling fan in the lamp unit blows, some flexing of the polychromatic filter is observed. This definitely affects the spatial uniformity of the irradiance at the measurement plane. The effects of the increase of the non-uniformity on the current and spectral measurements can be seen from the resulting curve in Figure 5.13 which is far from matching to the spectral response curve using the monochromatic method. The disagreement between the curves indicates that there are some differences between the measured currents and the currents calculated from the measured spectra which result in bad fitted coefficients. This finding also reveals that the tested PV device and the diffuser have received different amount of spectra when illuminated. This could be due to the ripple on the surface of the measured filter when it is placed in front of the light source.
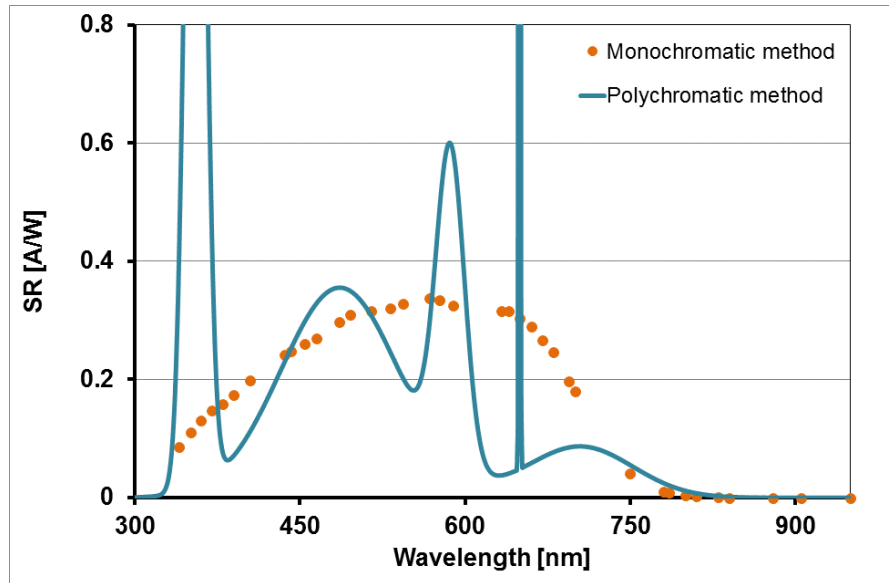
Figure 5.13: Spectral response determination of amorphous silicon PV device when the lighting gel filters are arranged in front of the light source

Therefore to improve the accuracy in the current and spectral measurements, another setup for the filter setting is arranged as shown in Figure 5.14. In this arrangement, the lighting gel filter is placed exactly in front of the tested PV device and the diffuser of the spectro-radiometer at 8m distance from the xenon lamps. In this way, both the tested PV device and the diffuser of the spectro-radiometer can receive exactly the same amount of irradiance when they are illuminated. However, this measurement setup limits the size of PV devices that can be measured in the measurement system, but is used here to verify the polychromatic concept can in principle be used for a large-area spectral response measurement. The distance between the input of the spectro-radiometer to the monitor cell and the tested PV device is kept the same as shown in Figure 5.12 in order to assess the impacts of the new arrangement on the measurement results. The monitor cell in the both measurement setups is used to monitor the stability of irradiance during the flash and at the end to correct the measured current.
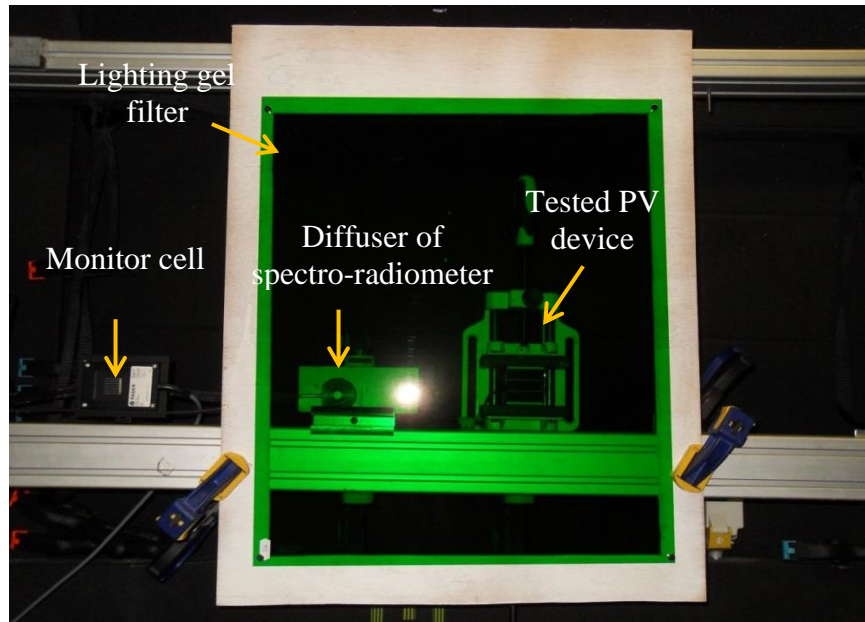
Figure 5.14: Lighting gel filters are arranged in front of a tested PV device and a diffuser of spectro-radiometer at the test area of PASAN solar simulator system

The measurement procedure for determining spectral response of a PV device using the polychromatic spectral response fitting method is shown in Figure 5.15. The measurement only needs to produce a set of short-circuit currents generated by a tested PV device when illuminated at different spectral conditions and the corresponding spectra produced by the pulsed xenon lamp.
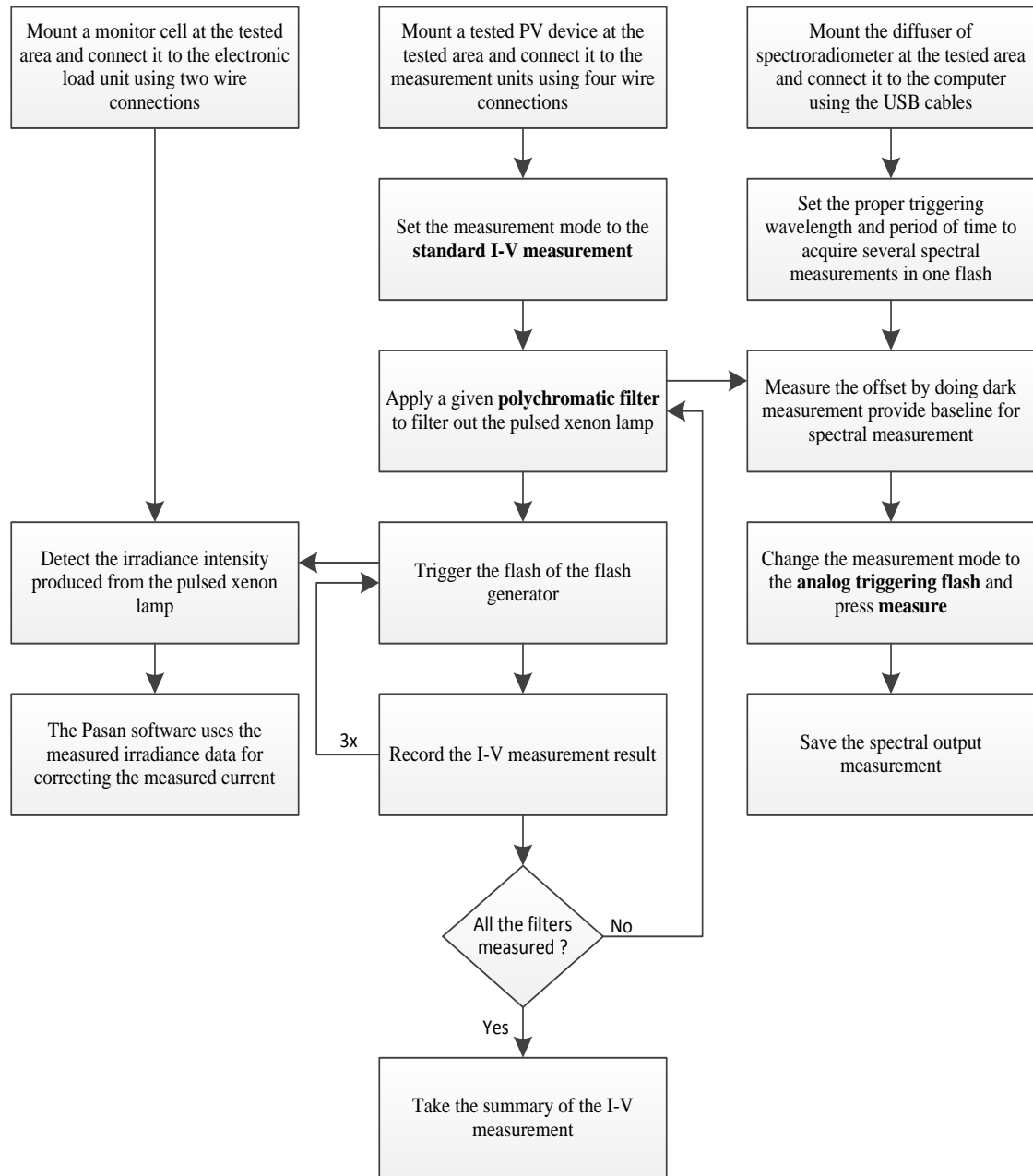
Figure 5.15: Procedure to perform the short-circuit measurement of a PV device at the PASAN solar simulator measurement system

To obtain accurate spectral measurements, room temperature is always kept constant during the I-V measurement. The spectral measurement is performed using two AstraNet charge couple device (CCD) spectro-radiometers [90]. Thermal offsets in the spectral measurement are corrected by measuring the dark response of the CCD detectors. This measurement is also used to provide a correct baseline and eliminate stray light in the spectral measurement. To reduce the uncertainty in the spectral

measurement, the operating temperature of the Si detector must be kept stable at 20°C during measurements. The dark measurement signal of the Si detector has been used to monitor its operating temperature. Once the level has reached a calibrated value that corresponds to the correct detector temperature, the spectro-radiometers are ready for measurement.

Due to the short pulse duration of the PASAN light source, measuring its spectral output is quite challenging compared to a continuous light source such as in the small-area system described in the previous chapter. The full spectrum from the visible to the near infrared must be captured within 10 ms. To reduce noises in the measurement and to compensate the unsynchronised measurements between the Si and InGaAs detectors, the spectro-radiometers must be able to measure 10 pulses within such a short time [90]. This can be obtained by setting the period time of one pulse at 1 ms. The spectro-radiometers can be triggered by an external pulse from the light source at each wavelength [91]. For the PASAN spectral measurement, the triggering wavelength has been set at 611.38 nm and the amplitude at 10.04 counts/ms in order to detect the spectral output of a given polychromatic filter. To maintain the accuracy in the measured spectra, a dark measurement is always taken beforehand. After the spectra of the lamps with each of the selected polychromatic filters have been measured, they need to be interpolated into 1 nm wavelength steps before inputting to the fitting algorithm of the polychromatic spectral response fitting method. The entire fitting process is identical to that of the small-area spectral response determination, but with different spectra and current input data. The validation of the method for large-area spectral response measurements is done by a direct comparison of the results with that are obtained using the monochromatic filter method.

5.4. Large-area Measurement Results

The results of the spectral response determinations of a small amorphous silicon PV device from the second measurement setup are shown in Figure 5.16 and their differences to the spectral response determination using the monochromatic method is shown in Figure 5.17.
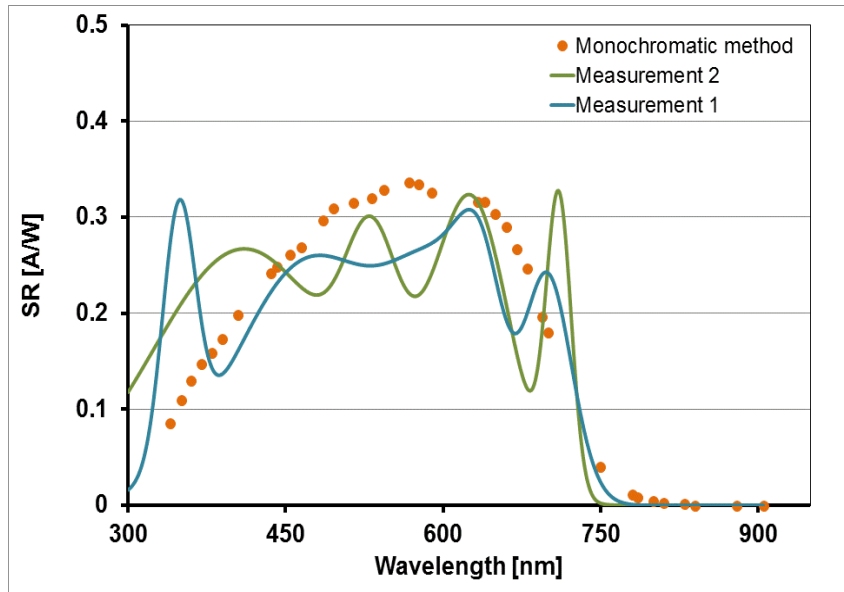
Figure 5.16: SR determinations of a small amorphous silicon PV device when the lighting gel filters are placed in front of a tested PV device

Figure 5.17: Differences in SR determinations of a small amorphous silicon PV device obtained using polychromatic method at the PASAN solar simulator system to their SR measured using the monochromatic method

As can be seen in Figure 5.16, the differences between the spectral response determinations obtained using the polychromatic method and that of the monochromatic method are still apparent, even though the filter has been placed directly in front of the tested PV device and the diffuser of spectro-radiometer and is

not affected by the movement that is caused by the lamp housing fans or degradation caused by the high intensity irradiance close to the lamps. The differences between the spectral response determinations obtained from two measurements using the polychromatic method and that are obtained using the monochromatic method are significant, (more than 100% in the ultraviolet range and up to 80% in the red range). The differences are also significant in the visible band, in the range of 10% to 40%.

To investigate further why the polychromatic method cannot produce a well-matched spectral response curve to the spectral response curve measured using the monochromatic method, another spectral response determination test has been performed. A new PV device which is made from the same PV material has been used. It is a mini module amorphous silicon PV device with a total area of 0.1230 m^2. It consists of 48 cells in series. The device spectral response curve has been measured by a calibrated PV laboratory in Europe. The device has been mounted in the same position as the small a-Si PV device and the second spectral response measurement setup was applied as shown in Figure 5.18.
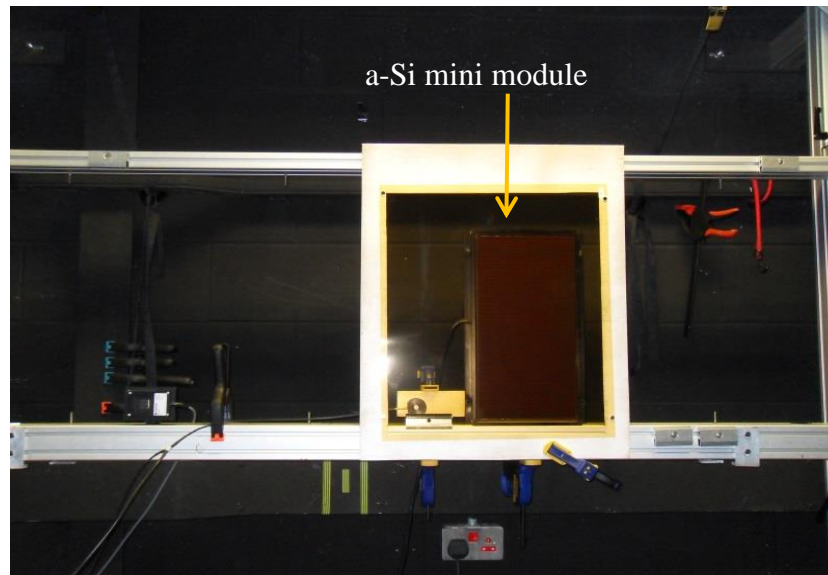
Figure 5.18: The SR measurement setup of a mini module amorphous silicon device in the PASAN measurement system

The results of the spectral response determinations are given in Figure 5.19. The spectral response determinations using the polychromatic method differ from that of the monochromatic method. These results are unsatisfactorily undesirable as the

spectral response curves apparently fluctuate over the wavelength range. The differences in the spectral response determinations across the entire wavelength regions between the polychromatic and monochromatic methods can be seen in Figure 5.20.
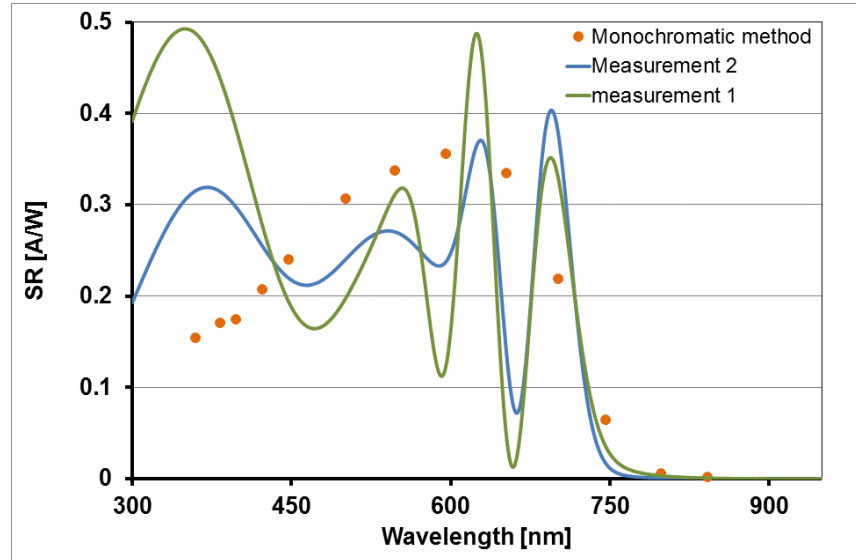
Figure 5.19: SR determination of amorphous silicon mini module when the lighting gel filters are arranged in front of the light source
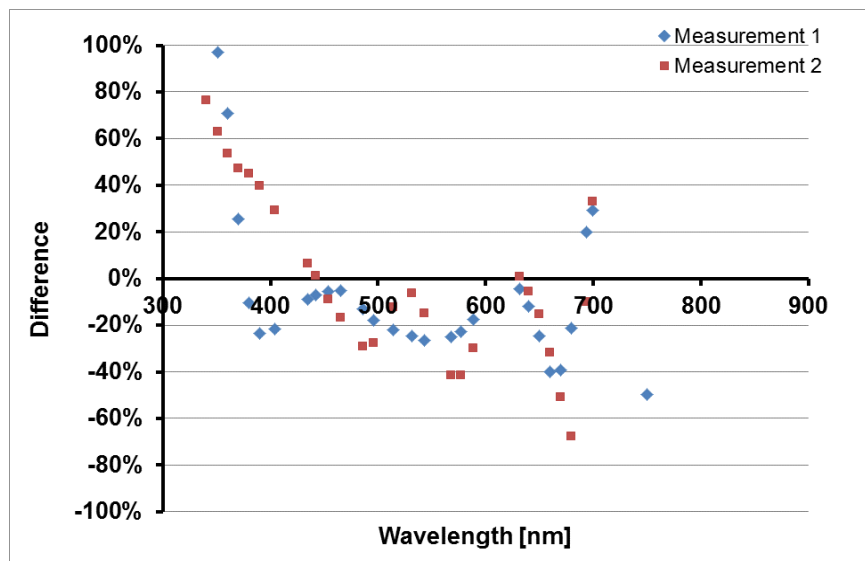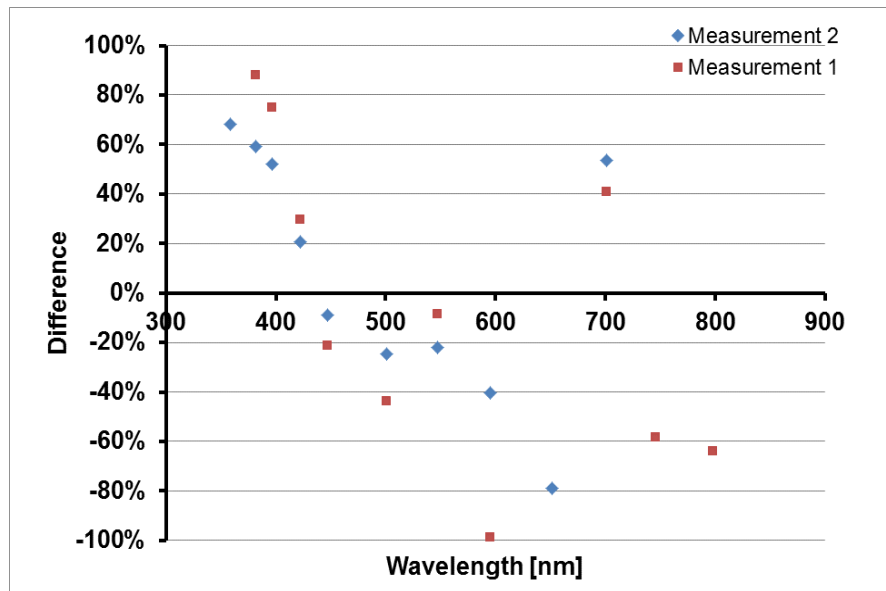

Figure 5.20: Differences in SR determinations of an amorphous silicon mini module obtained using polychromatic method at the PASAN solar simulator system to their SR measured using the monochromatic method

Compared to the findings of the first validation in the small-area measurement system, the findings from these large-area spectral response measurements indicate that there are some faults in this large-area measurement system as the spectral response determinations of both tested PV devices have been failed to be matched. To verify whether this condition also applies for other PV technologies, another set of measurements is carried out using mono-crystalline and poly-crystalline PV devices as tested devices. These PV devices have been used in the previous work to validate the polychromatic method in the small-area spectral response measurement in Chapter 4. The arrangement of the selected PV devices on the measurement rig is kept the same as shown in Figure 5.12. Results of the measurements are shown in Figure 5.21 and Figure 5.23.
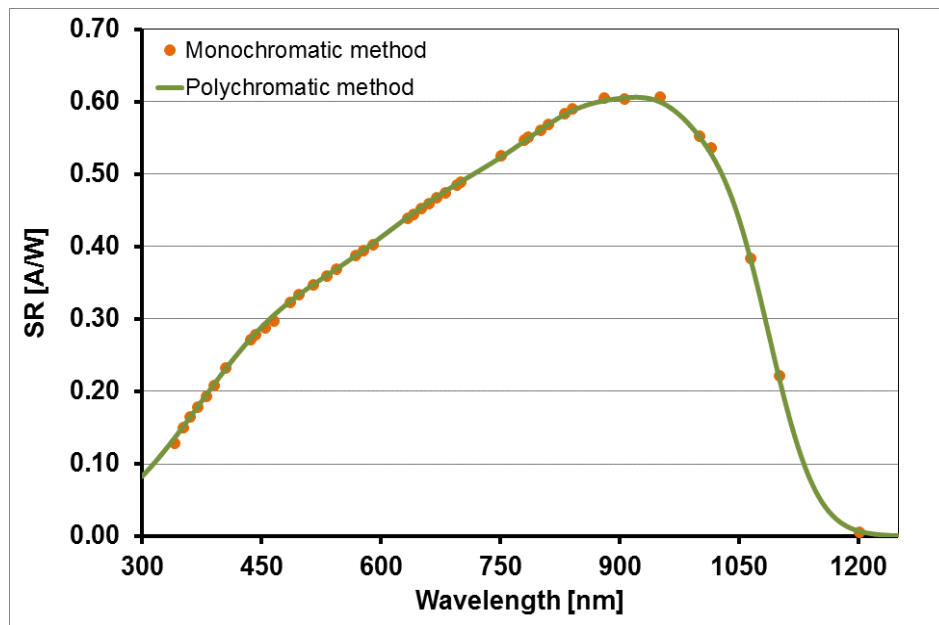
Figure 5.21: SR determination of a mono-crystalline PV device after the correction factor is applied
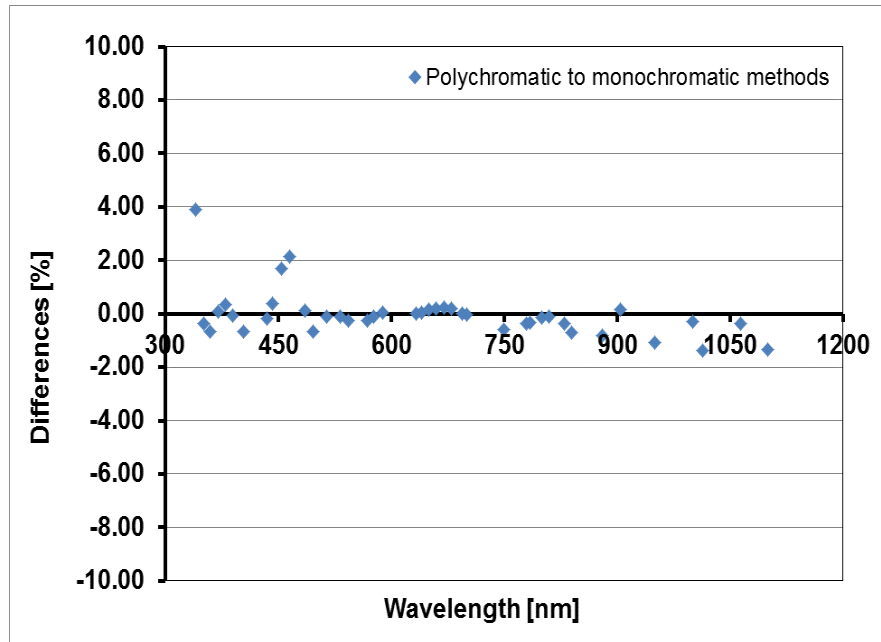
Figure 5.22: Differences in SR determinations of a mono-crystalline PV device using polychromatic method at the PASAN solar simulator system to their SR measured using the monochromatic method
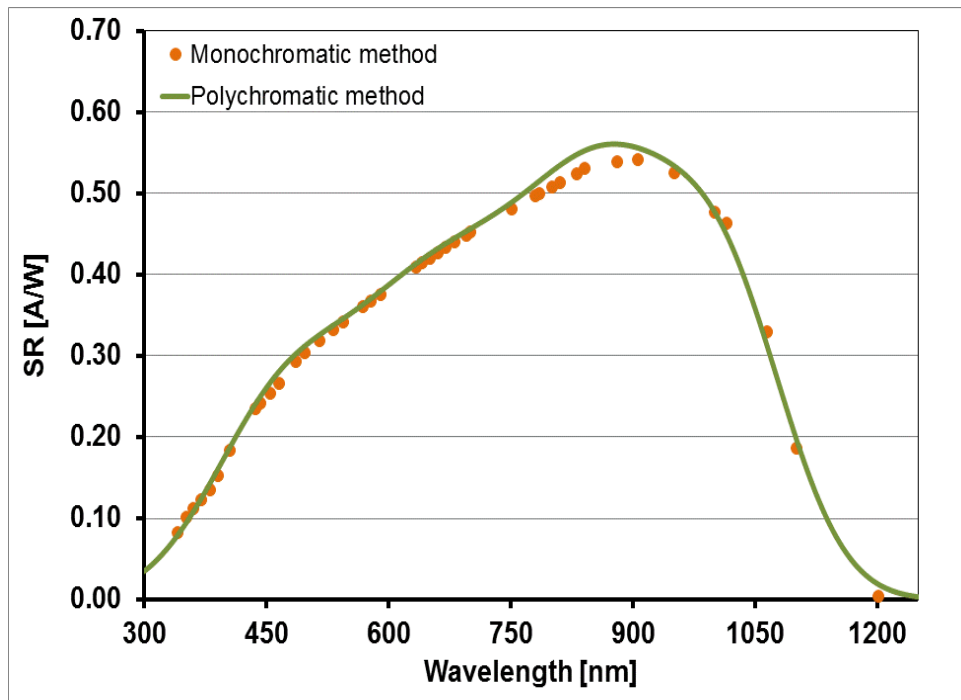
Figure 5.23: SR determination of a poly-crystalline PV device after the correction factor is applied
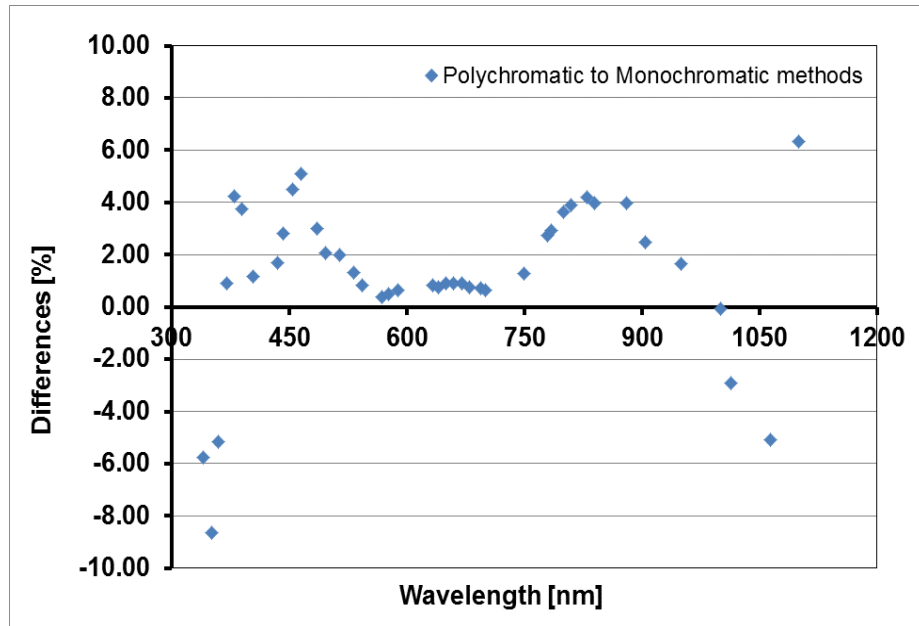
Figure 5.24: Differences in SR determinations of a poly-crystalline PV device using polychromatic method at the PASAN solar simulator system to their SR measured using the monochromatic method

As shown in Figure 5.21 and Figure 5.23, both spectral response curves from the different PV devices are well-matched to their corresponding curves of the monochromatic method with differences less than ±1.5% for the mono-crystalline PV device across its response range and less than ±4% for the poly-crystalline device as shown in Figure 5.22 and Figure 5.24. The good agreements between the spectral response curves of using the polychromatic and monochromatic methods can be achieved after the measured spectra of those devices are corrected with certain scaling factors which are obtained using the calibrated reference solar cell. The measured spectra should be corrected after it is noticed that the measured currents of the reference solar cell differ from its calculated currents using equation (2.1) as shown in Figure 5.25.

144
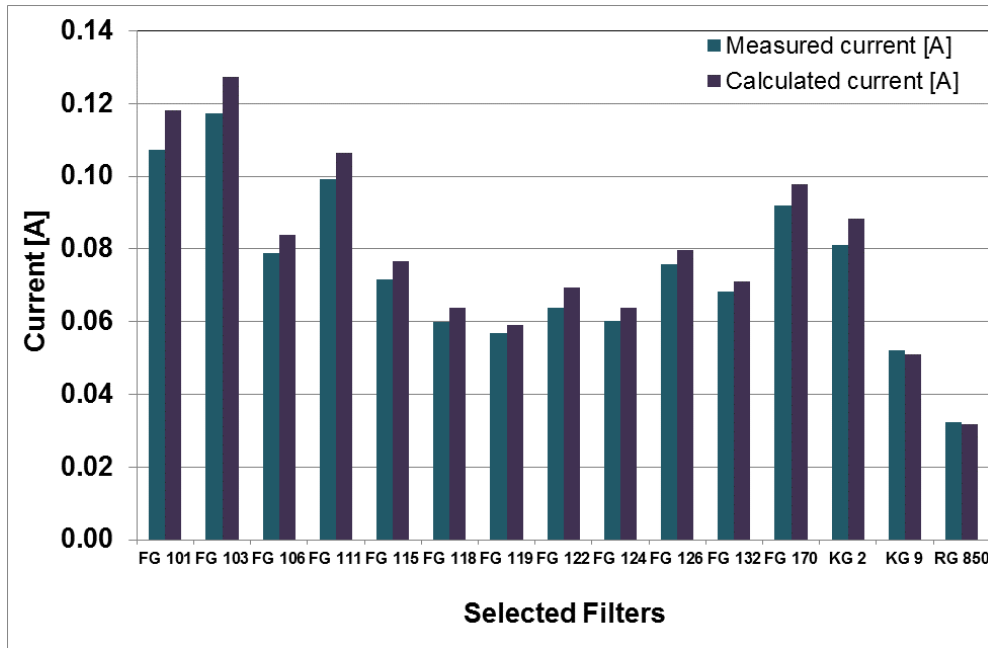
Figure 5.25: Comparison of the measured and calculated currents of a reference solar cell for all selected polychromatic filters

The calculated currents are higher by 5% to 10% from the measured currents. As the uncertainty in the current measurement is approximately ±2.6% with a coverage factor of 2, the accuracy in the current measurement is very acceptable. The only contributor to the increase in the calculated currents is the overestimated spectral measurement. This premise can be justified when the measured spectra are corrected using the scaling factors and the agreements between the spectral response curves are achievable as shown in Figure 5.21 and Figure 5.23. A similar approach has been applied to obtain a well-matched spectral response curve of the amorphous silicon devices either a small-area solar cell or a mini module. In this approach, the measured spectra are corrected using the scaling factors which are determined by comparing their measured currents to their calculated currents at certain spectral conditions. The results of this correction approach are shown in Figure 5.26 for a small solar cell and Figure 5.28 for a mini module.
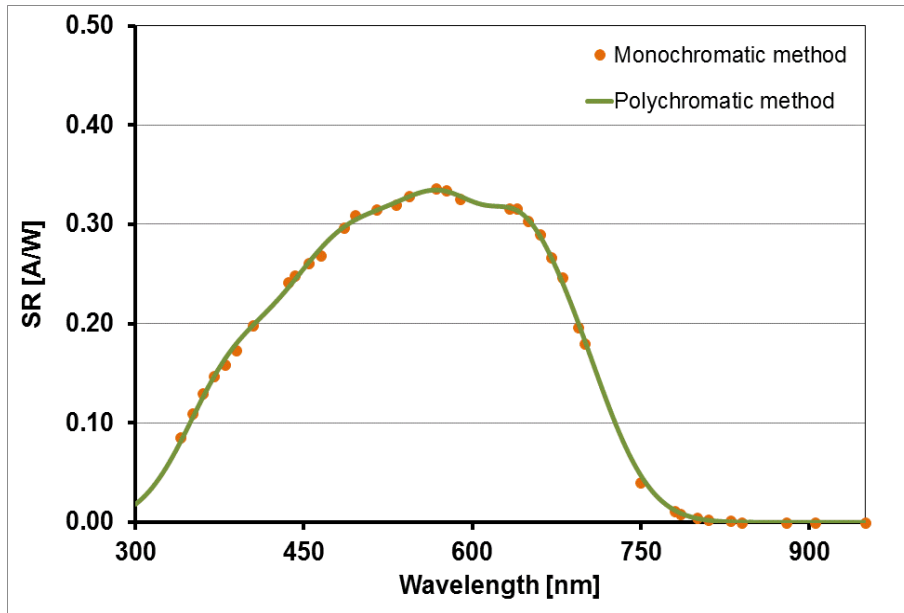
Figure 5.26: SR determination of a small amorphous silicon PV device after the correction factors are applied

As can be seen from the figure, there is an improvement in the spectral response curve using the polychromatic method after the correction factors are applied. A good agreement between the two SR curves is established. The differences between the SR curves are within ±2% across the spectral range of the tested amorphous silicon device as shown in Figure 5.27.
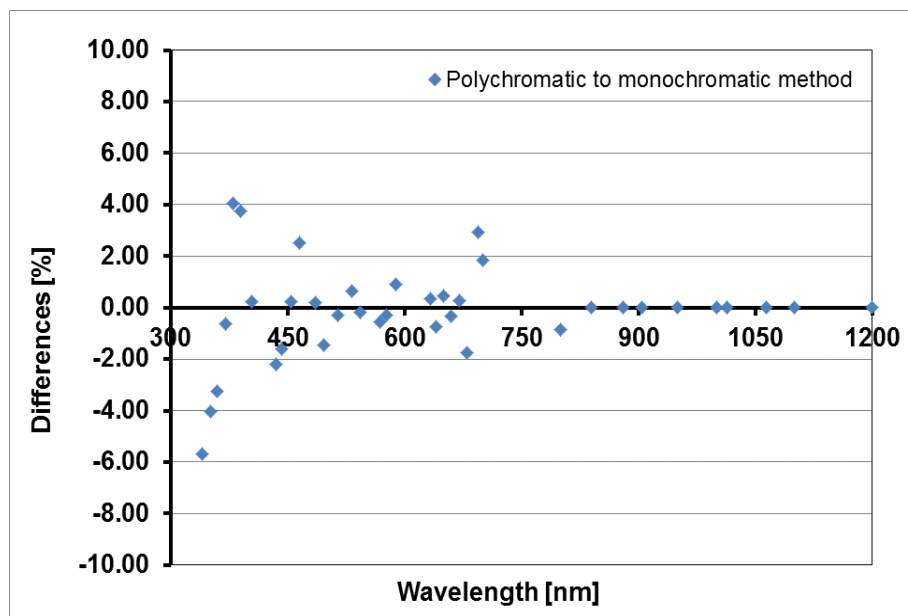
Figure 5.27: Differences in SR determinations of a small amorphous silicon PV device after the correction factor is applied to the measured spectra

The same improvement is also exhibited by the amorphous silicon mini module. Its SR curve which is obtained using the polychromatic method correlates well to that of using the monochromatic method with differences within ±2% as shown in Figure 5.29.
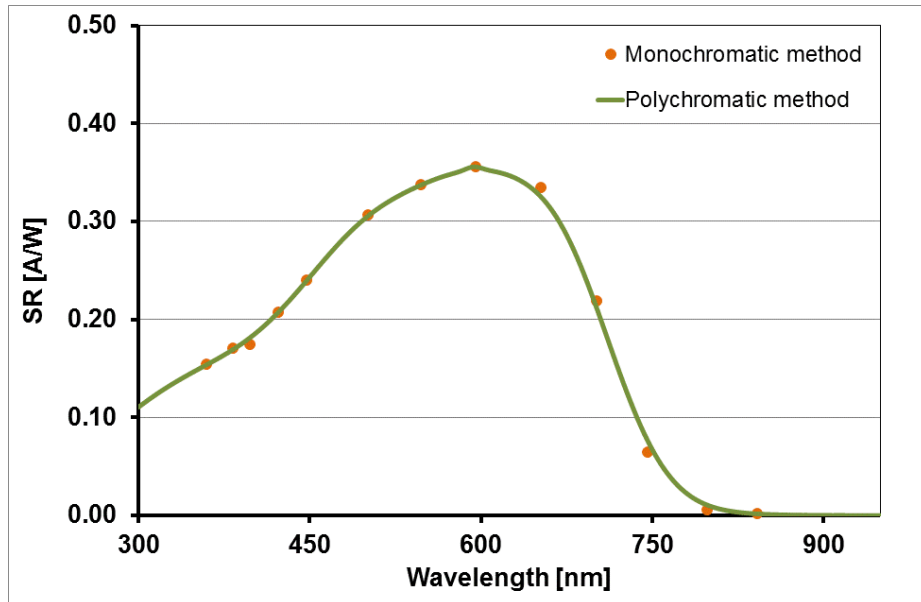
Figure 5.28: SR determination of amorphous silicon mini module after the correction factor is applied
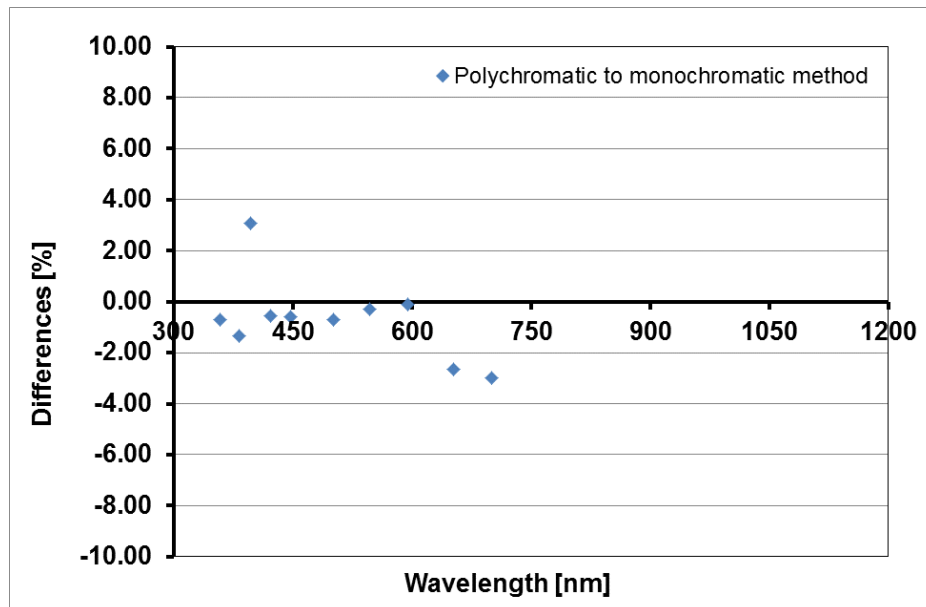
Figure 5.29: Differences in the corrected SR determinations of an amorphous silicon mini module obtained using polychromatic method at the PASAN solar simulator system to their SR measured using the monochromatic method

These findings reveal that the polychromatic filter method is feasible for a large-area spectral response determination. However, this measurement technique is very sensitive to the errors in the current and spectral measurements. Therefore, high precision and accuracy of current and spectral instruments are highly required for accurate SR determinations of PV devices. Understanding any possible defects in the applications of the polychromatic filter method is important for determining an accurate SR determination of a PV device. The following section will investigate some possible errors in the spectral response measurement using the polychromatic filter method.

5.5. Error Analysis in Large-area SR Measurements

As shown in the Chapter 4, there are three error sources found in the polychromatic method for spectral response determinations of a PV device. These errors are the current measurement, the spectral measurement and the chosen initial values for the coefficients of the chosen spectral response model. The errors in the current and spectral measurements can be contributed by the non-uniformity of irradiance at the measurement plane and the errors in the instruments themselves. From the homogeneity test as shown in section 5.3, the uniformity of irradiance on the measurement plane is very good, ±1.9% only with the pulsed xenon lamp and ±1.4% with a polychromatic filter but in a reduced illumination area. However, a simple homogeneity test has been carried out in order to convince that the chosen test area has a good spatial uniformity as shown in Figure 5.30. The measurement setup for this measurement is made similar to that of the spectral response measurement. The measurement requires a calibrated PV device (a reference solar cell) to detect changes in the irradiance along the test plane, a monitor cell to monitor the irradiance produced from the pulsed xenon lamp and a spectro-radiometer to observe changes in the spectral irradiance of the pulsed xenon lamp. There are no polychromatic filters applied in this measurement.
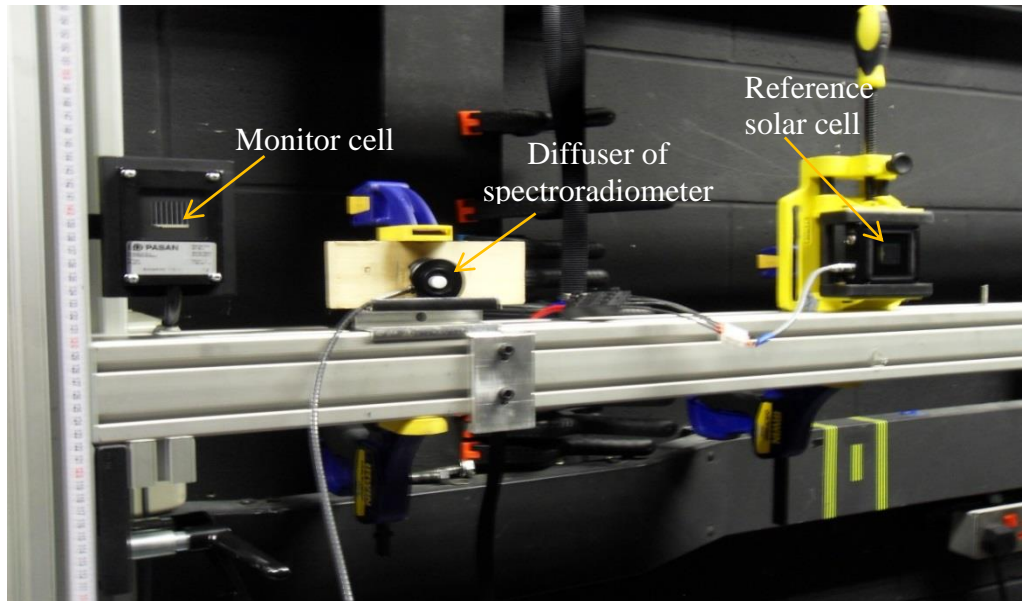
Figure 5.30: Spatial uniformity measurement of a tested area using a calibrated mono-crystalline solar cell (a reference solar cell)

The reference solar cell is moved to different positions along the measurement bar, with a measurement of the short-circuit current and the spectral irradiance taken at each position. The result of the spatial uniformity test is given in Figure 5.31.
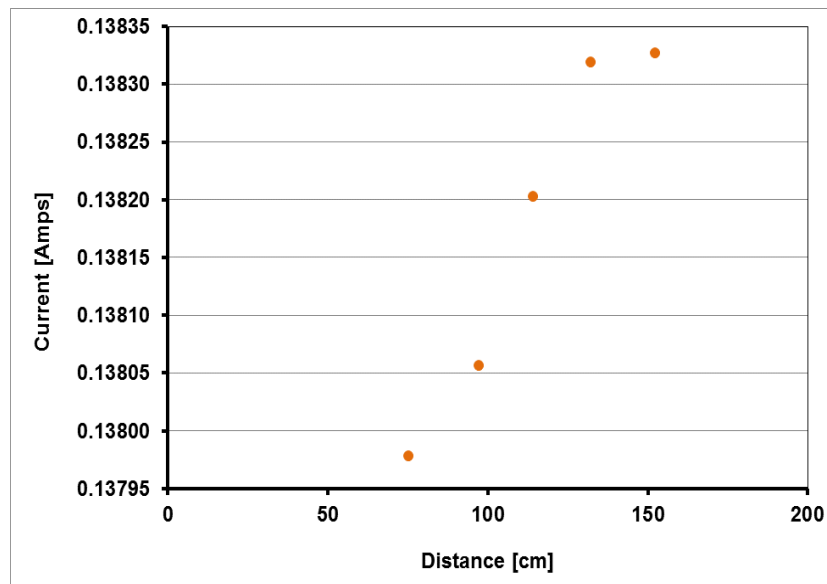
Figure 5.31: Variations in the short-circuit current of a calibrated reference solar cell with distance measured at the PASAN measurement system

As seen in Figure 5.31, variations in the short-circuit currents of the reference solar cell with distance are minimum, approximately 0.016%. This finding confirms that the spatial uniformity is not a problem in the spectral response measurement.

To observe faults in the current measurements, the short-circuit current produced by the reference solar cell is used as an indicator. The short-circuit currents generated by the reference solar cell have been measured at STC for 5 consecutive days. Ten I-V measurements were taken for each day. The accuracy in the current measurement can be determined by comparing the measured short-circuit currents of the reference solar cell to its calibrated value. Results of this comparison are shown in Figure 5.32. There is a slight difference between the measured short-circuit currents to the calibrated value. However these differences are not so significant since their variations are in a range 0.1% to 0.4%. This indicates that the current measurement of the PASAN measurement system is highly accurate. To verify the repeatability in the current measurements, the short-circuit currents produced by the tested PV devices from the two separate measurements are compared as shown in Figure 5.33.
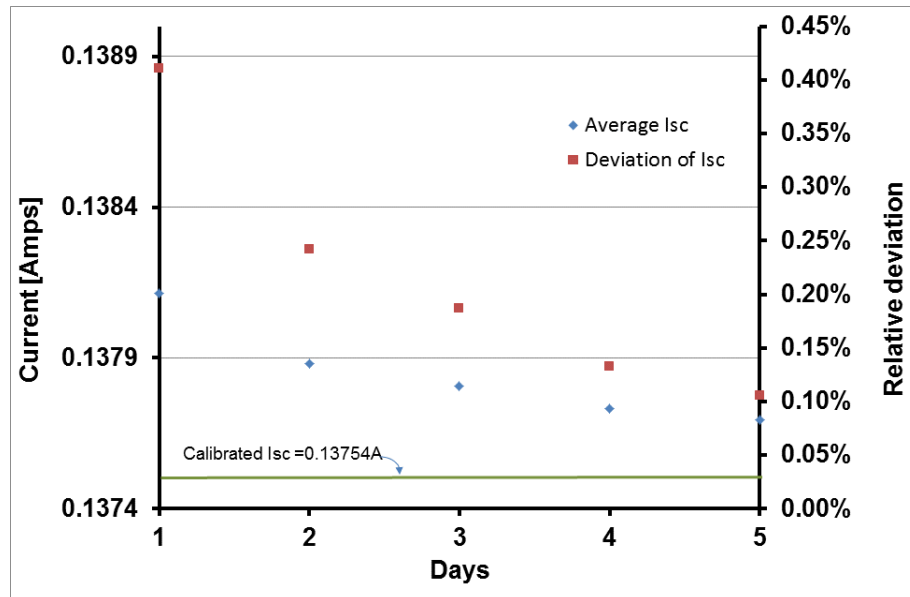
Figure 5.32: Comparison of short-circuit currents of a calibrated mono-cSi measured at CREST' PASAN solar simulator system and a calibrated laboratory (ESTI)
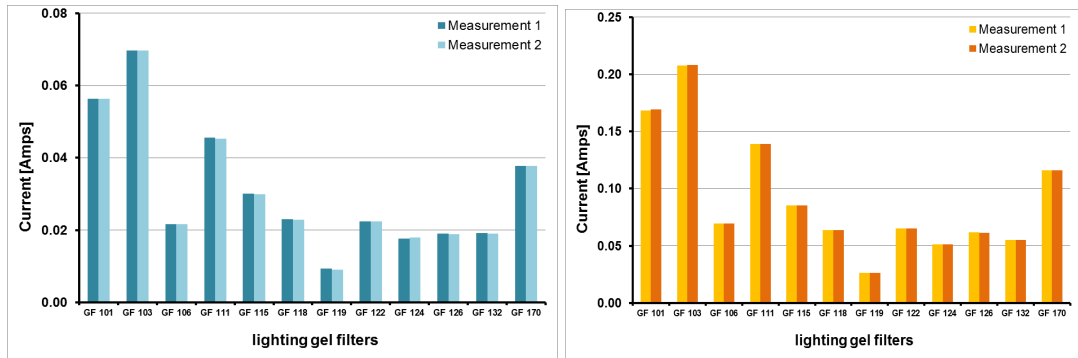
a. Small a-Si b. Mini module a-Si

Figure 5.33: Repeatability of current measurements performed on tested PV devices

As be seen in the figures, the short-circuit currents from the two tested PV devices are reproducible. This comparison and the earlier results have demonstrated conclusively that there is no fault in the current measurements.
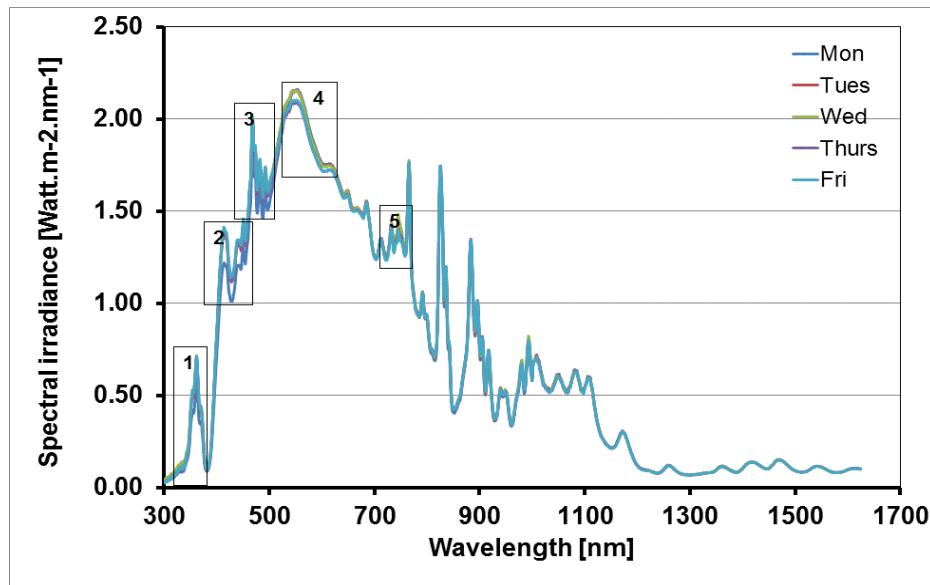
Figure 5.34: Weekly variations of the spectral irradiance distributions of the pulsed xenon lamp measured using spectro-radiometer at the PASAN measurement system

As can been seen from Figure 5.34, there are some significant variations in the spectral measurement results particularly around the peak of the wavelength spectrum and in the blue region. The high differences in the spectral response determinations of the amorphous silicon device correspond to high variations in these spectral ranges. The variations cannot be caused by temperature inside the room or

151

the lamp age as the room temperature is always kept constant during the measurement and the currents produced from the calibrated reference cell are repeated. The repeatability is assessed using the relative standard deviation, shown in Figure 5.35.
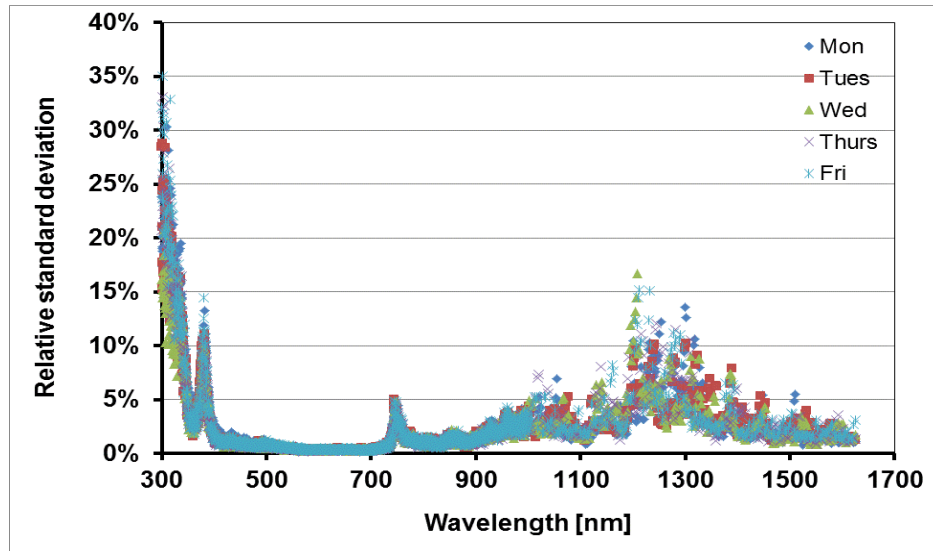
Figure 5.35: Weekly relative standard deviation of spectral irradiance distributions of the pulsed xenon lamp measured using spectro-radiometer at the PASAN measurement system

To examine the variability in the spectral measurement, there are 20 spectral measurements taken each day for five consecutive days. The variations are calculated by taking the ratio of daily average and standard deviation. Daily variations in the ultra violet range are very high (up to 35%) as well as in the blue range (up to 15%), while variations in the green to red regions are below 1%. High variations in the ultraviolet range and the near infrared onward are believed to be due to the low signal to noise ratio of the spectro-radiometer or systematic measurement errors in those ranges. To verify this assumption, the spectral transmittance of each gel filters as measured using a calibrated spectrophotometer presented in section 3.5 was compared to the values determined using the Astranet spectro-radiometer. Determination of the spectral transmittances using the spectrophotometer is straightforward, by giving a baseline signal at 100% and 0% transmittances to eliminate offset in the measurement then radiating the sample to measure its transmittance. For measuring the spectral transmittance using the Astranet spectro-

radiometer, it must be calculated by comparing the throughput of a given polychromatic filter to the spectrum of the pulsed xenon lamp. The procedure to obtain the measured spectra using the Astranet is the same as shown in Figure 5.15. A comparison of the spectral transmittance of a sample of the filters, measured in the two systems, is shown in Figure 5.36.
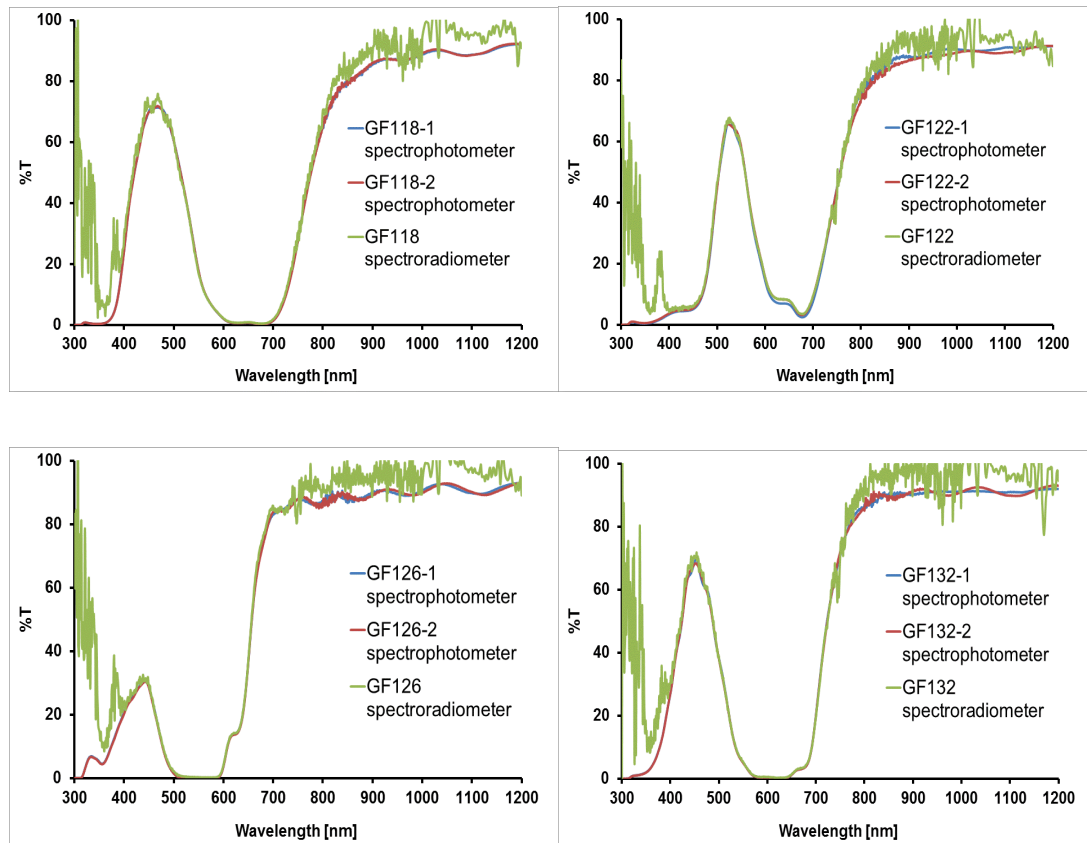
Figure 5.36: Comparisons of spectral transmittances of some selected lighting gel filters measuring using the spectrophotometer and the spectro-radiometer

To check for any changes in the spectral transmittance of the gel filters, they were measured twice using the spectrophotometer, once before they were used in the spectral response measurements and again after all the spectral response measurements were finished. As shown in Figure 5.36, no changes were detected, allowing the spectral transmittance of the filters to be used to check the validity of the spectral measurement using the Astranet spectro-radiometer. It is apparent that differences in the spectral transmittance measured using the spectrophotometer and spectro-radiometer (Astranet) are very high in the ultraviolet and violet ranges. The deviations that are detected at wavelengths below 400 nm are up to 50% and at 700

nm onwards about below 5%. This justifies that there is a high systematic error in the spectro-radiometer in those ranges. The percentage differences in the spectral transmittance between the two measurements for the other filters are presented in Figure 5.37.
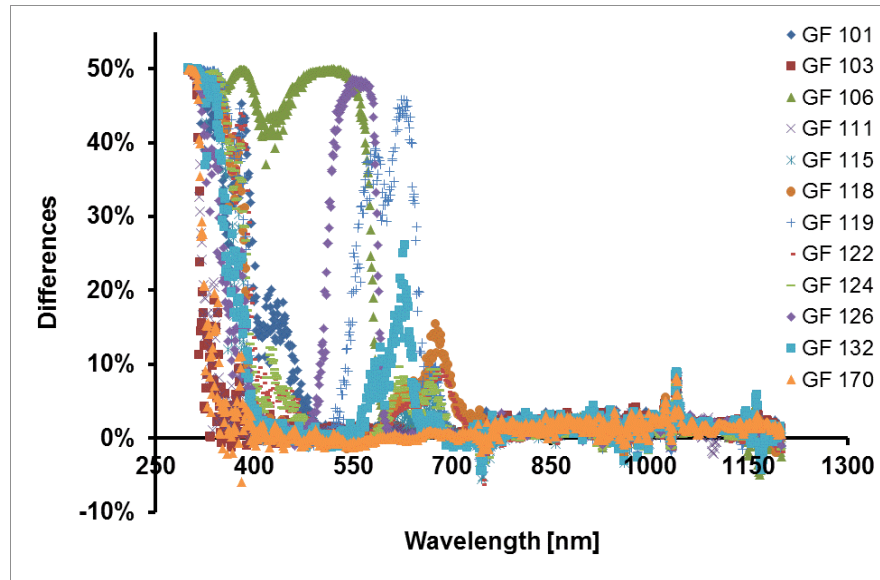
Figure 5.37: Variations in the spectral transmittances of lighting gel filters measured using the spectro-radiometer and the spectrophotometer in use at CREST

Errors in the spectral measurement have a significant impact on the output of the polychromatic spectral response fitting method. As it has been analysed in section 4.5, highly accurate spectral measurements with uncertainty less than 4% are required to enable the fitting algorithm to produce the appropriate fitted coefficients. To quantify the effects of the errors in the spectral measurements on the calculation currents, the measured spectra of the pulsed xenon lamp from the five consecutive days are applied to calculate the currents of the calibrated reference cell. By applying the photocurrent formula as presented in equation (3.1) in section 3.2, the calculated photocurrents of the reference cell are determined as shown in Figure 5.38. The differences between the calculated photocurrents and their measured values are significant, up to 6%. These findings also confirm that there is a systematic error in the spectral measurement. Therefore, the spectra that are measured using the Astranet spectro-radiometer need to be corrected using certain scaling factors in order to obtain accurate spectral measurements as have been discussed in the previous section (5.4).

154
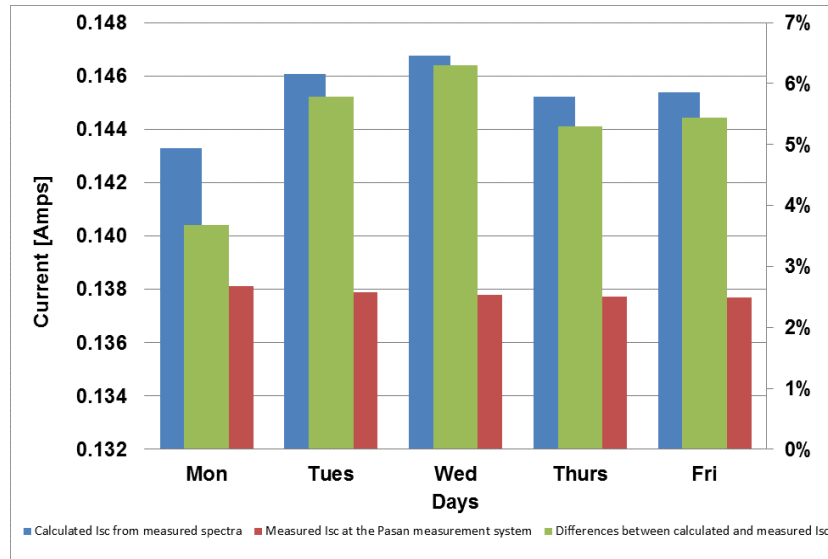
Figure 5.38: Effects of errors in the spectral measurements to the calculated currents of a calibrated reference solar cell

Further examination is carried out to determine whether there is another cause of failure in the fitting algorithm itself. From the error sensitivity analyses that have been done in section 4.5 of Chapter 4, errors in choosing a set of initial values for the chosen spectral response model essentially cause defects in the spectral response determinations. Therefore the accuracy of the chosen initial values for the spectral response model is analysed. It is done by simulating the spectral response determination process using the polychromatic method and applying the chosen initial values to the fitting algorithm to obtain the spectral response of a tested PV device. The result of this simulation is compared to the device spectral response obtained using the monochromatic method. The entire simulation process is the same as that has been done in section 3.6 in Chapter 3. Results of these spectral response simulations are presented in Figure 5.39. From the figures, it is obvious that the chosen initial values for the spectral response model are viable, since the output matches the monochromatic measurements.

155
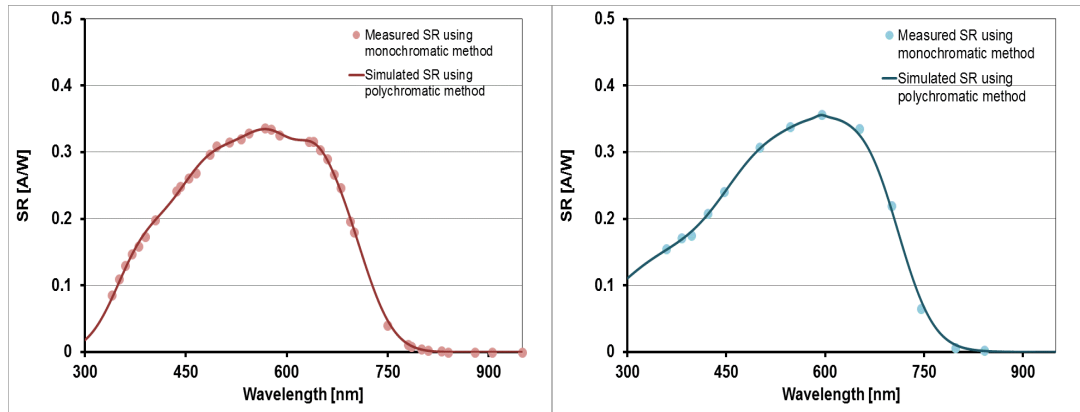
a. Small a-Si   b. Mini module a-Si

Figure 5.39: Comparison of SR determinations obtained by simulation using the polychromatic method and measured using the monochromatic method

Based on the error tracing analysis, it is clear that the failures in the spectral response determinations using the polychromatic spectral response fitting method are due to inaccurate spectral irradiance measurements. This spectral error has caused the fitting algorithm to fail to produce a set of coefficients for accurate spectral response determinations if it is not corrected using certain scaling factors.

5.6.   Conclusions

The implementation of the spectral response characterisation tools using the polychromatic spectral response fitting method to the PASAN measurement system are practical as it only requires the addition of the spectro-radiometer and the polychromatic filters to provide spectral variations at the test plane. If the cheap filter materials can be found, the building cost of the spectral response measurement system would be more effective. Even though there is no temperature issue emerged in the spectral response measurement, the applications of the polychromatic filters which are made from the polymeric materials to filter out the powerful pulsed xenon lamp of the PASAN solar simulator are unsuitable. This is due to the high irradiance and temperature stress produced by the pulsed xenon lamps which have degraded the filter material physically. Polychromatic filters which are made from a suitable material such as glass which can withstand high irradiance and temperature stress should be found to replace the polymeric material filters.

The application of the polychromatic spectral response fitting method for measuring spectral response using the pulsed xenon lamp is more challenging than using a continuous xenon lamp particularly when spectral measurement is required. This is due to very short duration time of the pulse signal produced by the xenon lamp within 10 ms illuminating the measurement plane. An accurate current measurement can be achieved by using the full current-voltage mode. Systematic errors in the spectral measurement can introduce errors in the spectral response determinations and at the end lead to failure. Compared to other spectral response measurement methods, the polychromatic spectral response fitting method can provide high irradiance throughputs at the measurement plane if appropriate polychromatic filters are utilised. This will improve the signal-to-noise ratios particularly in the ultraviolet and near infrared ranges. Implementation of the polychromatic method for a large-area SR determination has proven that the proposed spectral response method is feasible as a new technique for determining a large-area spectral response of a PV device. However, high precision instruments for measuring spectra and current are significantly required for an accurate SR determination.

Chapter 6

Conclusions and Recommendations for Future Research

6.1. Conclusions

The objective of this work was to develop a novel spectral response (SR) measurement approach for a large area SR determination of a photovoltaic (PV) device. To achieve this objective, the following main tasks were completed:

- Development of an original SR measurement concept for SR determinations of a PV device
- Proving the proposed SR measurement concept through a computer simulation
- Validation of the proposed SR measurement concept by means of a small scale laboratory measurement
- The upgrading the SR measurement approach for a large-area SR determination in the PASAN solar simulator system

The conclusions that can be drawn after completing those works as follows:

6.1.1. Development of Spectral Response Measurement Concept

Problems associated with the application of the monochromatic method for the spectral response determination have been identified. One of these problems is low irradiance throughput of a monochromatic filter on the measurement plane, which results in weak signal strength generated from a tested PV device. A simple solution

is proposed by introducing **polychromatic filters** to replace the use of monochromatic filters for spectral response determinations. This new measurement approach is known as **the polychromatic SR fitting method** or in short, it referred as **the polychromatic method**. The irradiance throughput of the polychromatic filters has much higher intensity than that of using the monochromatic filters. This increases the signal strength produced from a tested PV device almost 20 times higher than that of using the monochromatic filters.

The polychromatic SR method offers a simple measurement setup which consists of a light source, a set of polychromatic filters, a spectro-radiometer, and a current meter. In this technique, **a new spectral response model was introduced** for the SR determination of a PV device. This SR model is an **empirical model** based on **the fifth order Gaussian function**. As the fifth order Gaussian function is not a physical based model, it could not be used to determine certain device's optical properties that might be important in the fabrication process to improve PV device performance.

6.1.2. Proving the Spectral Response Measurement Concept through a Computer Simulation

The feasibility of the polychromatic SR fitting concept was demonstrated by modelling the SR measurement process using a computer simulation. A fitting algorithm based on the non-linear least squares method was developed to generate the appropriate coefficients for the chosen SR model. The simulation demonstrated that there were correlations in the spectral response curves between the polychromatic and the monochromatic methods, with deviations within $\pm 2\%$. From the simulation, it was found that employing 15 polychromatic filters are adequate to produce an accurate spectral response curve. This can reduce the cost for building up the spectral response measurement system.

6.1.3. Validation of the Spectral Response Measurement Concept in a Small Scale Laboratory Measurement

The validations were demonstrated using a continuous xenon lamp as a light source in a small-area measurement system. Some issues related to the spectral measurement were identified, which are the homogeneity of illumination on the measurement plane and the accuracy of the spectro-radiometer. It was found that the spatial non-uniformity of the irradiance on an illumination area of 120 mm x100 mm was approximately 8.5%, which was still considered satisfactory for PV measurement tests. The accuracy in the spectral measurement was improved by applying certain scaling factors which were determined using a reference solar cell.

The small-scale laboratory measurement confirmed that the SR determinations using the polychromatic method were not different from those of the monochromatic method. This demonstrates that the proposed polychromatic SR method is feasible for the SR determination of a PV device. However, to obtain an accurate SR curve, the polychromatic method requires high precision current and spectral measurement units with the uncertainty should not be greater than $\pm 4\%$.

6.1.4. Implementation of the Spectral Response Measurement Concept for a Large-area Spectral Response Determination

The potential of up-scaling the polychromatic filter method for a large-area SR measurement was examined by adding the spectro-radiometer and employing the 15 selected polychromatic filters into the PASAN solar simulator system. There are two significant problems encountered in the measurement. These are the physical damage of the polychromatic filters made from the polymeric material after experiencing 19 consecutive flashes within 30 ms and a systematic error in the spectral measurement. The first finding shows that the filters made from the polymeric material are not suitable to be employed in the PASAN measurement system. It is only suitable for a small-area SR measurement system. Therefore durable materials which are able to

sustain high irradiance and temperature stress over longer periods of time are required to substitute the polymeric materials.

The large-area verification demonstrates that the potential for implementing the polychromatic SR method is feasible for a large-area SR determination of a PV device. The simplicity in the measurement setup which is offered by this SR measurement method makes it easy to be integrated into the PASAN measurement system. As a result, the cost for building the SR measurement would become cheap and this can reduce the cost for measuring the spectral response curve of a PV device in the future.

6.2. Future Research

The potential of the polychromatic method for a large-area spectral response measurement investigated in this work was focused on the crystalline silicone and amorphous silicon PV devices. The findings were satisfactory despite the polychromatic filters which are made from polymeric materials are failed to withstand high irradiance output of the PASAN measurement system. To improve the performance of the polychromatic filters for a large-area SR determination, **a robust and durable filter material is required**. Therefore, further research would be still required to source appropriate materials for the polychromatic filter to replace the polymeric materials. Should this be achieved, future development on my present findings would prove to be most worthwhile from scientific and financial standpoint.

List of Publications

I.D.sara, T.R.Betts, R.Gottschalg. Analysis of uncertainty in PV device spectral response measurement, presented in the proceedings of Photovoltaic science applications and technology the PVSAT-7 conference, 6-8 April 2011, ISBN 0 904963 77 2.

I.D.sara, T.R.Betts, R.Gottschalg. Factors influencing the Short-circuit Current of a Tandem Photovoltaic Device. The PVSAT-8 conference, 2-4 April 2012, ISBN 0 904963 78 0.

I.D.sara, T.R.Betts, R.Gottschalg. Analysis of a suitable model for spectral response measurement. The EUPVSEC-27 conference, 24-28 September 2012.

I.D.sara, T.R.Betts, R.Gottschalg. Determining Spectral Response of a Photovoltaic Device using Polychromatic Filters. The PVSAT-9 conference, 9-11 April 2013.

I.D.sara, T.R.Betts, R.Gottschalg. Determining Spectral Response of a Photovoltaic Device using Polychromatic Filters. Invited paper for special issue going to be published at IET Renewable power generation journal.

References

[1] IEC 60904-3, "Photovoltaic devices - Part 3: Measurement Principles for Terrestrial PV Solar Devices with Reference Spectral Irradiance Data," 2008.

[2] G. Masson, M. Latour, M. Rekinger, I. T. Theologitis and M. Papoutsi, "Global market outlook for photovoltaics 2013-2017," European Photovoltaic Industry Association (EPIA), Belgium, May 2013.

[3] IEC 61215, "Crystalline silicon terrestrial photovoltaic (PV) modules - Design qualification and type approval," 2005.

[4] IEC 60904-8, "Photovoltaic devices - Part 8: measurement of spectral response of a photovoltaic (PV) device," 1998.

[5] The German Energy Society (Deutsche Gesellschaft fur Sonnenenergie), *Planning and Installing Photovoltaic Systems: A Guide for Installers, Architects, and Engineers.* Earthscan, 2008.

[6] S. R. Wenham, M. A. Green, M. E. Watt and R. Corkish, Eds., *Applied Photovoltaics.* London, UK: Earthscan, 2007.

[7] E. E. van Dyk and E. L. Meyer, "Analysis of the effect of parasitic resistances on the performance of photovoltaic modules," *Renewable Energy,* vol. 29, pp. 333-344, 3, 2004.

[8] J. Nelson, *The Physics of Solar Cells.* Imperial college press, 2003.

[9] R. Gottschalg, M. Rommel, D. G. Infield and M. J. Kearney, "The influence of the measurement environment on the accuracy of the extraction of the physical of solar cells," vol. 10, pp. 796-804, 1999.

[10] J. Merten, J. M. Asensi, C. Voz, A. V. Shah, R. Platz and J. Andreu, "Improved equivalent circuit and analytical model for amorphous silicon solar cells and modules," *Electron Devices, IEEE Transactions on,* vol. 45, pp. 423-429, 1998.

[11] A. Virtuani, H. Mullejans and E. D. Dunlop, "Comparison of indoor and outdoor performance measurements of recent commercially available solar modules," *Progress in Photovoltaics,* vol. 19, pp. 11-20, 2011.

[12] P. Merhej, E. Dallago and D. Finarelli, "Effect of capacitance on the output characteristics of solar cells," in *Ph.D. Research in Microelectronics and Electronics (PRIME), 2010 Conference on,* 2010, pp. 1-4.

[13] R. Gottschalg, "Environmental Influences on the Performance of Thin Film Solar Cells," 2001.

[14] J. Meier, S. Dubail, S. Golay, U. Kroll, S. Faÿ, E. Vallat-Sauvain, L. Feitknecht, J. Dubail and A. Shah, "Microcrystalline silicon and the impact on micromorph tandem solar cells," *Solar Energy Mater. Solar Cells,* vol. 74, pp. 457-467, 10, 2002.

[15] M. Meusel, C. Baur, G. Siefer, F. Dimroth, A. W. Bett and W. Warta, "Characterization of monolithic III–V multi-junction solar cells—challenges and application," *Solar Energy Mater. Solar Cells,* vol. 90, pp. 3268-3275, 11/23, 2006.

[16] M. Meusel, R. Adelhelm, F. Dimroth, A. Bett and W. Warta, "Spectral mismatch correction and spectrometric characterization of monolithic III-V multi-junction solar cells," *Prog Photovoltaics Res Appl,* vol. 10, pp. 243-255, 2002.

[17] M. Meusel, C. Baur, G. Létay, A. W. Bett, W. Warta and E. Fernandez, "Spectral response measurements of monolithic GaInP/Ga(In)As/Ge triple-junction solar cells: Measurement artifacts and their explanation," *Prog Photovoltaics Res Appl,* vol. 11, pp. 499-514, 2003.

[18] J. Burdick and T. Glatfelter, "Spectral Response and IV Measurements of Tandem Amorphous-Silicon Alloy Solar-Cells," *Solar Cells,* vol. 18, pp. 301-314, 1986.

[19] S. R. Kurtz, P. Faine and J. M. Olson, "Modeling of two-junction, series-connected tandem solar cells using top-cell thickness as an adjustable parameter," *Journal of Applied Physics,* vol. 68, pp. 1890-1895, 1990.

[20] J. Yang, B. Yan and S. Guha, "Amorphous and nanocrystalline silicon-based multi-junction solar cells," *Thin Solid Films,* vol. 487, pp. 162-169, 9/1, 2005.

[21] K. Yang and J. Yang, "The analysis of light trapping and internal quantum efficiency of a solar cell with DBR back reflector," *Solar Energy,* vol. 83, pp. 2050-2058, 11, 2009.

[22] R. Gottschalg, T. R. Betts, D. G. Infield and M. J. Kearney, "The effect of spectral variations on the performance parameters of single and double junction amorphous silicon solar cells," *Solar Energy Mater. Solar Cells,* vol. 85, pp. 415-428, 1/31, 2005.

[23] R. Gottschalg, T. R. Betts, D. G. Infield and M. J. Kearney, "On the importance of considering the incident spectrum when measuring the outdoor performance of amorphous silicon photovoltaic devices," *Measurement Science and Technology,* vol. 15, pp. 460, 2004.

[24] P. J. Faine, S. R. Kurtz and J. M. Olson, "Modeling of two-junction, series-connected tandem solar cells using top-cell and coating thicknesses as adjustable parameters," in *Photovoltaic Specialists Conference, 1990., Conference Record of the Twenty First IEEE,* 1990, pp. 339-344 vol.1.

[25] I. D. Sara, T. R. Betts and R. Gottschalg, "Factors influencing the short-circuit current of a tandem photovoltaic device," in *The 8th PVSAT,* Edinburgh, UK, 2011, .

[26] H. Al Buflasa, R. Gottschalg and T. Betts, "Modeling the effect of varying spectra on multi junction A-SI solar cells," *Desalination,* vol. 209, pp. 78-85, 4/30, 2007.

[27] Y. Hirata, T. Inasaka and T. Tani, "Output variation of photovoltaic modules with environmental factors - II: Seasonal variation," *Solar Energy,* vol. 63, pp. 185-189, 1998.

[28] R. P. Kenny, A. Ioannides, H. Mullejans, W. Zaaiman and E. D. Dunlop, "Performance of thin film PV modules," *Thin Solid Films,* vol. 511, pp. 663-672, 2006.

[29] K. Ichida, S. Fukushige, A. Nakajima, T. Minemoto and H. Takakura, "Impact of environment factors on solar cell parameters of a-Si∥μc-Si photovoltaic modules," *Solar Energy Mater. Solar Cells,* vol. 93, pp. 879-883, 6, 2009.

[30] T. Huld, R. Gottschalg, H. G. Beyer and M. Topic, "Mapping the performance of PV modules, effects of module type and data averaging," *Solar Energy,* vol. 84, pp. 324-338, 2010.

[31] B. Marion, "A method for modeling the current-voltage curve of a PV module for outdoor conditions," *PROGRESS IN PHOTOVOLTAICS,* vol. 10, pp. 205-214, 2002.

[32] D. L. King, "Photovoltaic module and array performance characterization methods for all system operating conditions," *Nrel/snl Photovoltaics Program Review - Proceedings of the 14th Conference: A Joint Meeting,* pp. 347-368, 1997.

[33] D. L. King, J. A. Kratochvil, W. E. Boyson and W. I. Bower, "Field experience with a new performance characterisation procedure for photovoltaic arrays " in *The Proceeding of the 2nd World Conference and Exhibition on Photovoltaic Solar   Energy   Conversion* Vienna, 1998, .

[34] D. L. King, M. A. Quintana, J. A. Kratochvil, D. E. Ellibee and B. R. Hansen, "Photovoltaic module performance and durability following long-term field exposure," *Ncpv Photovoltaics Program Review,* vol. 462, pp. 565-572, 1999.

[35] D. L. King, W. E. Boyson and J. A. Kratochvil, "Analysis of factors influencing the annual energy production of photovoltaic systems," in *Photovoltaic Specialists Conference, 2002. Conference Record of the Twenty-Ninth IEEE,* 2002, pp. 1356-1361.

[36] D. L. King, G. M. Galbraith, W. E. Boyson, S. Gonzalez, A. T. Murray, J. W. Ginn and W. I. Bower, "Array performance characterization and modeling for real-time performance analysis of photovoltaic systems," *Conference Record of the 2006*

IEEE 4th World Conference on Photovoltaic Energy Conversion, Vols 1 and 2, pp. 2308-2311, 2006.

[37] R. Perez, J. Doty, B. Bailey and R. Stewart, "Experimental evaluation of a photovoltaic simulation program," *Solar Energy,* vol. 52, pp. 359-365, 4, 1994.

[38] C. A. Gueymard, "Direct and indirect uncertainties in the prediction of tilted irradiance for solar engineering applications," *Solar Energy,* vol. 83, pp. 432-444, 2009.

[39] J. A. Duffie and W. A. Beckman, *Solar Engineering of Thermal Processes.* Hoboken, New Jersey, USA: John Wiley & Sons, Inc, 2013.

[40] N. Veissid, "The I-V silicon solar cell characteristic parameters temperature dependence an experimental study using the standard deviation " in *The Proceeding of the 10th European Photovoltaic Solar Energy Conference* Lisbon Portugal, 1991, .

[41] N. Veissid, D. Bonnet and H. Richter, "Experimental investigation of the double exponential model of a solar cell under illuminated conditions: Considering the instrumental uncertainties in the current, voltage and temperature values," *Solid-State Electronics,* vol. 38, pp. 1937-1943, 11, 1995.

[42] N. Veissid, P. Nubile and A. F. Beloto, "Results of the solar cell experiment of the first Brazilian satellite," *Solar Energy Mater. Solar Cells,* vol. 46, pp. 1-16, 4/1, 1997.

[43] M. W. Wanlass, K. A. Emery, T. A. Gessert, G. S. Horner, C. R. Osterwald and T. J. Coutts, "Practical Considerations in Tandem Cell Modeling," *Solar Cells,* vol. 27, pp. 191-204, 1989.

[44] R. J. Matson, K. A. Emery and R. E. Bird, "Terrestrial solar spectra, solar simulation and solar cell short-circuit current calibration: A review," *Solar Cells,* vol. 11, pp. 105-145, 3, 1984.

[45] C. A. Gueymard, D. Myers and K. Emery, "Proposed reference irradiance spectra for solar energy systems testing," *Solar Energy,* vol. 73, pp. 443-467, 12, 2002.

[46] C. A. Gueymard and H. D. Kambezidis, "Solar spectral radiation," in *Solar Radiation and Daylight Models (Second Edition)*Anonymous Oxford: Butterworth-Heinemann, 2004, pp. 221-301.

[47] IEC 60904-1, "Photovoltaic devices - Part 1: Measurement of photovoltaic current-voltage characteristics," 2006.

[48] A. Luque and S. Hegedus, Eds., *Handbook of Photovoltaic Science and Engineering.* England UK: John wiley & sons Ltd, 2003.

[49] IEC 60904-9, "photovoltaic devices - part 9: Solar simulator performance requirements," 2007.

[50] W. Hermann, S. Zamini, F. Fabero, T. Betts, N. van der Borg, K. Kiefer, G. Friesen, H. Muellejans, H. D. Mohring, M. Vasques and D. Fraile, "PV module output power characterisation in test laboratories and in the PV industry - results of the european performance project," in *The 25th EU PVSEC / WCPEC-5,* Valencia, Spain, 2010, pp. 1-5.

[51] (14 August 2013). *Measurement of Cell Efficiency: Illumination Sources*. Available: http://www.pveducation.org/pvcdrom/characterisation/illumination-sources.

[52] J. Kuurne, A. Tolvanen and J. Hyvarinen, "Sweep time, spectral mismatch and light soaking in thin film module measurement," in *Photovoltaic Specialists Conference, 2008. PVSC '08. 33rd IEEE,* 2008, pp. 1-3.

[53] IEC 60904-7, "Photovoltaic devices - Part 7: Computation of the spectral mismatch correction for measurements of photovoltaic devices," 2008.

[54] H. Mullejans, A. Ioannides, R. Kenny, W. Zaaiman, H. A. Ossenbrink and E. D. Dunlop, "Spectral mismatch in calibration of photovoltaic reference devices by global sunlight method," vol. 16, pp. 1250-1254, 2005.

[55] G. Friesen, D. Chianese, S. Dittmann, D. Domine, E. Bura, D. Strepparava, B. Margni, M. Denicola, R. Meoli and I. Pola, "Performance intercomparison of 13 different PV modules based on indoor and outdoor tests," in *The 25th European Photovoltaic Solar Energy Conference and Exhibition / the 5th World Conference on Photovoltaic Energy Conversion,* Valencia, Spain, 6-10 September 2010, pp. 3780-3784.

[56] B. L. Sopori, "A spectral response measurement system for large-area solar cells," *Solar Cells,* vol. 22, pp. 287-294, 12, 1987.

[57] J. S. Hartman and M. A. Lind, "Spectral response measurements for solar cells," *Solar Cells,* vol. 7, pp. 147-157, 11, 1982.

[58] L. P. Boivin, W. Budde, C. X. Dodd and S. R. Das, " Spectral response measurement apparatus for large area solar cells," 1986.

[59] K. Emery, D. Dunlavy, H. Field and T. Moriarty, "Photovoltaic spectral responsivity measurements," in *The 2nd World Conference and Exhibition on Photovoltaic Solar Energy Conversion,* Vienna, Austria, 6-10July 1998, .

[60] S. S. Hegedus and W. N. Shafarman, "Thin-film solar cells: device measurements and analysis," *Prog Photovoltaics Res Appl,* vol. 12, pp. 155-176, 2004.

[61] H. Mullejans, T. Wagner, F. Merli, A. Jäger-Waldau and E. D. Dunlop, "Changes in spectral response with temperature and irradiance intensity," *Thin Solid Films,* vol. 451–452, pp. 145-151, 3/22, 2004.

[62] S. Kohraku and K. Kurokawa, "New methods for solar cells measurement by LED solar simulator," in *Photovoltaic Energy Conversion, 2003. Proceedings of 3rd World Conference on,* 2003, pp. 1977-1980 Vol.2.

[63] K. K. Jun Koyanagi, "A fundamental experiment of solar cell's I-V characteristics measurement using LED solar simulator," in *Renewable Energy,* 2006, pp. 270-273.

[64] Y. Tsuno, Koichi Kamisako and K. Kurokawa, "New generation of PV module rating by LED solar simulator - A novel approach and its capabilities," in *Photovoltaic Specialists Conference, 2008. PVSC '08. 33rd IEEE,* 2008, pp. 1-5.

[65] Martin Bliss, "Measurement system for fast power and energy rating of photovoltaic devices," 2011.

[66] Y. Hishikawa, Y. Tsuno and K. Kurokawa, "Spectral response measurement of PV modules and multi-junction devices " in *The Proceeding of the 22nd European Photovoltaic Solar Energy Conference* Milan, Italy, 2007, .

[67] M. Pravettoni, R. Galleano, A. Virtuani, H. Mullejans and E. D. Dunlop, "Spectral response measurement of double-junction thin-film photovoltaic devices: the impact of shunt resistance and bias voltage," *Measurement Science and Technology,* vol. 22, pp. 045902, 2011.

[68] S. Winter, T. Fey, I. Kroger, D. Friendrich, K. Ladner, B. Ortel, S. Pendsa and D. Schlussel, "Laser-DSR facility at PTB: Realization of a next generation high accuracy primary calibration facility," in *The 27th European Photovoltaic Solar Energy Conference and Exhibition,* Frankfrut, Germany, 24-28 September 2012, pp. 3049-3051.

[69] M. Pravettoni, A. Komlan, R. Galleano, H. Müllejans and E. D. Dunlop, "An alternative method for spectral response measurements of large-area thin-film photovoltaic modules," *Prog Photovoltaics Res Appl,* pp. n/a-n/a, 2011.

[70] J. Carabe, "A new approach to measuring spectral responses of non-linear solar cells," *Solar Cells,* vol. 31, pp. 39-46, 2, 1991.

[71] E. F. Zalewski and J. Geist, "Solar cell spectral response characterization," vol. 18, pp. 3942-3947, 1979.

[72] R. L. Mueller, "Spectral response measurements of two-terminal triple-junction a-Si solar cells," *Solar Energy Mater. Solar Cells,* vol. 30, pp. 37-45, 6, 1993.

[73] A. Schonecker and K. Bucher, "Influence of non-uniform illumination on spectral response and efficiency measurements of large area solar cells," in *Photovoltaic Specialists Conference, 1991., Conference Record of the Twenty Second IEEE,* 1991, pp. 203-208 vol.1.

[74] H. Field, "Solar cell spectral response measurement errors related to spectral band width and chopped light waveform," in *Photovoltaic Specialists Conference, 1997., Conference Record of the Twenty-Sixth IEEE,* 1997, pp. 471-474.

[75] J. Blifford, "Factor Affecting the Performance of Commercial Interference Filters," vol. 5, pp. 105-111, 1966.

[76] J. Hohl-Ebinger and W. Warta, "Investigation of large area cell and module spectral response measurement," in *19th European Photovoltaic Solar Energy Conference,* Paris, France, 7-11 June 2004, pp. 2611-2614.

[77] J. Hohl-Ebinger and W. Warta, "Uncertainty of the spectral mismatch correction factor in STC measurements on photovoltaic devices," *Prog Photovoltaics Res Appl,* vol. 19, pp. 573-579, 2011.

[78] B. H. Hamadani, J. Roller, B. Dougherty and H. W. Yoon, "Versatile light-emitting-diode-based spectral response measurement system for photovoltaic device characterization," vol. 51, pp. 4469-4479, 2012.

[79] G. Zaid, N. P. Park, S. Park and D. H. Lee, "Differential spectral responsivity measurement of photovoltaic detectors with a light-emitting-diode-based integrating sphere source," vol. 49, pp. 6772-6783, 10 December, 2010.

[80] P. Espinet, I. Rey-Stolle and C. Algora, "Advanced characterization of multijunction solar cells with electroluminescence," in *Electron Devices, 2009. CDE 2009. Spanish Conference on,* 2009, pp. 390-393.

[81] IEC 60904-10, "Photovoltaic devices - Part 10: Methods of linearity measurement," 2009.

[82] H. Schade and Z. E. Smith, "Optical properties and quantum efficiency of a-Si[sub 1 - x]C[sub x]@B:H/a-Si@B:H solar cells," vol. 57, pp. 568-574, January 15, 1985.

[83] I. D. Sara, T. R. Betts and R. Gottschalg, "Analysis of a suitable model for spectral response of a photovoltaic device," in *The 27th European Photovoltaic Solar Energy Conference,* Frankfrut Germany, 24-28 September 2012, pp. 471-475.

[84] Press,William H. Teukolsky, Saul A. Vetterling, William T. Flannery, Brian P., *Numerical Recipes the Art of Scientific Computing* Cambridge University Press, 2007.

[85] D. Domine, M. Pravettoni, A. Virtuani, D. Pavanello, M. Bernasocchi and G. Friesen, "Spectral characterization tools used at SUPSI for indoor performance

measurement of single and multi-junction photovoltaic modules," in *The 26th European Photovoltaic Solar Energy Conference,* Hamburg, Germany, 2011, pp. 3450-3453.

[86] M. Pravettoni, M. Nicola and G. Friesen, "A filtered pulsed solar simulator for spectral response measurements of multi-junction modules of commercial size," in *The 27th European Photovoltaic Solar Energy Conference,* Frankfrut, Germany, 2012, .

[87] (26 May 2011). *TUV Rheinland sets up spectral sensitivity measurement test stand for PV modules at Cologne site*. Available: http://www.pv-tech.org/news/tuev_rheinland_sets_up_spectral_sensitivity_measurement_test_stand_for_pv_m.

[88] M. Schweiger, U. Jahn and W. Herrmann, "Spectral analysis of various thin film modules using high precision spectral response data and solar spectral irradiance data," in *The 27th European Photovoltaic Solar Energy Conference,* Frankfrut, Germany, 24-28 September 2012, .

[89] C. J. Hibberd, F. Plyta, C. Monokroussos, M. Bliss, T. R. Betts and R. Gottschalg, "Voltage-dependent quantum efficiency measurements of amorphous silicon multi-junction mini-modules," *Solar Energy Mater. Solar Cells,* vol. In Press, Corrected Proof, .

[90] M. Bliss, A. Smith, B. Mihaylov, T. R. Betts and R. Gottschalg, "Spectral changes of solar simulator xenon flash bulbs over lifetime and its effects on measurement uncertainty," in *The Proceedinhs of PVSAT-9,* Swansea, Wales UK, 10th - 12th April 2013, pp. 107-110.

[91] T. W. Cannon, "Spectral measurements on pulse solar simulators," The National Renewable Energy Laboratory, Denver, Colorado USA, Tech. Rep. PV907401, 8-11 September 1998.